Ministry of Higher Education
and Scientific Research
University of Diyala
College of Science

PREPARATION AND CHARACTERIZATION OF SOME METAL OXIDES NANOPARTICLES AND USING THEM TO REMOVE HEAVY METALS FROM INDUSTIRAL WASTE WATER

A Thesis Submitted to Council of College of Science, University of Diyala in Partial Fulfillment of the Requirements for the Degree of Master of Science in Chemistry

by

Eman Rahman Mahdi
BSc. Chemistry, College of Science, University of Diyala 2011

Supervised by
Prof. Dr. Karim H. Hassan

2016 AD **IRAQ** **1438 AH**

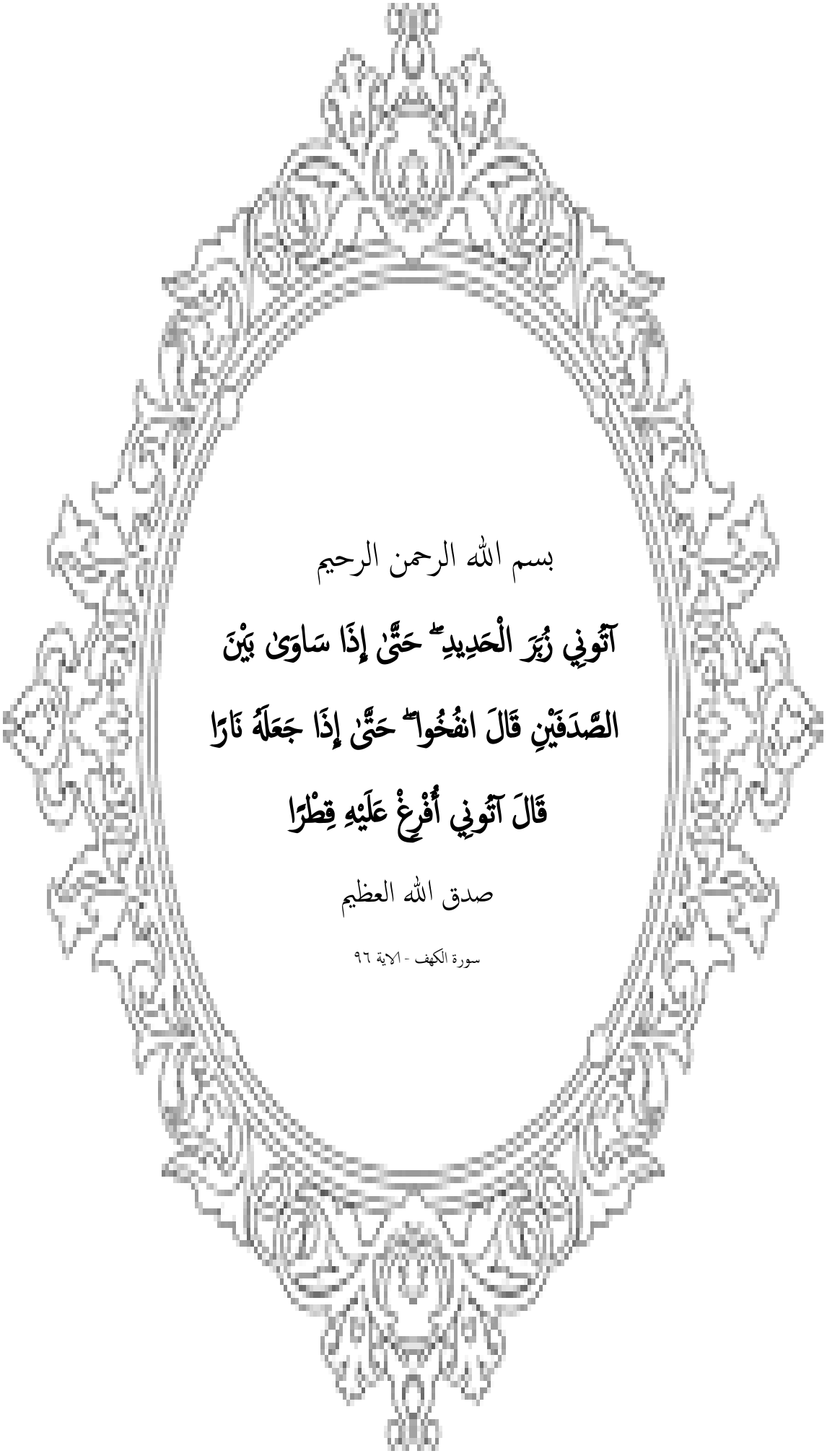

بسم الله الرحمن الرحيم

آتُونِي زُبَرَ الْحَدِيدِ ۖ حَتَّىٰ إِذَا سَاوَىٰ بَيْنَ

الصَّدَفَيْنِ قَالَ انفُخُوا ۖ حَتَّىٰ إِذَا جَعَلَهُ نَارًا

قَالَ آتُونِي أُفْرِغْ عَلَيْهِ قِطْرًا

صدق الله العظيم

سورة الكهف - الاية ٩٦

DEDICATIONS

I would like to dedicate my humble effort to

The memory of my late uncle "Ahmed"

(May Allah have mercy on his soul and grant him the highest level of paradise)

My Father, my Mother

Whose love, support, and prays make me completing this work

My Brothers and Sisters

Whose support and helping in all study period

Eman..

ACKNOWLEDGMENT

First of all , I thank Almighty Allah who has enable me to continue this work and overcome all difficulties .

I would like to express my sincere gratitude to my supervisor ***Prof. Dr. karim H. Hassan****, for his encouragement, guidance, and scientific support throughout this study.*

Special thanks are extended to the Dean , Chairman, and the staff of the chemistry Department, College of science, Diyala University for their assistance.

I would like to express my appreciation to ***Prof. Dr. Nabeel Ali*** *Physics Department, College of science , Diyala University for helping me.*

I would like to express my gratitude to my uncles ***Prof. Dr. Aziz M. Abed*** *and* ***Asst. Prof. Dr. Abbas M. Abed*** *and my aunt* ***Asst. Prof. Dr. Suhad M. Abed*** *for their continuous support and encouragement throughout this study.*

My gratitude is dedicated to all my colleagues especially ***Fayha'a, Asia, and Mohammed*** *for their help.*

Special thanks to my buddy all the work time ***Noor Hatam*** *for her help and trouble all the work time.*

I would like to express my gratitude to my dearest friends ***Saja Khalil,*** *and* ***Noor Kathium*** *for their assistance .*

Finally , my big thanks to ***my sweet and loving dad*** *,* ***mom*** *for their love, trust, encouragement, support, pray, and to* ***my dearest brothers (Mohamad, Mohanad,*** *and* ***Hussam)*** *and* ***my lovely sisters (Noor, Kawthar)*** *for support and help and everything.*

Eman....

Supervisor Certification

We certify that this thesis (***Preparation and Characterization of Some Metal Oxides Nanoparticles and Using Them to Remove Heavy Metals from Industrial waste water***) was carried out under our supervision in Chemistry Department, College of Science, Diyala University in partial fulfilment of the requirement for the degree of Master of science in chemistry by the student (**Eman Rahman Mahdi**).

Signature:
Name: Dr. Karim H. Hassan
Title: Professor
Date: / / 2017
Supervisor

In view of the available recommendation, we forwarded this thesis for debate by the examination committee.

Signature:
Name: Dr. Wassan B. Ali
Title: Lecturer
Date: / / 2017
Head of Chemistry Department
College of Science
Diyala University

Scientific Amendment

I certify that the thesis entitled "***Preparation and Characterization of Some Metal Oxides Nanoparticles and Using Them to Remove Heavy Metals from Industrial Waste Water*** " presented by **(Eman Rahman Mahdi)** has been evaluated scientifically, therefore, it is suitable for debate by examining committee.

Signature :

Name : Dr. Dhia H. Hussain

Title : Professor

Date : / / 2017

Linguistic Amendment

I certify that the thesis entitled " ***Preparation and Characterization of Some Metal Oxides Nanoparticles and Using Them to Remove Heavy Metals from Industrial Waste Water*** " presented by **(Eman Rahman Mahdi** has been corrected linguistically, therefore, it is suitable for debate by examining committee.

Signature :

Name : Massarra Majid Ibrahim

Title : Assistant Prof.

Date : / / 2017

Examination Committee Certificate

We certify, that we have read the thesis entitled (***Preparation and Characterization of Some Metal Oxides Nanoparticles and Using Them to Remove Heavy Metals from Industrial Waste Water***), presented by (**Eman Rahman Mahdi**), and as an examining committee, we examined the student on its contents, and in what is related to it and our opinion it meets the standard for the degree of master in Chemistry Science.

Signature:
Name: Dr. Ramzi R. Ali
Title: Professor
Date: / / 2017

Signature:
Name: Dr. Ahmed N. Abd
Title: Assistant Prof.
Date: / / 2017

Signature:
Name: Dr. Sameer H. Kareem
Title: Assistant Prof.
Date: / / 2017

Signature:
Name: Dr. Karim H. Hassan
Title: Professor
Date: / / 2017

Approved by The Council of College of the Science, University of Diyala.

Signature:
Name: Dr. Tahseen H. Mubarak
Title: Assistant Prof.
Date: / / 2017

ABSTRACT

In this study, three different oxides nanoparticles are prepared by simple precipitation method including iron oxide nanoparticles (Fe_3O_4), (Fe_2O_3), and copper oxide nanoparticles (CuO). They are characterized by XRD, SEM, and AFM techniques. XRD spectrum reveals that particle size obtained is around (12.04, 39.11, and 7.43 nm) for (Fe_3O_4), (Fe_2O_3), and (CuO) nanoparticles respectively, which agreed fairly well with SEM and AFM data. Surface morphology as a main nanoparticles phenomenon is studied in terms of SEM and AFM. The prepared oxides nanoparticles are used to remove nickel and lead ions from industrial wastewater by using prepared aqueous solution of these ions determining the best removal percentage at different contact time (30, 60, 90, and 120 min) and different initial concentration of aqueous solutions (100, 200, and 300 mg/L) with other constant condition such as pH of 3.5, adsorbent dosage (0.1g), and room temperature (25˚C).

The result shows the percentage removal of nickel and lead ions increase with the contact time increasing, and the highest adsorption with 100 mg/L has been observed for the three oxides nanoparticle. Also the percentage removal seems to decrease with the increase in the initial concentration of adsorbate.

The correlation coefficient for the linear Langmuir isotherm regression fits is larger than that for the Freundlich one for (Fe_3O_4) nanoparticles, so the Langmuir model could describe the adsorption isotherm for the uptake ions of nickel from its aqueous solution on (Fe_3O_4), nanoparticles surfaces. (Fe_2O_3), and(CuO) nanoparticles show the otherwise because they fit better the model of Freundlich isotherm than the model of Langmuir isotherm. Thus Freundlich model could describe the adsorption isotherm for nickel ions removal from the aqueous solution on both oxides nanoparticles surfaces. For lead ions removal from aqueous solution the Freundlich model describes the adsorption isotherm on the three oxide nanoparticles surfaces.

The kinetics results of adsorption showed that the adsorption of nickel and lead ions by the three oxide nanoparticles surfaces obey pseudo-second order equation.

List of Contents

List of Tables

List of Figures

List of Abbreviations and Symbols

Abbreviation or Symbol	Definition
AAS	Atomic absorption spectrometry
AFM	Atomic force microscope
Avg	Average
EDS	Energy dispersive spectroscopy
EPA	Environmental protection agency
FESEM	Field emission scanning electron microscope
FETEM	Field emission transmission electron microscope
FTIR	Fourier transform infrared spectroscopy
FWHM	Full width at half maximum
ICP-MS	Mass spectrometry with inductively coupled plasma
JCPDS	Join committee on power diffraction standars
min	Minute
pH	Power of hydrogen
RMS	Root mean square
rpm	Revolution per minute
SEM	Scanning electron microscope
T	Temperature
TEM	Transmission electron microscope
V	Volume of solution
WHO	World health organization
XRD	X- ray diffraction
a	Langmuir constant related with adsorption capacity
B	Full width at half maximum
b	Langmuir constant related with energy of adsorption
C_1	Initial concentration of adsorbate before the adsorption
C_2	Concentration of adsorbate at any time after the adsorption
C_e	Equilibrium concentration of adsorbate
C_o	Initial concentration of adsorbate
C_t	Concentration of adsorbate after any time
D	Crystallite size
d	Distance between atomic planes
k_1	Rate constant of pseudo-first order adsorption
k_2	Rate constant of pseudo-second order adsorption
K_f	Freundliuch constant related with adsorption capacity
m	Weight of adsorbent
n	Freundliuch constant related with adsorption intensity
Q_e	Adsorption capacity of the adsorbent at equilibrium time t
Q_t	Adsorption capacity of the adsorbent at any time
R%	Percentage removal of adsorbate
R^2	Correlation coefficient
$ʎ_{max}$	Wave length at maximum
θ	Bragg's angle
ΔG	Gibbs free energy
ΔH	Enthalpy
ΔS	Entropy

Chapter One

Introduction

1.1: Introduction

Environment means surrounding and everything that affects an organism during its lifetime or it is sum total of water, air and land inter relationships and also their relationship with the human being, other living organisms and property. It involves all the physical and biological surrounding and their interactions [1]. So, pollutants entrance to a natural environment leads to disorder, instability, damage or discomfort of the ecosystem i.e. physical systems or living organisms known as the environmental pollution [2].

There are many types of environmental pollution such as water pollution, light pollution, air pollution, noise pollution, soil pollution, thermal pollution, radiation pollution, and the agents which cause environmental pollution known as pollutants [3]. Three parameters located the pollutant severity including its concentration, its chemical nature, and its persistence [4]. Water pollution, known as the water bodies pollution (for example rivers, lakes, oceans and ground water) is one of the most serious environmental problems. It is caused by a variety of human activities such as industrial, agricultural and domestic takes place when contaminates are sent in direct way or indirectly into water bodies without enough remediation to remove harmful compounds [5].

Wastes of industrial process are different from one industry to other and from certain location to another. Some industries produce wastes containing high level of organic substance, such industries involve food processing plants, dairy and meat-packing houses. The other industries discharge wastes with low level of inorganic substance but which are high in toxic chemicals including: mining facilities, chemical plants, and textile mills [6].

Water industrial contaminants contain many chemicals materials such as aromatic hydrocarbons, organic solvents, pesticides, metals and heavy metals which are one of the pollutants in industrial waste. They are discharged into natural water and tend to be collected in the chain of food. Then they are adsorbed by living organisms because of high solubility in the aquatic environments, so these toxic metals must be removed or are decreased from wastewater before discharging them to environment [7, 8].

Adsorption is a very effective process and economical method for metal ions removal from wastewaters; In order to be a good adsorption process, there must be choice of the type of adsorbent as having many properties such as a good compatibility with adsorbate, high surface area, high adsorption capacity, quick response of adsorption capacity to temperature change, high thermal conductivity, high mass diffusivity and thermal stability [9].

A great change is observed in the adsorbents properties whether chemical, physical, optical and mechanical when the particle size decreases to a nano level. The main change is observed on the surface area of the nanomaterial which increases tremendously and leads to the higher capacity of adsorption for the removal of heavy metals [10].

Metal oxides nanoparticles are classified as the promising adsorbent for removal of heavy metals from aquatic systems due to their large surface areas and high activities , therefore increasing attention has been focused on metal oxide such as iron, aluminum, titanium, manganese, zirconium, and copper oxides [11].

As far as the present study is concerned, iron and copper oxides nanoparticles are prepared and applied to remove heavy metals ions from industrial waste water . Sample analysis is made which contains high concentration of nickel and lead ions and an aqueous solution are prepared of different concentrations of these ions and calculation removal percentage

at different contact time. Then determination of the suitable adsorption isotherm model, calculation as well as determination order of the adsorption kinetic are made.

1.2: Heavy Metals

The term 'heavy metal' is applied to a group of metals (and metal-like elements) with atomic number above 20 and density greater than 5 g/cm^3 [12]. Twenty metals at least are classified as toxic and fifty percent of these are sent into the environment in magnitude that acts hazard to human health [13]. These elements are naturally found on earth crust and can be introduced into environment as a results of human activities and fast manufacturing [14]. Large amounts of probably toxic heavy metals are introduced into the environment from industrial processes[15]. Many processes such as smelting activities, battery industrial, plating and mining discharge of municipal sewage and industrial wastewater include heavy metals such as chromium, copper, cadmium, lead, nickel, mercury, and zinc [16]. Also heavy metal pollution is present in aqueous effluent of many industries such as refining ores, paint and pigments, chloralkali, sludge disposal, tanneries, radiator manufacturing, and alloy industries [17]. Heavy metals exist in discharged and untreated wastes , pollute water bodies and pose menace to ecosystem [18].

The removal of heavy metals from wastewaters is so important because of their high toxicity and tendency to be collected in living organisms. Moreover, heavy metals cannot be destroyed or degraded [19], and tend to accumulate in living organisms, causing different life threatening disorders [20].

Heavy metal contamination of water and water bodies is a dangerous environmental trouble which affects the quality of water. The consequences

are : decrease in water supply and aquatic production, increase in cost of purification and eutrophication of water bodies [21].

The heavy metals include in particular cadmium, lead, copper, zinc and mercury, these elements are highly undegradable, capable to accumulate in various tissues of organisms. Such accumulation in human body may cause damage to kidney structure and function, bones, central nervous system, hematopoietic disorders. It may also influence the course of the fundamental biochemical reactions and have adverse reproductive effects [22].

1.2.1: Nickel element

1.2.1.1: Definition and uses

Nickel, a silver-grayish solid , is found naturally below the crust of earth (volcanic rocks and soils) and has a crystalline structure [23]. It is a one of transition metals. It is ductile and hard [24]. It is highly resistant to attack by air and water [25]. It is 24^{th} most abundant metal the crust of earth and its ores are basically of two types sulphides and oxides [26].

Nickel is one of the five ferromagnetic elements, and it is also a naturally magnetostrictive material, meaning that in the presence of a magnetic field, the material succumb a small change in length, it takes place most commonly in combination with sulphur and iron in pentlandite, with sulphur in millerite, with arsenic in mineral nickeline, and with arsenic and sulphur in nickel glance. Nickel is primarily found combined with oxygen or sulphur as oxides or sulphides found naturally in the earth's crust. Nickel combined with other elements and is present in all soils, in meteorites, and is emitted from volcanoes [24].

It is found in numerous kind of foods. In spite of nickel content of the soil in which they are grown, widespread items being rich in contents include rye, oats, sunflower seeds, red kidney beans, tea, gelatin, baking

powder kippered herrings, soya, strong licorice, peas peanuts, hazelnuts, and whole wheat, cocoa, and dried fruits [27]. Like any other heavy metal, nickel is toxic, non-biodegradable and is usually introduce into environment as a consequence of anthropogenic activities. Other ways of nickel introducing into the environment are through weathering of rocks and soils and leaching of the minerals [23]. Nickel ions and its toxic compounds are water soluble and have a distinctive green color and its compounds have no characteristic of smell or taste [28,29].

Different nickel compounds have been used in many industrial applications which involve stainless steel, aircraft parts, cosmetics, electroplating, automobile, batteries, spark plugs, coins, and production of nickel–cadmium batteries on an industrial scale [23].

Nickel forms many alloys with another metals. Its alloy with iron, nickel steel, is extremely hard and corrosion resistant. For this reason most of the nickel produced world-wide is used for the industry of stainless steel, which is usually used to produce food processing tools and containers. It is also used to fashion jewelry manufacture, machinery parts, coins, finely-divided nickel is used as hydrogenation catalyst [25].

The most widespread metals or alloys are nickel titanium and stainless steel which are used in dentistry for endodontic treatment. However, an essential potential disadvantage of these materials is in corrosion [30].

1.2.1.2: Nickel toxicities and health effect

Nickel, having been classified very toxic represents a dangerous contaminants of environmental trouble. It is the most toxic element, and its elevated concentration lead to symptoms of poisoning like headache, cancer, tightness of the chest, reduction in cell growth, dizziness, nausea, dry cough, chest pain, shortness of breath vomiting, cyanosis, extreme weakness and rapid respiration. In accordance to the World Health

Organization (WHO 2006) the agreeable nickel border is 0.01 and 2.0 mg/L in drinking water and industrial effluent, respectively (WHO 2006) [16]. The toxicity limits for nickel according to WHO are 1.0 mg/m^3 for insoluble nickel compounds, 0.1 mg/m^3 for soluble nickel compounds, 0.05–0.12 mg/m^3 for nickel carbonyl and 1.0 mg/m^3 for nickel sulphide [31].The very common harmful health effect of nickel on people is an allergic reaction. Approximately 10–20% of people is sensitive to nickel. A person can become sensitive to nickel while being in direct contact with jewelry or another substance containing nickel or through lengthy contact with the cuticle. The most common reaction is a skin rash at the site of contact, such as dermatitis, hand eczema; workers who are insecure to nickel by breathing can become sensitized and have asthma attacks. Some sensitized individuals react when they eat nickel in food or water or breathe dust containing nickel. People who are not sensitive to nickel must eat very large amounts of nickel to suffer harmful health effects. Workers who fortuitously drank light-green water including 250 mg/L of nickel from a polluted drinking source are to have stomach aches and suffer from adverse effects such as red blood cells increase and protein increase in the urine in kidneys. This concentration of nickel is more than 100,000 times greater than the amount usually found in drinking water . The most serious harmful health effects resulted from exposure to nickel, such as chronic bronchitis, reduced lung function, lung cancer nasal sinus cancers occurred as a result of being exposed to more than 10 mg nickel/m^3 as nickel compounds that are hard to dissolve (such as nickel sub sulfide). Exposure to big concentration of nickel compounds, that soluble easily in water, may also cause cancer. It is due to the existence of nickel compounds or another materials which are cancer producing [28].

Nickel is known to be answerable for ‘Nickel Itch’ a form of skin reactions, conjunctivitis and inflammatory reaction. A concentration of

about 30 mg or more of nickel is capable to cause changes in vital organs; such as muscle, brain, lungs, liver and kidney etc. and eventually causes death [31].

1.2.1.3: Properties of nickel element

Some important properties of nickel element are given in **Table (1.1)**.

Table (1.1): Some of important properties of nickel element [32, 33]

Property	
Symbol	Ni
Atomic number	28
Atomic weight	58.6934 $g.mol^{-1}$
Group, block	group 10, d-block
Period	period 4
Element category	transition metal
Oxidation states	4, 3, 2, 1, 0, −1, −2
Color	silvery-white
Atomic radis	empirical: 124 pm
Electronic configuration	[Ar] $3d^8$ $4s^2$
Density	8.908 g/cm^3
Melting point	1728 K (1455 °C)
Poiling point	3186 K (2913 °C)
Solubility in acids	Dilute HCl & H_2SO_4
Crystal structure	Face-centered cubic
Heat of fusion	17.48 kJ. mol^{-1}
Heat of vaporization	379 k J. mol^{-1}
Electron affinity	112 k J. mol^{-1}
Specific heat capacity	0.44 $J.g^{-1}$ K^{-1}
Molar heat capacity	26.07 J/ (mol·K)
Phase	Solid
Isotopes	Five observationally stable isotopes (^{58}Ni, ^{60}Ni , ^{61}Ni , ^{62}Ni , ^{64}Ni)

1.2.2: Lead element

1.2.2.1: Definition and uses:

Lead is a common heavy metal. It is soft and flexible. Metallic lead has a bluish-white color after cutting it, but when exposed to air its color turns to a dull grayish. It is a bright and silvery metal with a very slight shade of blue in a dry atmosphere. Lead is also the heaviest non-radioactive element. It is harmful and a toxic element that is ubiquitous in environment due to various sources and is found both naturally and anthropogenically. Concentration of lead in the environment increases by pesticide spraying , waste, and cars exhaust [34,35], and many industries generated a big quantities of wastewater including different concentrations of lead such as storage batteries, automotive, aeronautical coating, and steel industries [36], and from lead smelting, tetraethyl lead manufacturing, and the mining, plating, ammunition, ceramic and glass industries [37]. It is also resulted from the industrial wastes of photographic materials, printing, explosive manufacturing, fossil fuels, rubber production, etc.[38] .

Lead is one of the essential contaminated in the wastewater discharged from industries of ore beneficiation, electroplating, tanneries, electrical and electronic, and hydrometallurgical processing [18], and it has been used as raw material in the production of pigments for lead paints [39]. It can be introduced to the food chain and will pose a great threat to human food security. Also it can pollute water, mud and soil because it is released from the breakdown of lead-based paint on buildings: Park tools and soil beside roads may have high lead levels from years of exhaust vapors and pollution from cars that once used leaded gasoline [40]. So all these different sources beside natural ores, deposited lead to the soil, water and air.

1.2.2.2: Lead toxicities and health effect:

Lead has been confirmed to be extremely toxic and its concentration in the environment has to be contained within a specified limit [40]**.** Lead contamination is wide world environmental problem due to its source variety in the environment and its high toxicity which causes a big damage to human beings and ecosystems [41, 42]. Usually lead is listed in the 2nd order between 275 human toxins in the priority list of hazardous substances because of its high toxicity and presence in the environment [43, 44]. Many processes cause lead entrance to human system, such as air breathing in workplace, or places of industries that use lead or eating and drinking water from lead pipes or ingesting polluted dust or air and water near waste places or breathing weed smoke or ingesting polluted food grown on soil containing lead or food covered with lead-containing dust or breathing fumes or eating lead from avocations using lead for example leaded glass and ceramics, etc. [45]. Lead is a extremely dangerous agent among the heavy metals, because of its side effects on the human health even at concentrations as low as 0.01–5 mg/L [19].

Lead does not introduce the metabolism of living organism, so it is considered non-essential and represents a serious cell toxicants even at low concentration percentage[40], 143000 death cases estimated annually along with 600000 new cases of children with intellectual disabilities result from lead exposure according to WHO , and the U.S. Environmental Protection Agency (EPA) has established an action level of 15 μg L^{-1} for lead in public drinking water to protect human health since 1991[46], and it causes plant and animal death and failure to provide adequate protection for food from lead pollution . However, this is causes increase in levels of lead in blood and decreases immunological defenses and impaired psychosocial faculties. Such increase in lead level depletes the body's stores of some

major nutrients especially in children, mental deficiency, encephalopathy, brain damage, vomiting, anorexia, anemia, kidney damage, behavioral disturbances, cognitive impairment, and malaise in humans and resultant death [17, 34].

1.2.2.3: Properties of lead element

Some important properties of lead element are given in **Table (1.2).**

Table (1.2): Some of important properties of lead element [32,47]

Property	
Symbol	Pb
Atomic number	82
Atomic weight	207.19
Group, block	group 14 (carbon group) , p-block
Period	period 4
Element category	post-transition metal
Oxidation states	4, 3, 2, 1, 0 ,−1, −2, −4
Color	Bluish-gray
Atomic radis	empirical: 175 pm
Electronic configuration	[Xe] $4f^{14}$ $5d^{10}$ $6s^2$ $6p^2$
Density	11.34 g/cm^3
Melting point	600.4 K (327.4 °C)
Poiling point	2022 K (1740 °C)
Solubility in acid	Nitric acid & Hot conc. sulfuric acid
crystal structure	Face-centered cubic
Heat of fusion	4.77 k $J.mol^{-1}$
Heat of vaporization	179.5 k $J.mol^{-1}$
Electron affinity	35.1 $kJ.mol^{-1}$
Specific heat capacity	0.13 J. g^{-1} K^{-1}
Molar heat capacity	26.650 J/ (mol.K)
Phase	Solid
Isotopes	Four observationally stable isotopes (^{204}Pb , ^{206}Pb , ^{207}Pb , ^{208}Pb)

1.3: Heavy Metals Removal from Polluted Aqueous Solution

With heavy metal contamination becoming one of the most serious environmental problems [48], removal of toxic metals such as Cr, Cd, Cu, Pb, Ni, Hg and Zn from waste waters become a necessity due to their toxicity and carcinogenicity [49]. Recently, more and more efforts of researchers all over the world with the best of their abilities have been made on wastewater polluted by toxic metals because it is a public health problem of global concern and severe environmental [16, 50, 51].

In order to tackle the threat caused by heavy metal pollution of water, several options have been adopted. These include oxidation and reduction [57], ion exchange, filtration [19,54,56,57,58,59,60,61], membrane separation, reverse osmosis[16,49,50], solvent extraction [53], electro dialysis[52,54],electrochemical treatments[14,51,52,55],biological methods [18,51], and chemical precipitation[14,16,49,51,52,54,55] is the most commonly used method for heavy metal removal from wastewater streams with high heavy metals concentrations. However, this method is not effective when the heavy metal concentration in the wastewater is lower (less than 100 mg/L) , while adsorption [14,16,49,51,52,54,55,56], gets increasing people's attention since adsorbents have strong adsorptive ability, high specific surface, , and are appropriate for treating a diversity of heavy metal ions of low concentration of wastewater. So, many studies have been carried out to propose effective and economic metal removal technologies. Some recently techniques tackled increase the interfacial surface area between adsorbent and adsorbate to remove metal ions from dilute solutions [57]. Several researches have been conducted using various materials as adsorbents, some of these adsorbents also contain other toxicants; some are expensive and are characterized with limited surface area for adsorption [52]. Typically, trace quantities of heavy metals in environmental samples are determined using spectrometric techniques such

as atomic absorption spectrometry (AAS) or mass spectrometry with inductively coupled plasma (ICP-MS). However, these methods require complex laboratory equipment, expensive chemicals and are hardly available. Instead of the mentioned methods, the electrochemical methods can be used (differential pulse voltammetry and/or cyclic voltammetry). These techniques are one of the best for metal detection because of their low detection limits, metal selectivity, high sensitivity, mobility and low cost [22].

1.4: Adsorption

Untold chemical, biological, and physical, processes occur at the confines between two phases, while others started at that interface. Concentration change of a given materials at the interface as compared with the neighboring phases is an indicating of adsorption [58].

Adsorption is the process whereby molecules from the gas (or liquid) phase are taken up by a solid surface. It is distinguished from absorption which refers to molecules entering into the lattice (bulk) of the solid material. The adsorptive is the material in the gas phase capable of being adsorbed, whereas the adsorbate is the material actually adsorbed by the solid [59].

Adsorption is a phase transport process that is vastly used in practice to eliminate materials from fluid phases (gases or liquids). It can also be observed as natural process in different environmental compartments. The most general definition describes adsorption as an enrichment of chemical species from a fluid phase on the surface of a liquid or a solid. In water remediation , adsorption has been confirmed as an active uptake process for an abundance of solutes [60].

It is one of the very vastly applied methods for environmental treatment. Its kinetics are of great significance to test the rendering of a given adsorbent and gain insight into the underlying mechanisms [61]. The major development of adsorption processes on a large, industrial scale deals mainly with the solid-gas and solid-liquid and interfaces, but in various laboratory separation techniques all types of interfaces are applied [58].

Adsorption is regarded as a practicable separation method for purification or bulk separation in newly developed material production processes, for example, high tech materials and biochemical and biomedical products [62]. The material that adsorbs is the adsorbate and the underlying material that we are concerned within this section is the adsorbent or substrate. The reverse of adsorption is desorption [63]. Purification of gases by adsorption has played a main role in air contamination control, and adsorption of dissolved impurities from solution has been vastly used for water purification. Adsorption is now viewed as a superior method for wastewater remediation and water reclamation. Adsorption applications for chemical processing, air pollution control and water treatment are well known [64].

Adsorption is a spontaneous process because of decreases in free energy of the system i.e. ΔG of the system must have negative value. Also we know, $\Delta G = \Delta H - T\Delta S$ and during this process of adsorption, randomness of the molecule decreases which ΔS is negative, so $\Delta G = \Delta H + T\Delta S$ and this lead ΔH to be negative and $|\Delta H| > |T\Delta S|$ [58].

1.4.1: Types of adsorption

Adsorption may occur in two different ways according to the interactions of the adsorbent and adsorbate. Table (1.3) shows the difference between chemical adsorption and physical adsorption:

Table (1.3): Comparison between chemical adsorption and physical adsorption [59, 63, 65].

Chemical adsorption	Physical adsorption
It arises when adsorbate molecules accumulated on the surface of adsorbent on account of chemical bond (ionic or covalent bond).	It arises when adsorbate molecules accumulated on the surface of adsorbent on account of Van der Waals forces.
The heat of adsorptions is high (40 - 400) $K.J.mole^{-1}$.	The heat of adsorption is low (20 - 40) $K.J.mole^{-1}$.
This process occurs at high temperature and increase with the increases in the temperature.	This process is observed under condensation of low temperature and decreased with the increases in the temperature.
It is highly specific.	It is not specific.
This process is irreversible.	This process is reversible, desorption can be occur by increasing temperature or decreasing of pressure.
It is required activation energy.	It does not require activation energy.
Monolayer adsorption, thus adsorbed layer is unimolecular thick.	Multilayer adsorption, thus adsorbed layer is several molecular thick .
It is increasing with the increase of surface area of adsorbent.	It is also increasing with the increase of surface area of adsorbent.
Electron transfer leading to bond formation between sorbent and surface.	No electron transfer although polarization of sorbent may occur.
Surface reactions may take place : Dissociation , reconstruction, catalyst.	No surface reactions.
It is otherwise known chemisorption .	It is otherwise known physisorption
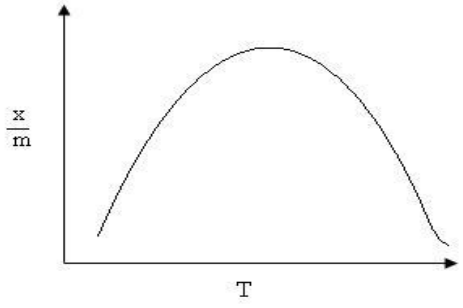 x = amount of absorbate m = amount of absorbent	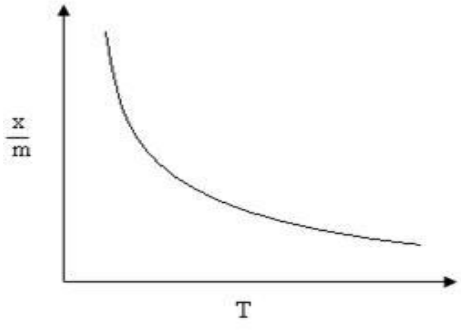 x = amount of absorbate m = amount of absorbent

1.4.2: Effective factors on the adsorption process

There are many factors which could affect the amount of molecules adsorb on surface:

1.4.2.1: The adsorbent nature and surface area

Adsorption represents surface phenomenon, the extent of adsorption depends upon the specific surface area which is defined as that portion of the total surface area that is exposed for adsorption, so the larger surface area of the adsorbent is simply greater adsorption capacity [66,67,68].

The properties of the adsorbent such as chemical nature, dimension of the pores, and the charge distribution of the adsorbent play an important role in the extent of adsorption. So more finely divided and more porous is solid greater is the amount of adsorption accomplished per unit weight of a solid adsorbent. The essential contribution to surface area is located in the pores of molecular dimension. As the adsorbent porosity increases, the adsorption of small molecules from the solution usually grows. It depended on the surface area and thus the greater the adsorption capacity is the more active sites are available. When the surface area of an adsorbent increases, the adsorption capacity would be the greater [67, 68]. Small particle sizes decrease internal diffusion and mass transfer limitation to the penetration of the adsorbate inside the adsorbent (i.e., equilibrium is more easily achieved and nearly adsorption capability can be attained) [66].

1.4.2.2: The adsorbate nature and concentration .

The physicochemical nature of adsorbate drastically affects both rate and capacity of adsorption, so the amount of material which is adsorbed by the adsorbent at certain temperature increases with the increase in the solute concentration. However, in some cases adsorption may be confined to only one layer of adsorbed solute. Thus increase of concentration of the solute

can produce no further adsorption because the surface of the crystal lattice of adsorbent covered [62,63]. Neutral molecules are adsorbed to a large extent than highly ionized molecules [66]. .

The solubility of the solute greatly influences the adsorption equilibrium, material slightly soluble in solvent will be more easily removed from solvent (i.e., adsorbed) than materials with high solubility. Generally, reverse relationship can be predictable between the range of adsorption of solute and its solubility in the solvent where the adsorption occurs [66,67] .When other effects are not present , for a given solvent , the more soluble solute are generally more weakly adsorbed than the less soluble solute [68].The extent of adsorption depends on the adsorbate nature, stereochemistry, size of adsorbed molecule, polarity, and the presence of different substituent groups in the molecule would govern the ability of the molecule to be adsorbed on certain surface [68].

1.4.2.3: Contact time

. The longer contact time is the more complete adsorption will be, therefore, the equipment will be larger [66].

1.4.2.4: The pH effect

The pH of the solution affects the extent of the adsorption because the distribution of the surface charge of the adsorbent can change. Also, the pH of the solution changing has a great effect on the extent of the adsorption through its influence on the adsorbate, the chemical state of the adsorbent, and the solvent. This effect can be observed through the competition on (H^+) and (OH^-) ions and their overlapping with the adsorbent surface or the adsorbate or the solvent. The degree of ionization of a species is affected by pH (e.g., a weak acid or a weak basis). This in turn affects adsorption. As a result of this interaction, the varying extent of

adsorption either increases, decreases, or remains unchanged according to the adsorbate functional groups [66,67,68].

1.4.2.5: Temperature

Another important factor is the temperature. Adsorption process is normally exothermic, it is a study of the temperature dependence on adsorption reactions which gives valuable information about the enthalpy and entropy changes during adsorption, thus decrease in temperature result in an increase of adsorption . On the other hand increasing adsorption with a rise in temperature means that process is endothermic. In chemisorption , the quantity adsorbed may increase or decrease with the rising temperature depending on the type of interaction and bonding between the surface and the adsorbed molecule , while in physisorption a decrease in temperature enhances the extent of adsorption [66,67,68].

1.5: Adsorbents

Adsorbents used are of two types either of natural origin or being the result of an industrial production and activation process. Typical natural adsorbents are clay minerals, natural zeolites, oxides, or biopolymers. Engineered adsorbents can be classified into carbonaceous adsorbents, polymeric adsorbents, oxidic adsorbents, and zeolite molecular sieves. Activated carbons produced from carbonaceous material by chemical activation or gas activation are the most widely applied adsorbents in water treatment.

Polymeric adsorbents made by copolymerization of nonpolar or weakly polar monomers show adsorption properties comparable to activated carbons, but high material costs and costly regeneration have prevented a broader application to date.

Oxides and zeolites are adsorbents with strong hydrophilic surface properties. The removal of polar, in particular ionic, compounds is therefore their preferred field of application. In recent decades, an increasing interest in using wastes and by-products as alternative low-cost adsorbents can be observed [60].

In the field of heavy metal removal, adsorption technology is represented as the most promising one among the techniques which are used for this purpose because of its low cost-effective, high efficiency, and being simple to operate for removing trace levels of heavy metal ions. So several types of materials above have been used to adsorb metal ions from aqueous solutions. Although traditional adsorbents could remove heavy metal ions, the low adsorption capacities and efficiencies limit their application deeply. To solve these defects of traditional adsorbents, nanomaterials are used as the novel ones to remove heavy metal ions. With novel size and shape dependent properties, nanomaterials have been extensively investigated over a decade in recent years. The development of nanoscience and nanotechnology has shown remarkable potential for the remediation of environmental problems [69].

1.6: Adsorption Isotherms

Adsorption process is studied through graphs known as adsorption isotherm which show the amount of solute adsorbed on the surface of adsorbent (Q_e) and the equilibrium concentration of the solute in the solution (C_e) at constant temperature [70].

An adsorption isotherm is an invaluable curve describing the phenomenon governing the retention (or release) or mobility of a substance from the aqueous media or aquatic environments to a solid phase at a constant temperature and pH [71].

Adsorption isotherms can be found in different shapes due to the adsorbent structure complexity and the interaction between each corpuscle as shown in **Figure (1.1)** and the different isotherm classified by Giles et al. (1960) to four types (S, L, H and C types) [70].

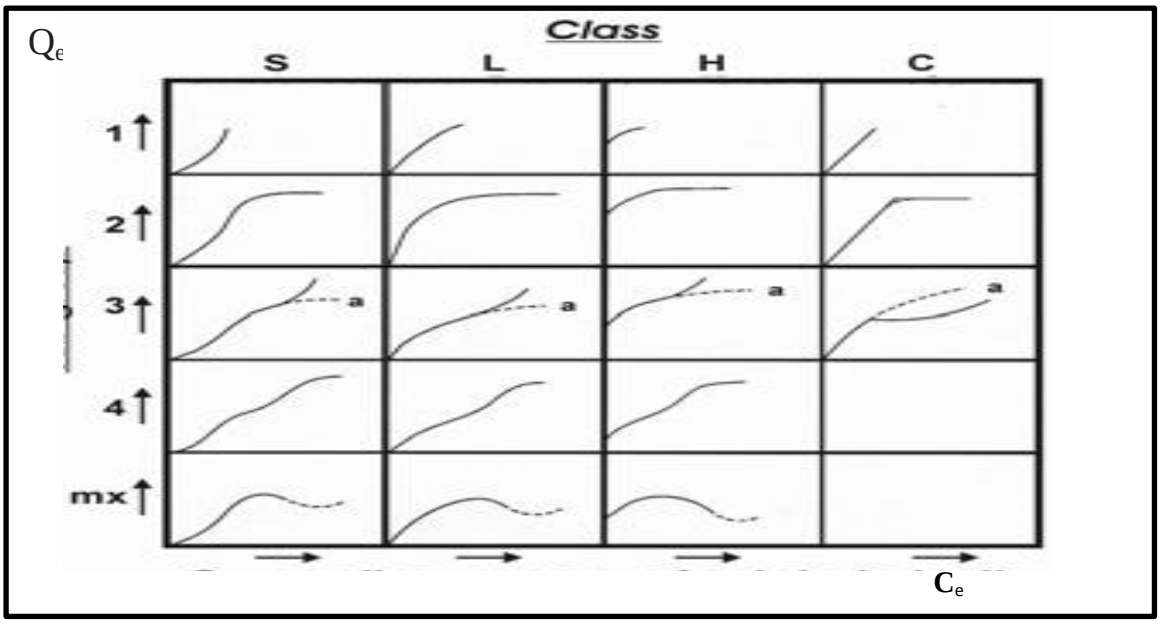

Figure (1.1): Adsorption isotherms as in Giles classification [72].

1. **S-curves :-** The S-curve isotherm is generally characterized by an initially small slope which increases with adsorptive concentration, or if the solvent is strongly absorbed ,there is a strong inter-molecular attraction within adsorbed layer, and the adsorbate which is mono functional
2. **L-curves:-** The L-curve isotherm is generally characterized by an initial slope which does not increase with adsorptive concentration**,** or it may be found when there is no stronger competition from solvent for sites on the surface. Another possibility is that the adsorbate has linear or planar molecules, the major axis is parallel to the surface**,** and it is also called Langmuir type.

3. **H-curves: -** The H-curve isotherm is characterized by a large initial slope suggestion a very high relative affinity of the adsorbent for the adsorbate which is shown even in very dilute solutions.
4. **C-curves: -** The C-curve isotherm is characterized by an initial slope which remain independent on adsorptive concentration until the maximum possible adsorption is achieved, and refers to constant partition linear curves given by substances which penetrate into the adsorbent more readily than the solvent does [72,73,74].

1.7: Type of Adsorption Isotherms

There are several types of adsorption isotherms and the most important one are:

1.7.1: The Langmuir isotherm

The Langmuir equation, which is valid for monolayer adsorption onto a completely homogeneous surface with a finite number of identical sites and with negligible interaction between adsorbed molecules, is represented in the linear form as follows [75,76,77].

$$\frac{Ce}{Qe} = \frac{1}{ab} + \frac{Ce}{a} \qquad (1.1)$$

Where

$\mathbf{Q_e}$: the quantity adsorbed at equilibrium in (mg/g).

$\mathbf{C_e}$: the equilibrium concentration of adsorbate in (mg/L).

a : the Langmuir constant which is a measure of adsorption capacity in (mg/g) .

b : also the Langmuir constant which isa measure of energy of adsorption in (L/mg).

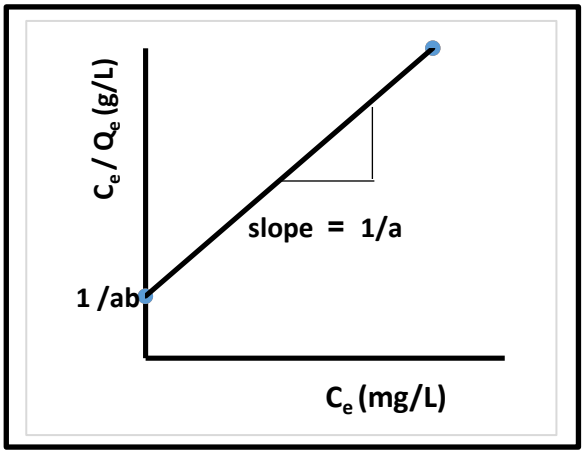

Figure (1.2): The linear form of Langmuir isotherm[77].

This form can be used as a linearization of expermental data by plotting C_e/Q_e against C_e as shown in **Figure (1.2).** The Langmuir constants (a) and (b) can be evaluated from the slope (1/a) and intercept (1/ab) of the linear equation [75].

1.7.2: The Freundlich isotherm

The Freundlich isotherm, assumes a heterogeneous sorption surface and is based on the idea that the adsorption depending on the energy of the adsorption sites. The Freundlich model can be represented as follows [77,78,79]:-

$$Q_e = K_f C_e^{1/n} \quad \ldots\ldots (1.2)$$

Where

Q_e : the quantity adsorbed at equilibrium in (mg/g)

C_e : the equilibrium concentration of the adsorbate in (mg/L).

K_f and **n:** the freundlich constants being indicators of the adsorption capacityand adsorption intensity, respectively.

Take logarithms of equation (1.2) give:

$\log Q_e = \log K_f + 1/n (\log C_e)$ .... (1.3)

If log **Q_e** is plotted against log **C_e** a straight line should be obtained as shown in **Figure (1.3).** The slope of the line will give the value of 1/n and the intercept on the Y-axis gives the value of log K_f .

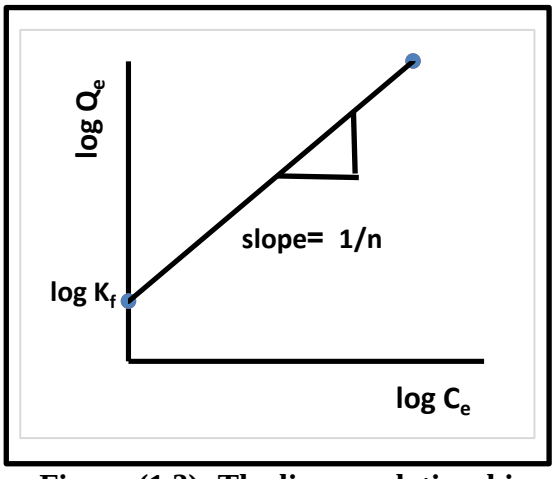

Figure (1.3): The linear relationship Freundlich isotherm[77].

1.8:Nanomaterials

The prefix “nano” has been found in last a century an ever increasing application to different fields of the knowledge. It comes from the ancient

Greek νᾶνος through the Latin nanus meaning literally dwarf and by extension, very small[80].

Nano material is defined as a physical substance with one dimension at the lowest between 1-100 nm, ($1nm=10^{-9}m$) have received considerable interest because of the unique properties different from their bulk counterparts [81, 82]. Nanotechnologies have applications in various disciplines from medicine to many through chemical technology to the construction industry, etc. [22].

Consequently nano metals find applications in diverse fields, such as homogeneous and heterogeneous catalysis, fuel cell catalysis, electronics, optics, magnetism, material sciences and even in medical and biological sciences. Nano-structured materials can be produced by two different approaches, namely, "top down" and "bottom up" approach, as shown in **Figure (1.2)**

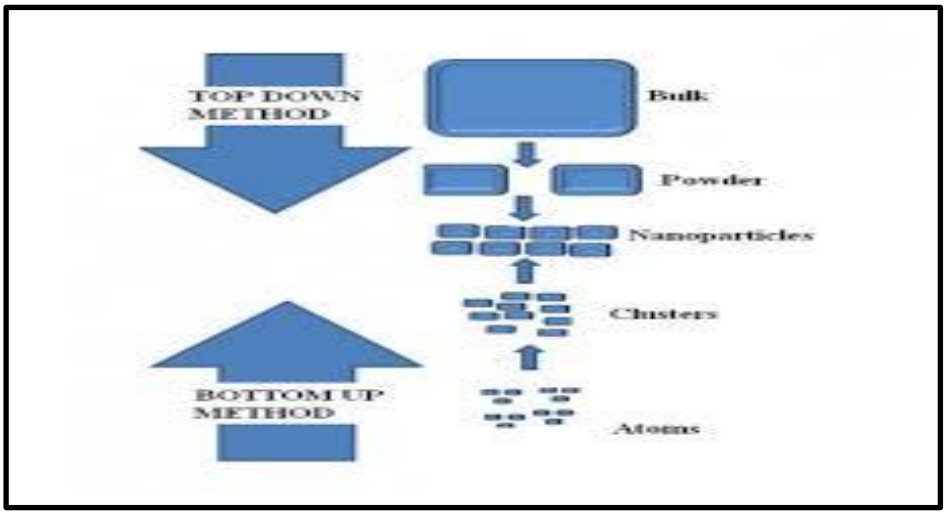

Figure (1.2): Nano materials production

The shape, size and composition of nanoparticles can be tuned depending on reaction conditions, such as pH, temperature, atmosphere, use of surfactants, and ionic strength of the medium or relative ratio of the reagents [83].

With the development of nanoscience and nanotechnology, many of the new nanosorbents are developed for the current water treatment

problems and removal of toxic metal very effectively due to large surface to volume ratio and the span life of these nanoparticles are very high. It can enhance huge planar surfaces of nanosorbents which enable and increase interface reactions with pollutants in environment. Various types of nano-sorbents such as metal oxides, clays, carbonaceous nanomaterials, zero-valent metals have been studied for their usefulness in the water treatments [50, 84].

1.9: Metal Oxide Nanoparticles

1.9.1: Iron oxide nanoparticles (Fe_3O_4, Fe_2O_3)

Iron nanomaterials have distinguished themselves by their unique properties, such as larger surface area-volume ratio with another special property of this kind magnetic materials are realized and utilized in the context of environmental remediation [55].

Iron oxides nanoparticles take many forms in nature such as magnetite Fe_3O_4, hematite α-Fe_2O_3 and maghemite γ-Fe_2O_3, and also different ferrite compounds are known as materials used in different biological and industrial applications [49,55]. The iron oxide nanoparticles have been utilized in various promising applications, such as catalysis, electronic devices, information storage, sensors, drug-delivery technology, biomedicine, magnetic recording materials, and environmental Remediation, biotechnology, and magnetic separation [56, 84]. It is used in many biological and biomedical applications such as targeted drug delivery, magnetic fluid hyperthermia, magnetic resonance imaging, and tissue engineering. For biological and biomedical applications, magnetic iron oxide nanoparticles are the primary choice because of their biocompatibility and chemical stability [85]. Magnetic nanoparticles are considered potential adsorbents for aqueous heavy metals due to their high

surface area and the unique advantage of easy separation under external magnetic fields [86].

Recently, due to the development in nano technology, the exploitation of iron oxide nanomaterials for heavy metal ion removal has attracted much attention because of their demonstrated excellent adsorption capacities and environmentally kindly nature. It has been proposed as inexpensive but efficient adsorbents become a raw material for treating the waste waters and soils, accelerating the coagulation of sewage, removing radionuclides, adsorbing organic dyes and cleaning up the contaminated soils [22,49,50,87].

The synthesis of iron oxide nanoparticles has seen a vast development, and many synthesis methods have been explored such as organic solvent heating method, reverse micelle and micro-emulsion technology, sol-gel synthesis, flow injection, polyol method, electrospray synthesis, the sonochemical method, hydrothermal synthesis or thermal decomposition thermolysis of precursors and co-precipitation method. As such, among the available methods for the synthesis of iron oxide nanoparticles, co-precipitation is the most commonly and the most effective technique which is used for preparing aqueous dispersions of iron oxide nanoparticles because the synthesis is conducted in water due to its simplicity and the possibility of obtaining large quantities of nanoparticles in a single batch . Particles with sizes ranging from 5 to100 nm are obtained [83,85,88]. However, control over particle size, morphology and composition is limited as particle growth is kinetically controlled. Additionally, factors such as the nature of the precursor salts used (chlorides, perchlorates, sulfates, nitrates, etc.), Fe (II) / Fe (III) ratio, pH and ionic strength of the medium are known to affect particle growth [83].

1.9.2: Copper oxide nanoparticles (CuO)

Copper oxide is one of the important metal oxide which has attracted recent research because of its low cost, abundant availably as well as its particular properties [89]. It is one of semiconductors material and gains considerable attentions due to its excellent optical, electrical, physical, and magnetic properties [89, 90]. CuO crystal structures possess a narrowband gap, giving useful photo catalytic and photovoltaic properties [91].

Copper oxide belongs to monoclinic structure system with the brownish-black appearance which finds their significant role in antibacterial agents to fabrics [89]. Copper oxide nanoparticles, have attracted particular attention because it is the simplest member of the family of copper compounds and shows a range of useful physical properties such as high temperature superconductivity, electron correlation effects, and spin dynamics [91].

Copper oxide nanoparticles has a monoclinic structure and semiconductor behavior with an indirect band gap of 1.21 – 1.51 eV. It has the advantage of a lower surface potential barrier than that of metals, which affects electron field emission properties, and is considered as a potential field emitter, an efficient catalytic agent, as well as a good gas sensing material [92]. It is extensively used in the many of fields like catalysis, heat transfer fluids, superconductors, batteries, ceramics as a kind of important inorganic materials etc. [89,90,91].

Copper oxide has gained the most interest because of its wide applications, such as in solar energy conversion, field emission, magnetic storage media, lithium ion batteries, gas sensor, drug delivery, magnetic

resonance imaging, and field emission device. Its treatment is known to induce a disruption of the blood–brain barrier in vivo in mice and rats. Under in vitro conditions, Copper oxide nanoparticles are also found to induce toxic effects in different types of neuronal cells[89]. .

Recently, application of nanoparticles for the removal of pollutants has come up as an interesting area of research. The unique nanosorbents properties provide unprecedented opportunities for the removal of metals in highly efficient and cost-effective approaches, and various nanoparticles and a synthetic polymer with a branching which are for this purpose. Nanoparticles exhibit good adsorption efficiency especially due to higher surface area and greater active sites for interaction with metallic species. Furthermore, adsorbents with specific functional groups have been developed to improve the adsorption capacity [93].

Copper oxide nanoparticles have been prepared with different sizes and shapes via several methods such as sonochemical, alcohothermal synthesis, vapor deposition , electrochemical methods, combustion, colloid thermal synthesis process, and microwave irradiation, thermal oxidation, pulsed wire explosion methods, radiolysis methods, plasma methods, quick precipitation [89,90,94]. There are some methods for the preparation of copper oxide nanoparticles which have been reported recently such as the sol-gel technique, one-step solid state reaction method at room temperature, thermal decomposition of precursors and co-implantation of metal and oxygen ions [95]. Most of these methods are complicated and have drawbacks like use of hazardous organic solvents, expensive reagent, toxic by product, drastic reaction condition, difficult to isolate nanoparticles, longer time etc. [94].

Among these processes, precipitation method is a facile way which attracts considerable interest in industries because of low energy and

temperature, inexpensive and cost-effective approach for large scale production and good yield. However, these CuO novel properties can be improved by synthesis in CuO nanostructures which shows excellent performance comparing to bulk counterpart. Different nanostructures of CuO are synthesized in form of nanowire, nanorod, nanoneedle, nano-flower and nanoparticle [90].

1.10: Literature Survey

1.10.1: Literature survey (adsorption and heavy metal ions removal)

(Elshazly and Konsowa , 2003), discussed Ni ions removal from waste water contaminated as $NiCl_2$ using a cation-exchange resin reactor with stirring store. The effect of each temperature, concentration of Ni ion, and stirring degree on the mass transfer coefficient of the diffusion-controlled reaction between Ni ions and the resin. It is example of the factors that was studied. The results showed that using a strong cation-exchange resin for remove of Ni ions is an encouraging technicality for waste water remediation due to get a removing of Ni ion rates up to 88.5% **[96]**.

(Onundi, **et. al 2010),** in their research presented the Cu, Ni and Pb ions adsorption from synthetic semiconductor industrial effluents using palm shell activated carbon . The results indicated that pH of 5 was very appropriate , when the largest adsorbent capacity was at a dosage of 1 g/L, giving an adsorption capacity of 1.337 mg/g for Pb, 1.581 mg/g for Cu and 0.130 mg/g for Ni. Percentage removal of metal was near from equilibrium within 30 min for lead, 75 min for Cu and Ni, with Pb showing 100 %, copper 97 % and nickel 55 % removal, having a trend of $Pb^{2+} > Cu^{2+} > Ni^{2+}$. The correlation coefficient of Langmuir isotherm model had a great value of 0.977, 0.817 and 0.978 for Cu, Ni and Pb respectively **[97]**.

(Jarullah, et. al, 2012), discuss the adsorption of nickel ion by using activated charcoal prepared from dry leaves of bitter orange tree (*Citrus aurantium*).The effects of its concentration, adsorbent dosage, particle size, pH and temperature on uptake of nickel ion have been studied. The adsorption of nickel ion is higher at lower concentration and progression decreases with increasing in the concentration. The pH of 5 was the most suitable. The uptake percentage of nickel ion increases with increase in the adsorbent dosage. The effect of the particle size reveals that the percentage removal of nickel ion decreases with increase in particle size of adsorbent. The effect of temperature shows that as temperature increases, the adsorption rate of nickel ion decreases **[98]**.

(Akkaya and Guzel, 2013), investigated the optimization of Cu and Pb uptake by a novel biosorbent , Cucumber peels biosorption efficiency for Cu and Pb ions were studied in batch mode. The best conditions for adsorption of copper and lead ions were found to be pH of 5, biosorbent dose of 0.1 g, contact time of 60 and 85 minutes, and initial concentration of 100 and 150 mg/L, respectively. The best description of the kinetic data were done by pseudo-second order model. The adsorption process is described by the Langmuir isotherm model. Highest monolayer adsorption capacities were 88.50 and 147.06 mg/g for copper and lead ions, respectively. Thermodynamic factors suggest that the adsorption process is endothermic and spontaneous **[17]**.

(Judith, et.al, 2014), in their research presented the kinetic, equilibrium and mechanistic studies of Ni removal using activated *Pistia stratiotes* leaves, which were prepared by acid remediation was examined for its activity in adsorption of Ni ion. The studied factors of the process involve contact time, temperature, adsorbent dose, initial concentration of Ni ion and pH. Adsorption followed 2^{nd} order. Freundlich and Langmuir isotherm models were applied to the equilibrium data. The adsorption capacity

obtained from the Langmuir isotherm plot at an initial pH of 6.5 and at 30, 40, 50, and 60℃. The effect of pH on nickel ion removal important and the removal was increased with temperature increasing **[52**].

(Saravanan, et. al, 2015), studied optimization of process factors for the uptake of Cr (VI) and Ni (II) from aqueous solutions using mixed biosorbents (custard apple seeds and Aspergillus niger) by using response surface methodology . Batch adsorption methods was implemented and it was affected by the different factors such as biomass loading, initial concentration of metal, temperature, and pH, the result showed the best conditions for the adsorption of Cr(VI) to be: pH of 3, Cr(VI) initial concentration was 100 mg/L, biosorbent loading being 10 g/L, and temperature of 36 °C. At these optimized conditions, the highest uptake of Cr (VI) was found to be of 95.7%. The best condition for the uptake of Ni(II) were found to be: pH of 5.6, Ni (II) initial concentration was100 mg/L, adsorbent loading was 10 g/L, and temperature of 30 °C. At these good conditions, the largest uptake of Ni(II) was found to be of 96.41%. Mixed adsorbents reveal best adsorption characteristic towards the removal of Cr (VI) and Ni (II) ions from the aqueous solutions **[29]**.

(Ali, et. al, 2016), studied the Cu (II) uptake from aqueous solutions by the peanut hull as an adsorbent without any physical or chemical remediation . Different factors effect such as particle size, contact time, initial concentration of Cu (II), initial pH, dosage of adsorbent, and temperature were examined for a batch adsorption method. The results indicated that the adsorption process followed the pseudo-second-order and intra-particle diffusion kinetic models, pointing that the adsorption mechanism is chemical and physical adsorption process. Langmuir and Freundlich adsorption isotherms have been tested. The thermodynamic factors were investigated, and it was confirmed that, removal of copper (II) using peanut hulls is nonspontaneous and endothermic. This study

convinced that the naturally peanut hulls proved to be an attractive , effective, economic, alternative, and environmentally friendly adsorbent for copper (II) adsorption from aqueous solution **[99]**.

(Al-Homaidan, et. al, **2016)**, investigated the adsorption of lead (II) from aqueous solutions by the nonliving biomass of the microalga (*cyanobacterium*) Spirulina platensis. The biomass was washed, exsiccated and utilized for the investigation. Lead (II) initial concentration of, pH, temperature, adsorbent dose, and effect of contact time on the adsorption of lead by the dry adsorbent were examined. The tests were executed in 250 ml flasks containing 100 ml of solutions using an orbital incubator at 150 rpm. The result showed high rates of lead (II) uptake (more than 91%). The best conditions for a maximum removal by Spirulina platensis were found to be adsorbent dose (2 g), pH of 3, incubation at 26 ° C, initial concentration of lead was 100 mg/L, and 60 min contact time. The empirical data fitted well with Freundlich isotherm model with correlation coefficient values greater than 0.97 **[40]**.

(Liu, et. al, 2015), studied the Pb, Cd, Zn and Cu uptake from local solid waste sludge incinerator fly ash by thermal and chlorination remediation. Results showed that without the addendum of chlorinating agents, temperature was a substantial factor and had considerable effect on heavy metal uptake, whilst the residence time had a low effect. Between 900 and 1000 °C for 60 to 300 min, heavy metals reacted with chloride-inherent in the fly ash, and about 80% - 89% of lead, 48% - 56% of cadmium, 27% - 36% of zinc, and 6% - 24% of copper were separated. After adding chlorinating agents, the vaporization percentage of the heavy metals amended dramatically, where the vaporization percentage of copper and zinc were greater than that of lead and cadmium. As the quantity of increment chlorinating agents boosted, the uptake effect of heavy metals increased the effect of the kind of chlorinating agent on the chlorination of

heavy metals different frequently, while sodium chloride had the weakest influence on the uptake percentage of copper, cadmium, and zinc. In terms of resource recapture and refinement, magnesium chloride and calcium chloride were the good choices because of their efficient removal of Zn **[100]**.

(Egirani and Wessey, 2015), in their research showed the effect of clay and goethite mineral system on lead removal from aqueous solution, and pH, ionic strength, and particle concentration and residence time related to simulated contaminated waters inclusive effluent discharge. Adsorption isotherms showed that adsorption capacities of the different clay minerals, goethite and their mixtures were dependent on the particle size. Mixed mineral systems of kaolinite / montmorillonite and kaolinite / goethite presented various sorption attitudes from the odd mineral components, constriction lead uptake over the range of pH inspected. Increased ionic strength and solid concentration showed a complex response leading to lower lead sorption. Enhanced lead sorption on some of the mixed mineral systems as ageing increased may be linked to excessed hydroxylation of the mineral surface performing in the fashioning of new reactive sites **[18]**.

1.10.2: Literature survey (nanoparticles)

(Dozier, et. al, 2010), in their research showed the preparation of iron oxide nanoparticles for biomedical and biological applications. It is needed to output nanoparticles that are water soluble and biocompatible. So they report the preparation of iron oxide nanoparticles plated with biological molecules (for example, gluconic acid, lactobionic acid, or polyacrylic acid) by a co-precipitation techniqe. These nanoparticles have small magnitude distribution and are much soluble in water. Due to the biological covering, they will have large potential in abundant biomedical applications such as tissue engineering **[85]**.

(Min, et. al, 2011), investigated the removing of cadmium (II) by composite adsorbent nano iron oxide (Fe_3O_4) / bacterial cellulose, it was prepared through blending method. The process of adsorbing cadmium (II) involves its isotherm and kinetics studies. Results show that the adsorption efficiency is amended because of huge surface area and surface coordination of nano iron oxide (Fe_3O_4) particles. Its adsorption capacity is 27.97 mg/g and the maximum of cadmium (II) uptake is 74%. The adsorption kinetics obeyed pseudo-second equation model and the adsorption equilibrium by Langmuir type. Cd^{2+} can be desorbed effectively by Ethylene diamante tetra acetic acid and hydrochloric acid from the composite adsorbent, which can use it once again **[56]**.

(Cheng, et. al, 2012), studied the enforcement of maghemite (γ-Fe_2O_3) nanoparticles for the eclectic uptake of toxic heavy metals from electroplating influence. The maghemite nanoparticles of 60 nm were prepared by using a co-precipitation technique. Batch tests were implemented for the removal of lead ions from aqueous solutions by maghemite nanoparticles. The effects of contact time, initial concentration of lead ions, pH, and brininess on the amount of lead removed were studied. Result showed a highly dependence on pH and which made the nanoparticles selectively adsorb lead from wastewater. The adsorption of lead ion arrived equilibrium speedily within 15 minutes and the data of adsorption were good agreed with the Langmuir isotherm **[55].**

(Andujar, et. al, 2012), studied illustrating the morphological and structural development of iron oxide nanoparticles created by sodium carbonate in aqueous medium.. They found that by agent for the preparation of uncovered iron oxide nanoparticles, and the reaction yields slowly enough to a detailed research of each of the reaction path and products. Many factors were studied such as temperature and reaction time on particle size, pH, crystalline phase, morphology, and its magnetic

properties. The product nanoparticles indicated an increase in average particle size. The optimization of the particle factor leads to super paramagnetic nanoparticles with a high saturation magnetization of 82 A m^2 kg^{-1} at 300 K when prepared at pH of 9 **[83].**

(Predescu and Nicolae, 2012), studied the adsorption of zinc, Copper and cadmium from influence by means of maghmite nanoparticles ,Nano-sized crystals of maghemite iron oxide (γ-Fe_2O_3) were synthesized, with a size of 10 nm. Subsequently, a nano-composite from γ-Fe_2O_3 with cationic exchange resin was prepared. The products have been subjected to characterization with several spectroscopic techniques as well as (TEM) measurements or (XRD) analysis. These investigations emphasize the formation of maghemite nanoparticles on resin surface. The nano-composite indicated remarkable adsorption efficiency in uptake of some toxic metal ions such as zinc, copper, and chromium **[49]**.

(Meng and Shibao, 2012), discussed the uptake of cadmium, lead and copper from water using humic Acid (HA) and thiol functionalized Fe_2O_3 nanoparticles , the humic acid (HA) and 3-mercapto propyl tri ethoxy silane were successfully coated onto Fe_2O_3 (α and γ) nanoparticles surface. Result showed that the sorption of cadmium, lead and copper ions via the nanoparticles can be agreed well by using Langmuir isotherm; and all the adsorbents appeared firmly adsorption ability to cadmium, lead and copper ions in solution. Maximum adsorption and affinity of adsorption on the nanoparticles for lead were usually higher than copper and cadmium, the maximum adsorption for the lead, cadmium and copper followed the order lead > copper > cadmium. Among the nano adsorbents, the Fe_2O_3 (α and γ) nanoparticles covered with HA showed largest adsorption ability to ions of metal than the exposed and thiolated Fe_2O_3 nanoparticles, the adsorption maxima of α-Fe_2O_3 / HA for lead arrived 151.5 mg/g, which was higher

than the values of 116.3 and 84.0 mg/g noticed for α-Fe_2O_3 and α-Fe_2O_3/MPTES particles. However, no increasing in the maximum adsorption was noticed for the thiolated Fe_2O_3 nanoparticles (Fe_2O_3/MPTES) for the metal ions compared with the uncovered Fe_2O_3 nanoparticles in this work. The whole capability of Fe_2O_3/HA to adsorb cadmium, lead, copper refers to its potential using another favorable method to treat the metals which polluted the water **[50].**

(Palanisamy, et. al, 2013), discussed the interest of magnetic iron oxide nanoparticles stabilized by carrier oils in uptake of Cu, Ni and Cr, from its aqueous solution by carrier oils intermediate iron oxide nanoparticles filtration , super paramagnetic iron oxide nanoparticles were synthesized by co-precipitation technique by using salts with a various Fe^{3+}/Fe^{2+}. Carrier oils such as olive oil, and flaxseed oil were used as the coating material **[84]**.

(Bhargav and Prabha, 2013), discussed the uptake of heavy metals like As (V) and Cu (II) from the contaminants in wastewater supply by the process of adsorption to make it safer for domestic purpose. For this magnetite (Fe_3O_4) nanoparticles are used for uptake of pollutants in municipal water by applying external magnetic fields. It is synthesized by co-precipitation technique obtained by an aging stoichiometric mixture of ferrous and ferric salts in aqueous medium. Precipitation of Fe_3O_4 is anticipated at a pH between 8 and 14. Magnetite (Fe_3O_4) nanoparticles with size smaller than 30 nm have a great surface area and remain non-magnetized under external magnetic field. The shape and size of the nanoparticles can be controlled by ionic strength, adjusting pH, temperature and the nature of the salts. At optimized pH the obtained Fe_3O_4 nanoparticles are coated with coating agents which develops surface functionalized groups. The sorption of metals like arsenic (V) and copper

(II) take place on these aggregates which are removed with help of external magnetic field leaving the supernatant free from Cu and As **[88]**.

(Phiwdang, K., et. al , 2013), discussed the synthesis of CuO nanoparticles by precipitation technique using various precursors as copper nitrate and copper chloride with post-heating comparing between as prepared and after calcinations. Relevant properties of as prepared nanoparticles were investigated by (XRD), (SEM) and (FTIR) spectroscopy. The results suggest that the formation of CuO nanostructures with various shape, size and morphology can be achieved using different precursors via this process. The improvement in their crystallinity and purification can be further attained by post calcinations process **[90]**.

(Farghali, et. al, 2013), in their research showed the removal of Pb ions from aqueous solutions by using copper oxide nanostructures , Various morphologies of CuO nanostructures (oval, cluster, leaves, small rod, porus nanosheets) have been synthesized by novel simple method using microwave radiation. The produced were characterized by XRD analysis technique, (TEM), surface area analyzer (BET), and energy dispersive spectroscopy (EDS). The ability of CuO nanostructures as adsorbent was leading for adsorptive uptake of lead ions from the aqueous solutions. Different physicochemical factors such as initial concentration of ion, pH, and the equilibrium contact time were investigated. The best pH value for removal of Pb (II) from aqueous solutions was 6.5 and 4 hours was optimum contact time. The adsorption isotherms were obtained using concentrations of the lead ions ranging from 100 to 300 mg/L. It was seen that the process of adsorption was described by pseudo-second-order reaction kinetics, as well as Langmuir and Freundlich adsorption isotherms. The largest capacity of oval, cluster, leaves, small rod and pours nanosheets CuO nanostructures for Pb^2 are 125, 116, 117, 120 and 115 mg/g. Finally it

is revealed that CuO nano structures was an active adsorbent for uptake of lead ions from aqueous solutions **[93].**

(Srivastava, et. al, 2013), studied the synthesis and characterization of copper oxide nanoparticles. It was synthesized by the chemical route and calcinations at temperature from 300 ˚C to 400 ˚C. For the comparison (TEM) and (XRD) measurements, showed a good agreement between data produced by spectroscopy and the microscopic measurements **[92].**

(Predescu, et. al, 2014), investigated the synthesis, characterization and adsorption efficiency of iron oxide nanoparticles covered with cationic resin for wastewater remediation. The magnetic nanoparticles were obtained by co-precipitation method, and then covered with cationic resin. The products were then characterized by (TEM) and (XRD). The removal efficiency was tested on a column with magnetic separation. The results demonstrated the fast adsorption of heavy metal ions on magnetic nanoparticles and the possibility to remove with high efficiency the toxic materials from wastewaters **[51].**

(Nithya, et. al, 2014), studied the preparation and characterization of copper oxide nanoparticles by modified sol-gel method using sodium dodecyl sulphate as a surfactant. Calcination temperature effect on particle size, band-gap, crystallinity and morphology of the nanoparticles were studied with the help of particle size analysis, UV-Spectroscopy, (XRD) and (SEM) studies. Also the prepared nanoparticles were tested for their activity towards gas sensing **[89].**

(Ahamed, et. al, 2014), studied the structural and antimicrobial properties of CuO nanoparticles synthesized by a simple precipitation method. Copper (II) acetate was used as a precursor and sodium hydroxide as a reducing agent. X-ray diffraction pattern showed the crystalline nature of copper

oxide nanoparticles. Field emission scanning electron microscope (FESEM) and field emission transmission electron microscope (FETEM) demonstrated the morphology of CuO nanoparticles. The average diameter of CuO nanoparticles calculated by TEM and XRD was around 23 nm. Energy dispersive X-ray spectroscopy (EDS) spectrum and XRD pattern suggested that prepared CuO nanoparticles were highly pure. CuO nanoparticles showed excellent antimicrobial activity against various bacterial strains. Moreover, *E. coli* and *E. faecalis* exhibited the highest sensitivity to CuO nanoparticles while *K. pneumonia* was the least one **[91]**.

(Devi and Singh, 2014), discussed the preparation of copper oxide nanoparticles by using *Centella asiatica* (L.) leaves extracts at room temperature. This method is completely a green method, free from toxic and harmful solvent. Copper oxide particles such prepared are in nano scale and there morphology and size are characterized using SEM, UV–Visible spectroscopy, IR spectroscopy and EDX. Copper oxide nanoparticles synthesized by this method can be used for the photo catalytic degradation of methyl orange. These nanoparticles can reduce methyl orange in aqueous medium in the absent of reducing agents. It is more economic as compared to other methods. This catalytic effect of copper oxide nanoparticles can be contributed to its small size **[94]**.

1.11: The Aims of The Study

1- Preparation of (Fe_3O_4) nanoparticles, (Fe_2O_3) nanoparticles , and (CuO) nanoparticles by a simple precipitation method, and Characterization them by using X-ray diffraction (XRD) , scanning electron microscopic (SEM), and atomic force (AFM).

2- Measuring the efficiency of these oxides to remove nickel and lead ions from industrial wastewater after analyzing by using aqueous solutions containing these ions.

3- Determining the best adsorption of nickel and lead ions by using the three oxide nanoparticles (adsorbent) with a batch method at different contact time and initial concentration of aqueous solutions (adsorbate) with other constant condition such as pH value ,adsorbent dosage ,and temperature being the same .

4- Determining a suitable adsorption isotherm for each oxide to fit the adsorption and calculating the orders of the adsorption kinetics.

Chapter Two

Materials & Methods

2.1: Instruments and Apparatus

2.1.1: Instruments and Apparatus used in preparation

The instruments and apparatus used are shown in **Table (2.1)** together with their model and location:

Table (2.1): Instruments and apparatus used in preparation

No.	Instrument and Apparatus Name	Model	Location
1	**Electric Balance**	KERN $_{ACJ/ACS}$, ACS 120 – 4, WB 12 AE 0308 , max 120 g , d = 0.1mg	The laboratories of chemistry Department ,College of Science, Diyala University, Iraq .
2	**Labortary Thermal Oven**	BINDER ,Hotline International (20 –360 ^{o}C)	
3	**pH Meter**	pH/Ion Benchtop MetersWTW inoLab pH 7110 Benchtop Meters	
4	**Hot Plate Magnetic Stirrer**	MS – H280 – pro ISO LAB laboratory GmbH	
5	**Water Bath**	YCW - O1	
6	**Microwave Oven**	BINDER Service - Hotline (0 –250 ^{o}C)	
7	**Water Bath with shaker**	BS – 11 230 VAC – 50 Hz , Korea	
8	**Centrifuge**	HERMLE LABORTI CHINK Type Z200A, Germany , 6000 rpm	
9	**Distillation device**	LUZ DE AVISO AGUA INSUFICICENTE	
10	**Electrical Furnace**	Type – KR 170 E ,Max temperature 1150˚C ,220 V, 13.8 A , 50 /60 Hz , Japan origin	The laboratories of Physics Department ,College of Science ,Diyala University , Iraq .

2.1.2 : Instruments used in characterization

The instruments used are shown in **Table (2.2)** together with their model and location:

Table (2.2): Instruments used in characterization

No.	Instrument Name	Model	Location
1	**X-ray Diffraction Spectroscopy (XRD)**	XRD-6000 , Cukα(λ=1.5406A°),220/50 HZ , SHIMADZU , Japan	The central service laboratory , College of Education Ibn Al-Haitham , Baghdad University , Iraq
2	**Scanning Electron Microscope (SEM)**	Type AIS2300C , Angstrom Advanced.	
3	**Atomic Force Microscope (AFM)**	Scanning Probe Microscope , AA 3000 SPM 220 V- Angstrom Advanced Inc, AFM contact mode, USA .	College of Science, Baghdad University, Iraq.
4	**Atomic Absorption Spectroscopy (AAS)**	AURORA , TRACE AI 1200	The laboratories of chemistry Department ,College of Science ,Diyala University , Iraq.

2.2: Materials

2.2.1: Materials used in metal oxide nanoparticles preparation:

The materials used in metal oxide nanoparticles preparation were classified as :

2.2.1.1 : Chemicals used in iron oxide nanoparticles, Fe_3O_4 preparation are shown in **Table (2.3)**

Table (2.3): Chemicals used in iron oxide nanoparticles, Fe_3O_4 preparation

No.	Chemicals	Formula	Phase	purity	Source
1	Iron (II) sulphate	$FeSO_4.5H_2O$	Solid	99.5 %	BDH
2	Iron (III) chloride	$FeCl_3$	Solid	99%	Riedel-de Haen
3	Sodium hydroxide	NaOH	Solid	99 %	Alpha chemical

2.2.1.2 : Chemicals used in iron oxide nanoparticles Fe_2O_3 preparation are shown in **Table (2.4)**

Table (2.4): Chemicals Used in iron oxide nanoparticles, Fe_2O_3 Preparation

No.	Chemicals	Formula	Phase	purity	Source
1	Iron (III) chloride	$FeCl_3$	Solid	99%	Riedel-de Haen
2	Urea	CH_4N_2O	Solid	99.5%	Alpha chemical
3	Ethanol	C_2H_5OH	Liquid	99%	GCC

2.2.1.3 : Chemicals used in copper oxide nanoparticles, CuO Preparation are shown in **Table (2.5)**

Table (2.5): Chemicals used in copper oxide nanoparticles, CuO preparation

No.	Chemicals	Formula	Phase	purity	Source
1	Copper(II) acetate	$Cu(CH_3COO)_2.H_2O$	Solid	99%	Bean Town
2	Glacial acetic acid	CH_3COOH	Liquid	99.5%	BDH
3	Sodium hydroxide	NaOH	Solid	99%	Alpha chemical
4	Absolute ethanol	C_2H_5OH	Liquid	99%	GCC

2.2.2 : Materials used in separation of nickel and lead ions:

The materials used in separation of nickel and lead ions were divided into two parts :

2.2.2.1 : Chemicals

The chemical compounds used in aqueous solution preparations are shown in **Table (2.6)**

Table (2.6): Chemicals used in aqueous solution preparation

No.	Chemicals	Formula	Phase	purity	Source
1	Lead (II) Acetate	$Pb(CH_3COO)_2.H_2O$	Solid	99.5%	BDH
2	Nickel (II) Chloride	$NiCl_2.6H_2O$	Solid	99%	Strem chemical
3	Sulfuric acid	H_2SO_4	Liquid	98%	Fluka
4	sodium hydroxide	NaOH	Solid	99%	Alpha chemical

2.2.2.2 : Adsorbents

The following metal oxide nanoparticles were used as adsorbent for both nickel and lead ions removal :

1 - Iron oxide nanoparticles, Fe_3O_4 .

2- Iron oxide nanoparticles, Fe_2O_3.

3 -Copper oxide nanoparticles, CuO.

2.3 : Preparation of Metal Oxides Nanoparticles

2.3.1 : Iron oxide nanoparticle , Fe_3O_4 preparation

Iron oxide nanoparticle , Fe_3O_4 was prepared by precipitation method . In which 100 ml of 0.2 M iron (II) sulphate solution and 100 ml of 0.4 M iron (III) chloride solution shown in **Figure (2.1-a,b)** were mixed together as shown **in Figure (2.1-c)**, then 2 M sodium hydroxide solution was added to the above mixture to obtain *pH* value between (10-11), shown in **Figure (2.1-d),** with a continuous stirring by using of a magnetic stirrer for 1 hour at the room temperature , we noted that a dark precipitate was formed. This is filtered off and washed several times with deionized water as shown in **Figure (2.1-e)**, and finally it was dried at 150˚ C for 3 hours in an oven and grinded to fine powder as shown in **Figure (2.1-f)**. **Figure (2.2)** is flow diagram showing the steps of (Fe_3O_4) nanoparticle preparation by precipitation method [84]. .

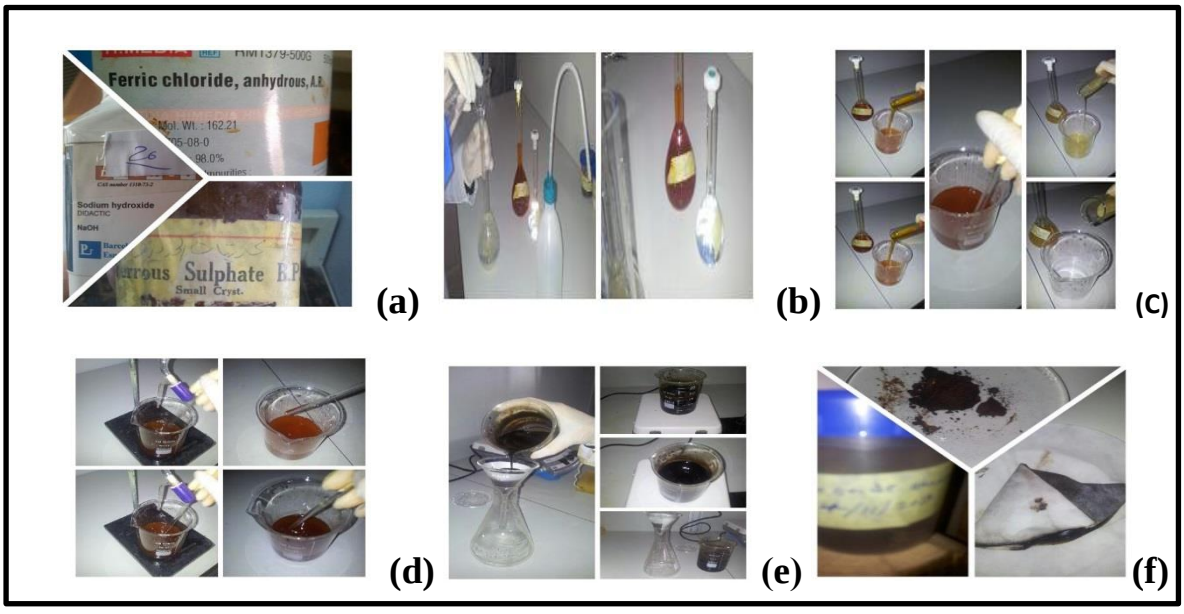

Figure (2.1) : Iron oxide nanoparticle Fe_3O_4 preparation steps :
(a,b) The materials and solutions **(c)** mixing .
(d) Addition of NaOH to adjust the *pH* value between (10 - 11).
(e) Continuous stirring for 1 hour, filtration and washing processes
(f) Iron oxide nanoparticle Fe_3O_4 powder after drying .

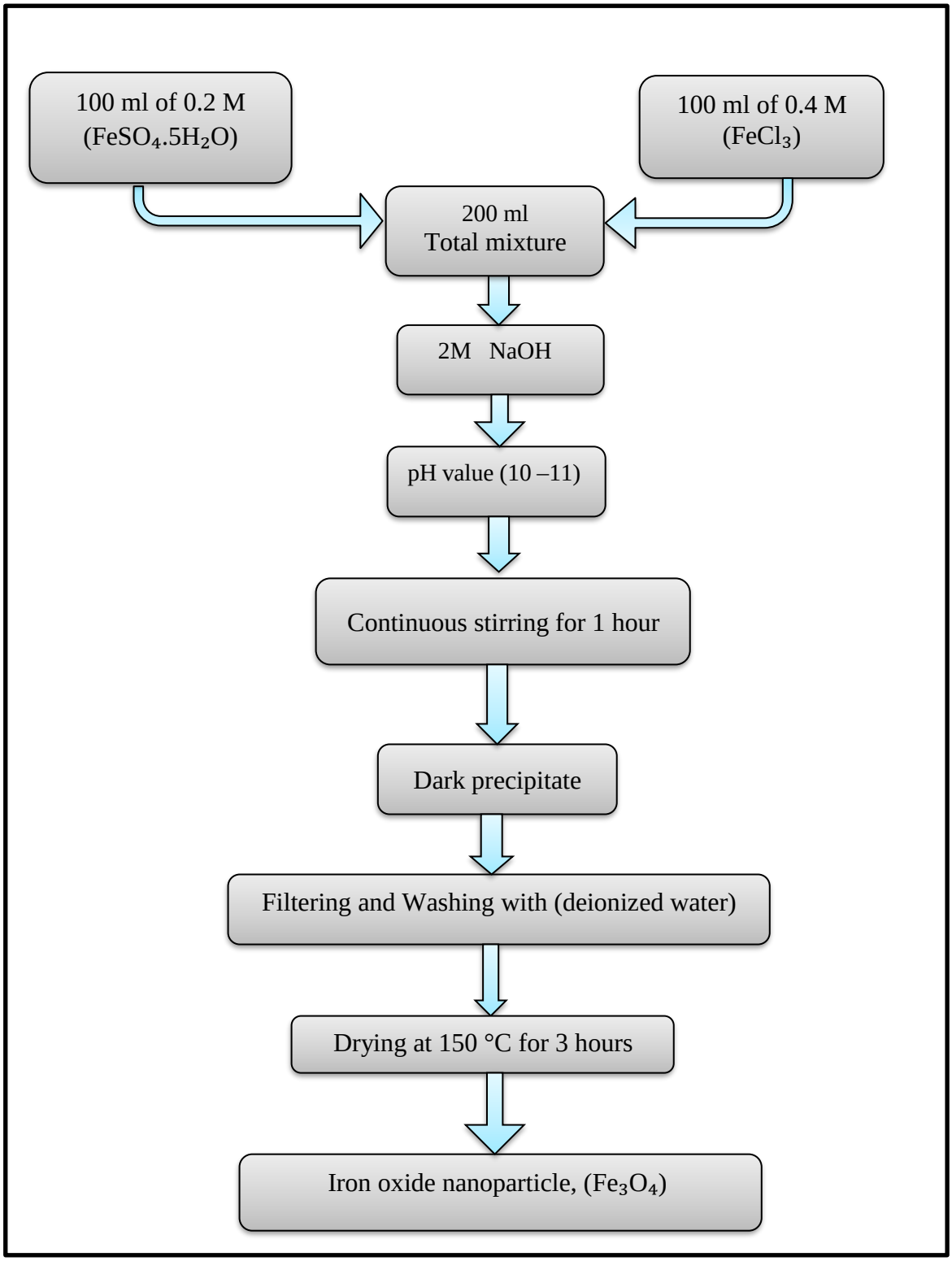

Figure (2.2): Flow diagram show the steps of iron oxide nanoparticle, Fe_3O_4 preparation.

2.3.2 : Iron oxide nanoparticle , Fe_2O_3 preparation

In synthesis of iron oxide nanoparticle, Fe_2O_3 specific molar ratio of iron (III) chloride and urea (1:2) were dissolved in deionized water as shown in **Figure (2.3 - a)**, after that the formed mixture was heated with a continuous stirring by using magnetic stirrer for 45 min at 90 °C under water bath shown in **Figure (2.3 - b)**, and then cooled to room temperature. The produced precipitate was centrifuged and filtered off and washed first by deionized water and then by ethanol as shown in **Figure (2.3-c)**.The precipitate dried at 80 °C for 10 hours and then the produced powder calcined at 650 °C for 2 hours as shown in **Figure (2.3-d)**. **Figure (2.4)** showing the steps of (Fe_2O_3) nanoparticle, preparation by precipitation method [55] . .

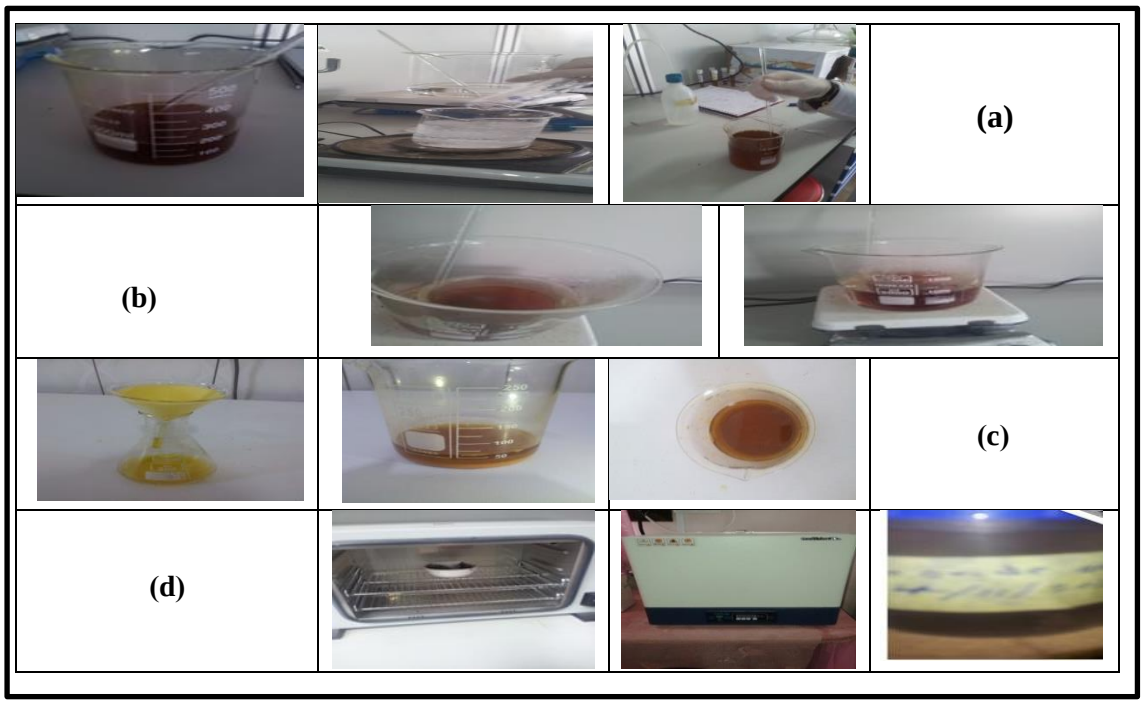

Figure (2.3): Iron oxide nanoparticle Fe_2O_3 preparation steps
(a) The materials and solutions and mixing
(b) Heating continuous stirring for45 min at 90° C in water bath.
(c) Cooled to room temperature and filtration washing processes
(d) Iron oxide nanoparticle Fe_2O_3 powder after drying at 80 C° for 10 hours calcining to 650 C° for 2 hours.

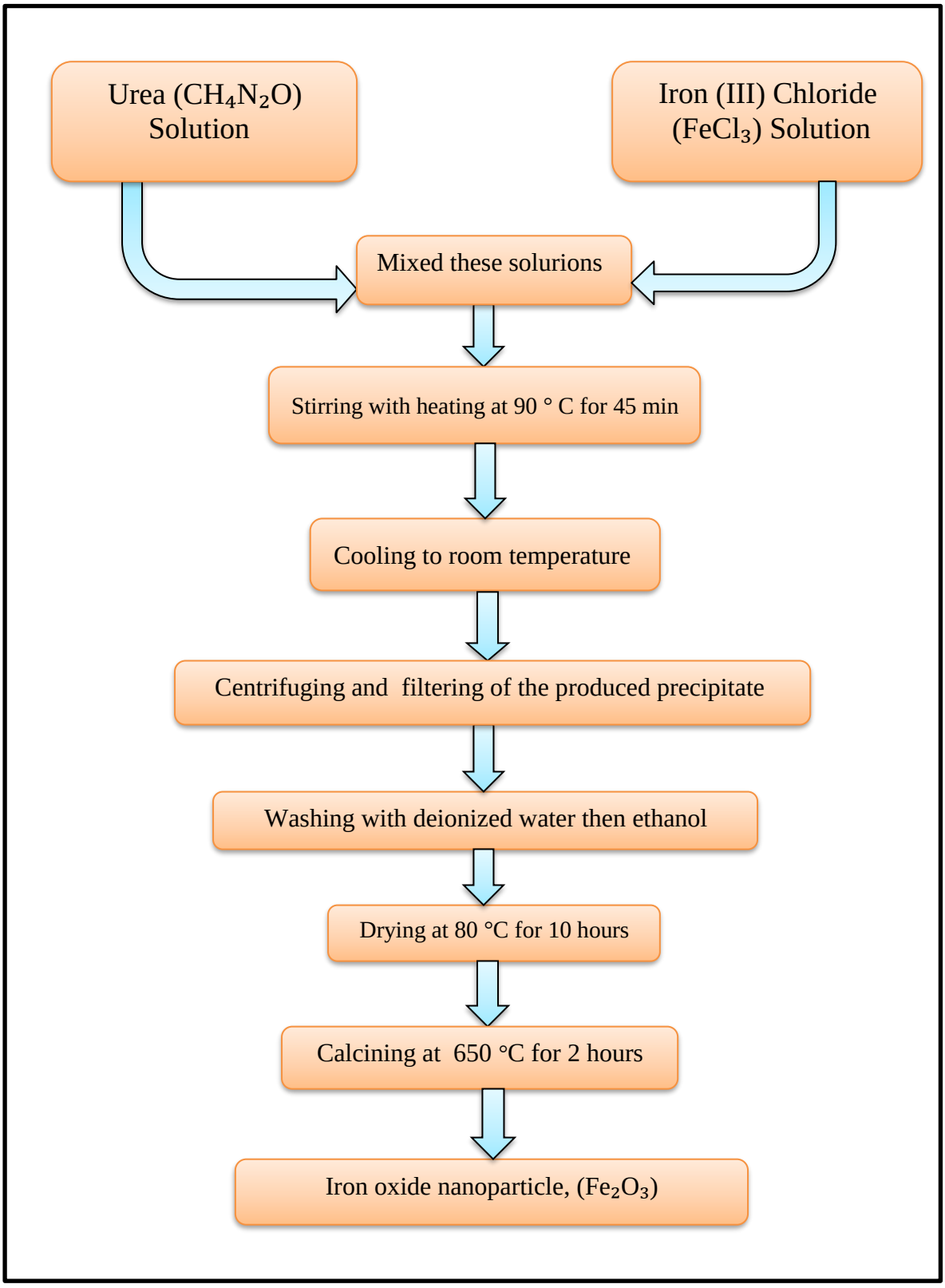

Figure (2.4): Flow diagram show the steps of iron oxide nanoparticle, Fe_2O_3 preparation by precipitation method

2.3.3 : Copper oxide nanoparticle , CuO preparation

Copper oxide nanoparticle ,CuO are synthesized by precipitation method , In which 600 ml of 0.2 M copper (II) acetate and 5 ml glacial acetic acid were mixed in beaker as shown in **Figure (2.5-a)** and the mixture heated to boiling as shown in **Figure (2.5-b)**.Then 30 ml of 6M sodium hydroxide solution was added to the mixture and notice the solution color turned from the blue color to black one directly and the black precipitate start forming as shown in **Figure (2.5- c)**, the reaction performed at boiling temperature with a continuous stirring for 3 hours .

The mixture thus obtained cooled to room temperature and separated by centrifuge and (CuO) nanoparticle, that obtained is filtered off and washed with deionized water and absolute ethanol for several times as shown in **Figure (2.5- d)** , and the precipitate was dried at 60 °C for 8 hours to produce (CuO) nanoparticle, as shown in **Figure (2.5 -e)**. **Figure (2.6)** show the steps of (CuO) nanoparticle, preparation by precipitation method.[89,95]

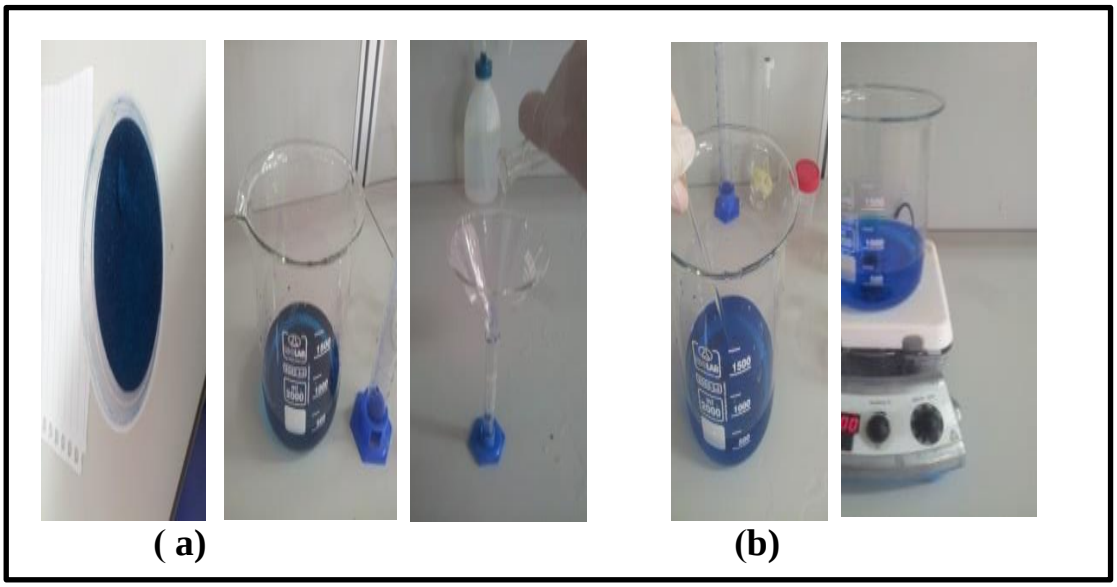

(a) **(b)**

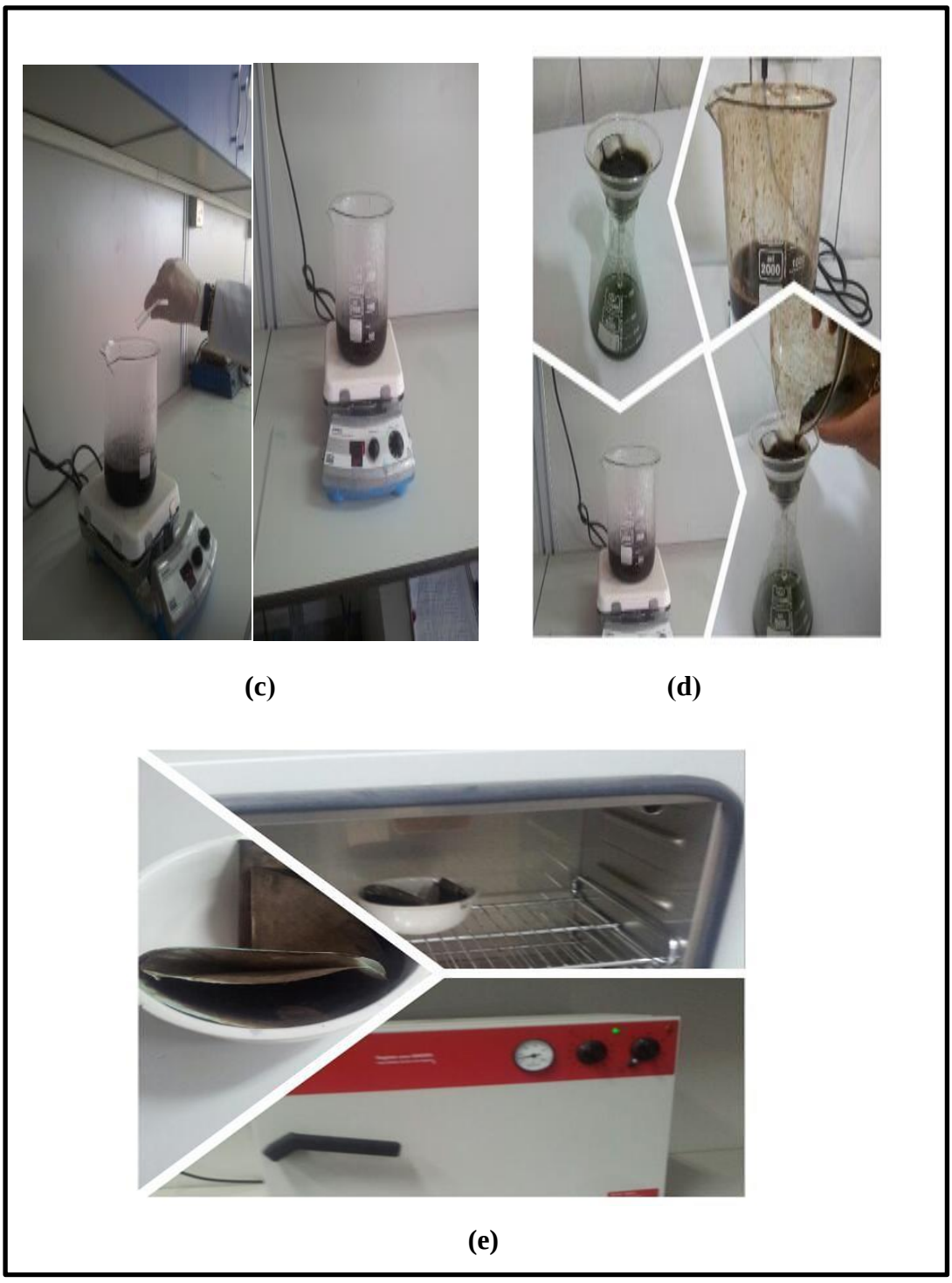

(c) **(d)**

(e)

Figure (2.5) : Copper oxide nanoparticle, CuO preparation steps :

(a) The materials and solutions

(b) Mixing and continuous stirring

. **(c)** Addition of NaOH and solution color turned to the black color directly

(d) Continuous stirring for 3 hour and filtration and washing processes .

(e) Copper oxide nanoparticle, CuO powder after drying at 60 °C for 8 hours.

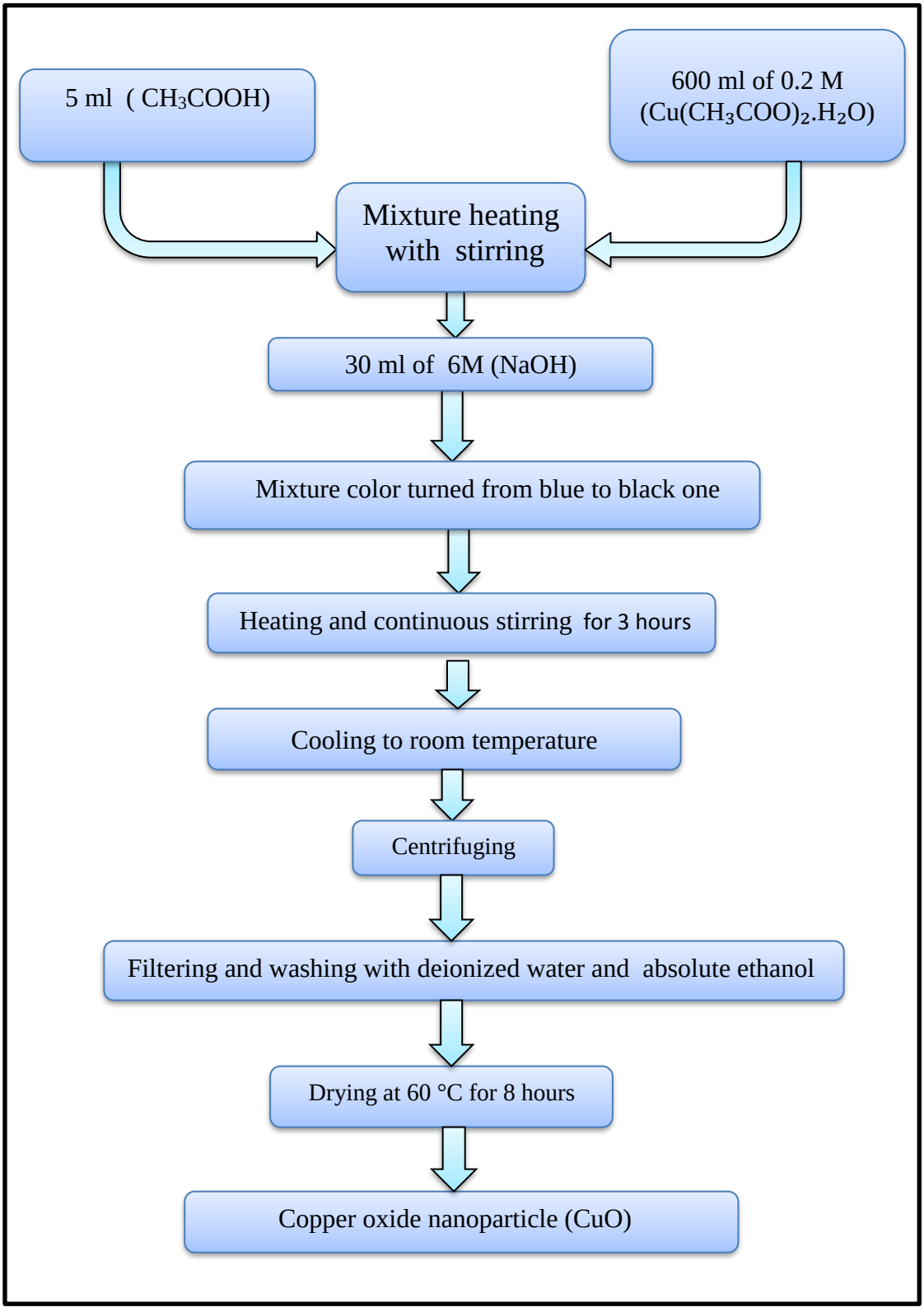

Figure (2.6): Flow diagram show the steps of copper oxide nanoparticle CuO preparation by precipitation method.

2.4: Characterization of Metal Oxide Nanoparticles

The devices and instruments used for characterization of the prepared nano oxides are:

.

2.4.1: X-ray diffraction

The crystal structure and characterization of the prepared metal oxide nanoparticles are investigated by X-ray diffraction which is one of the most important characterization tools used in material science and solid state chemistry. The one used is X-ray diffraction (XRD) with Cu-k_α radiation, and wave length λ= 1.54060 A˚, and Braggs angle (2θ =20˚– 60˚) and shown in **Figure (2.7).**

Figure (2.7): X-ray diffraction instrument used

XRD is an easy tool to determine the size and the shape of the unit cell for any compound .The scattered radiation requires several conditions such as the X-ray should be specularly reflected in any one atom plane and the rays that reflected of successive atom planes should constructively interfere. These two conditions lead to Bragg equation:

$$n\lambda = 2\,d \sin\theta \qquad \ldots\ldots\ldots\ldots\ldots \qquad (2.1)$$

Where, **n** , is an integer and is the order of the diffraction , **λ** , is the wave length of Cu-Kα radiation and θ is the angle of incidence at sample surface , and d : is the distance between atomic planes . **Figure (2.8)** show a description of exposure rays interacting with the various crystal planes.

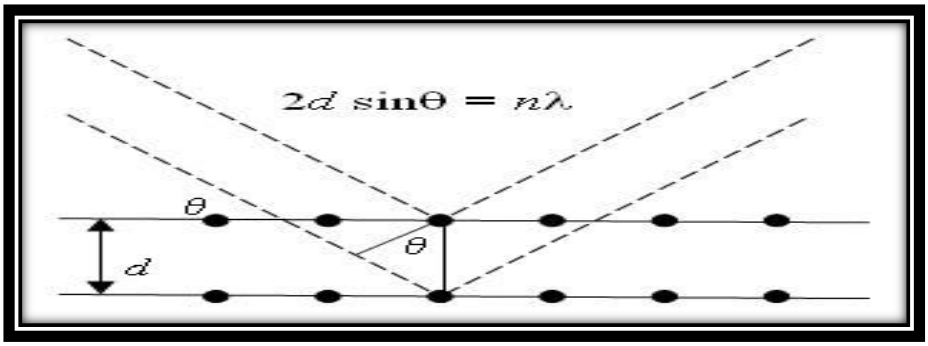

Figure (2.8) : Representation of reflected X-rays in crystal [102,103].

Since the details of the diffraction pattern are due to the specific nature of the crystal , diffraction can be used to determine the crystal structure .

From X- ray diffraction the average particle size of oxides sample can be determined from high intensity and using Debye–Scherrer equation as follow [101] :

$$D = 0.9\,\lambda / \beta \cos\theta \qquad \ldots\ldots\ldots\ldots \qquad (2.2)$$

Where **D** is the particle size, **λ** is the wave length of radiation, **θ** is the bragg's angle and **β** is the full width at half maximum (FWHM) [102,103].

. .

2.4.2: Scanning electron microscope

Scanning electron microscopy - SEM - is a powerful technique in the examination of materials. It is used widely in metallurgy, geology, biology and medicine .One can obtain high magnification images, with a good depth of field, and can also analyze individual crystals or other features. A high-resolution SEM image can show detail down to 25 Angstroms, or better.

An electron microscope uses an electron beam to produce the image of the object and magnification is obtained by electromagnetic fields; unlike light or optical microscopes, in which light waves are used to produce the image and magnification is obtained by a system of optical lenses. In a scanning electron microscope, the specimen is exposed to a narrow electron beam from an electron gun, which rapidly moves over or scans the surface of the specimen which causes the release of shower secondary electrons and other types of radiations from the specimen surface.

The intensity of these secondary electrons depends on the shape and the chemical composition of the irradiated object. These electrons are collected by a detector, which generates electronic signals. These signals are scanned in the manner of a television system to produce an image. The image is recorded by capturing it from the cathode ray tube (CRT). Modern variants have facility to record the photograph by digital camera.

The scanning electron microscope (SEM) uses a focused beam of high energy electrons to generate a variety of signals at the surface of the solid specimens. The signals that derive from electron sample interactions reveal information about the sample including external morphology (texture), chemical composition, and crystalline structure and orientation of materials making up the sample.

In most applications, data are collected over a selected area of the surface of the sample, and a 2 dimensional image is generated that displays spatial variations in these properties. Areas ranging from approximately (1 cm) to (5 microns) in width can be imaged in scanning mode using conventional SEM techniques (magnification ranging from 20X to approximately 30,000X , spatial resolution of 50 to 100 nm). The SEM is also capable of performing analyses of selected point locations on the sample, this approach is especially useful in qualitatively or semi quantitatively determining chemical compositions [101].

The scanning electron microscope used in imagining the nanoparticles is a scanning electron microscope AIS2300C that is Seron Technology's high competitive normal SEM which be equipped with optics designed for LOW KV performance and shown in **Figure (2.9)**.

Figure (2.9): Scanning electron microscope instrument used

2.4.3: Atomic force microscope:

The principle of operation of the AFM is very similar to that of a stylus profilometer - a sharp cantilever tip interacts with the sample surface sensing the local forces between the molecules of the tip and sample surface .It is high resolution type of scanning probe that gathers topographical information by scanning a special tip across the surface of sample .The advantage of this system over called the SEM , is that while the SEM can provides a detailed 2-d image of the surface, the AFM provides a 3 dimensional profile of the surface. AFM allows ones to see and measure surface features with unprecedented resolution and accuracy and almost any sample type can be imaged [104].

AFM is more than a surface-imaging tool in that force measurements can be used to probe the physical properties of the specimen, such as molecular interactions, surface hydrophobicity, surface charges, and mechanical properties. These measurements provide new insight into the structure-function relationships of microbial surfaces.

The Digital Instruments, Veeco Metrology group SPM, model AA 3000, 220V, AFM contact angstrum Advanced INC, USA was used for characterization of metal oxide nanoparticles surface and it shown in **Figure (2.10).**

Figure (2.10): Atomic force microscope instrument used

2.5: Sample Used For Adsorption

The analysis of waste water collected from Diyala Electrical Industries Company show that it contains mainly nickel and lead ions , so we prepare a standard aqueous solution for nickel and lead ions.

2.6: Separation of Nickel and Lead Ions

2.6.1 : Standard stock solution preparation

Standard stock solutions (500 mg / L) of Ni (II) and Pb (II) ions were prepared by dissolving nickel (II) chloride ($NiCl_2.6H_2O$) and lead (II) acetate ($Pb(CH_3COO)_2.H_2O$ in deionized water . several concentrations (100 , 200 , and 300 mg / L) of nickel and lead (II) ions were prepared from the standard stock solution by dilution . For absorption concentration determination the absorbance of these solutions were measured at a wavelength (λ_{max}) 283.3 nm for nickel and 232.0 nm for lead.

2.6.2 : Batch adsorption method studies

The effect of contact time and initial concentration of adsorbate on percentage metal removal (R%) were studied . .

2.6.2.1: Effect of contact time of adsorption of nickel and lead ions

Twelve volumetricflasks with the volume of (100 ml) and containing (50 ml) of Ni (II) ion solution with initial concentration (100 mg / L) were prepared. An amount of (0.1 g) of (Fe_3O_4) nanoparticles, was add into first four flasks, and of (0.1 g) of (Fe_2O_3) nanoparticles, was add into second four flasks, and of (0.1 g) of (CuO) nanoparticles was add into third four flasks and the pH value was adjusted to 3.5 by using H_2SO_4 and NaOH

solutions , and then the flasks covered with glass stopper placed in shaking water bath at room temperature of 25 ±1 ℃ with speed 130 rpm at various time intervals (30, 60, 90, 120) minute and after that the samples were filtered off and the concentration of nickel ion measured by atomic absorption spectrophotometer, and this procedure above was repeated with initial concentration (200, 300) mg/L.

All steps above were repeated for lead by using Pb (II) ion solution with initial concentration (100, 200, 300) mg/L also. .

2.6.2.2: Effect of initial concentration of adsorbate on metal removal (R%)

Adsorption experiments are carried out as mentioned in section (2.6.2.1) with different initial concentration of Ni(II) and Pb(II) ions (100 , 200, and 300) mg /L .

2.6.3 : Measurement the concentration of nickel and lead Ions

The analytical technique used to measure the concentration of nickel and lead was atomic absorption spectroscopy (AAS) that is produce by AURORA TRACE AI 1200, and it is shown in **Figure (2.11).**

Figure (2.11): Atomic absorption spectroscopy instrument

2.6.4: Calculation of Metal Removal

The percentage metal removal (R %) was calculated using equation [97,105]:

$$R\ \% = [(C_o - C_t) / C_o\ ] * 100\% \quad \ldots\ldots \quad (2.3)$$

Where

R % : The percentage metal removal.

C_o : The initial concentration of metal ion (mg /L).

C_t : The concentration of metal ion after adsorption at any time **t** (mg /L).

2.6.5: Adsorption isotherms of nickel and lead ions

The adsorption Isotherms for nickel and lead ions solutions were determined by using the following procedure:

(50ml) of nickel or lead ions solution of a known concentration ranged from (100 - 300) mg/L were added separately to volumetric flasks containing (0.1g) of (Fe_3O_4) nanoparticles , or(Fe_2O_3) nanoparticles, or (CuO) nanoparticles , at room temperature of 25 ±1 °C , the flasks covered with glass stopper placed in shaking water bath with constant shaking speed of 130 rpm at various time intervals (30 , 60 , 90 , 120) minute , and then the mixture filtered and the equilibrium metal concentrations measred using atomic absorbtion spectrometer .

The adsorption capacity of adsorbent was calculated using the equation below [97,105] :

$$Q_e = (C_o - C_e)V/\ m \quad \ldots\ldots\ldots\ldots \quad (2.4)$$

Where

Q_e : Quantity adsorbed at equilibrium (mg adsorbate / g adsorbent).

C_o : Initial concentrations of adsorbate (mg/L).

C_e : Equilibrium concentrations of adsorbate after adsorption (mg/L).

V : Volume of solution (L).

m : Weight of adsorbent (g).

2.6.6 : Kinetic study of adsorption of nickel and lead ions

To study the kinetic of adsorption of nickel and lead ions on the metal oxides nanoparticles, the following procedure was used:

(50ml) of nickel or lead ions solution of a known concentration (100) mg/L were added separately to volumetric flasks containing (0.1g) of (Fe_3O_4) nanoparticles, or (Fe_2O_3) nanoparticles, or (CuO) nanoparticles , at room temperature of 25 ±1° C, pH of 3.5, the flasks covered with glass stopper placed in shaking water bath with constant shaking speed of 150 rpm and left at intervals times of (30 , 60 , 90 , 120) minute , and then the mixture filtered and the equilibrium metal concentrations measured by using atomic absorption spectrometer. The order of adsorbate – adsorbent interaction was investigated by using various kinetic models which was described by the following equations :

The pseudo-first order model (k_1) $C_2= C_1\exp(k_1t)$

$$\mathbf{\ln C_2/C_1 = - (k_1t)} \quad \ldots\ldots \quad \mathbf{(2.5)}$$

The pseudo-second order model (k_2) $k_2= 1/t*[(1/C_2)-(1/C_1)]$

$$\mathbf{1/C_2 = k_2t + 1/C_1} \quad \ldots\ldots \quad \mathbf{(2.6)}$$

Where

t :Time in (minute).

C_1: Initial concentration of adsorbate before the adsorption in (mg/L).

C_2: Concentration of adsorbate at any time after the adsorption in (mg/L).

Chapter Three

Results & Discussion

3.1 : Characterization of Metal Oxide Nanoparticles :

3.1.1 : X-ray diffraction

3.1.1.1 : Structural characterization

X-ray diffractometer is used to investigate the structure of metal oxide nanoparticles. XRD patterns of metals oxides nanoparticles are shown in **Figures (3.1, 3.2 and 3.3)** for (Fe_3O_4) ,(Fe_2O_3) ,and (CuO) nanoparticles respectively, also the data of strongest three peak for them are shown in **Tables (3.1, 3.2 and 3.3).** The positions and intensities of peaks are in a good agreement with those reported in JCPDS file **NO. 19-0629** for (Fe_3O_4) nanoparticles, and **NO. 33-0664** for (Fe_2O_3) nanoparticles and **NO. 48-1548** for (CuO) nanoparticle. .

Table (3.1): Strongest three peaks in XRD of iron oxide nanoparticles, Fe_3O_4

No.	2θ (deg)	d (Å)	FWHM (deg)	Intensity
1	35.6106	2.51910	0.6933	124
2	62.8434	1.47756	0.76000	54
3	30.2031	2.95666	0.68000	44

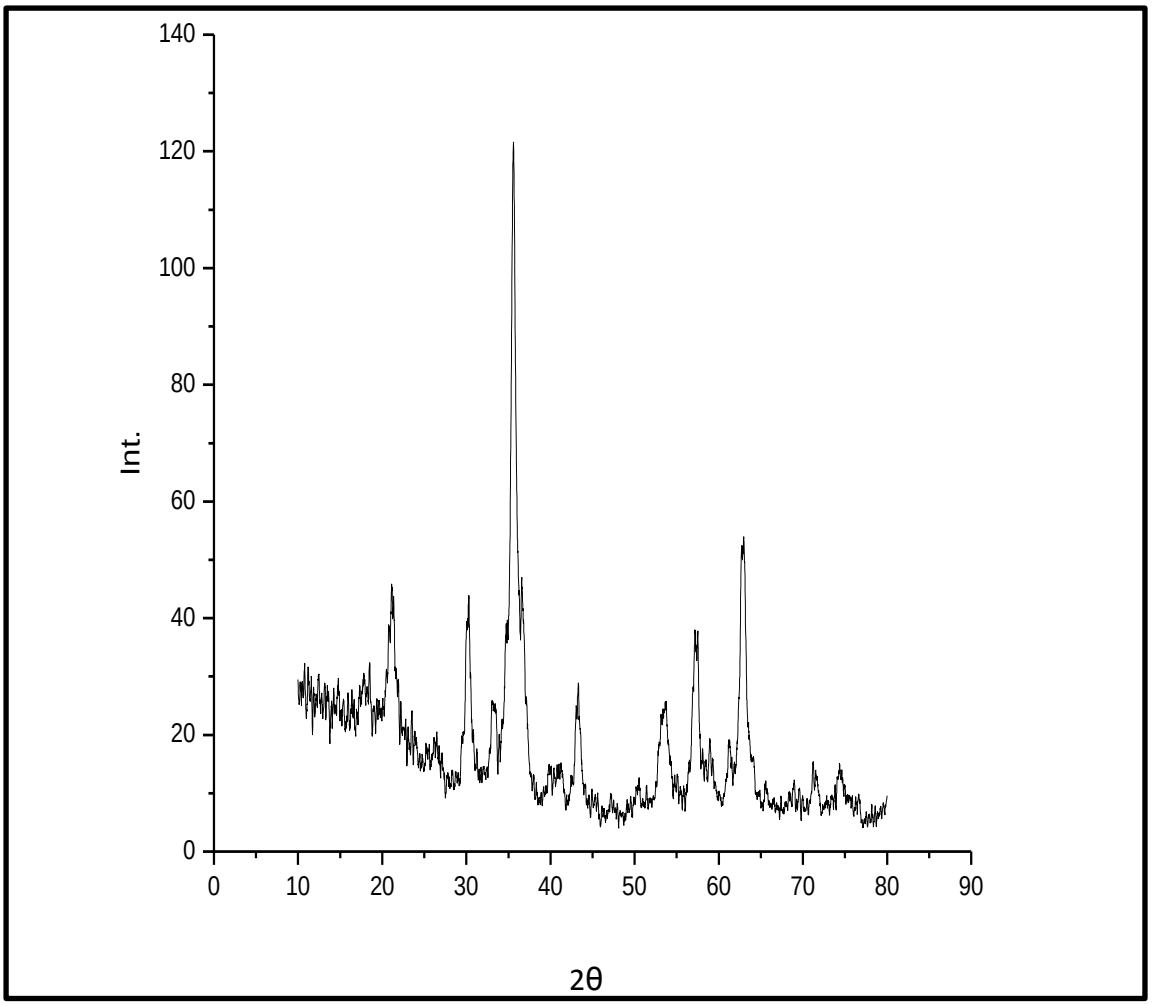

Figure (3.1): XRD pattern of iron oxide nanoparticles, Fe_3O_4

Table (3.2): Strongest three peaks in XRD of iron oxide nanoparticles, Fe_2O_3

No.	2θ (deg)	d (Å)	FWHM (deg)	Intensity
1	33.4455	2.67706	0.21220	502
2	54.3418	1.68686	0.18260	263
3	35.9183	2.49823	0.21450	224

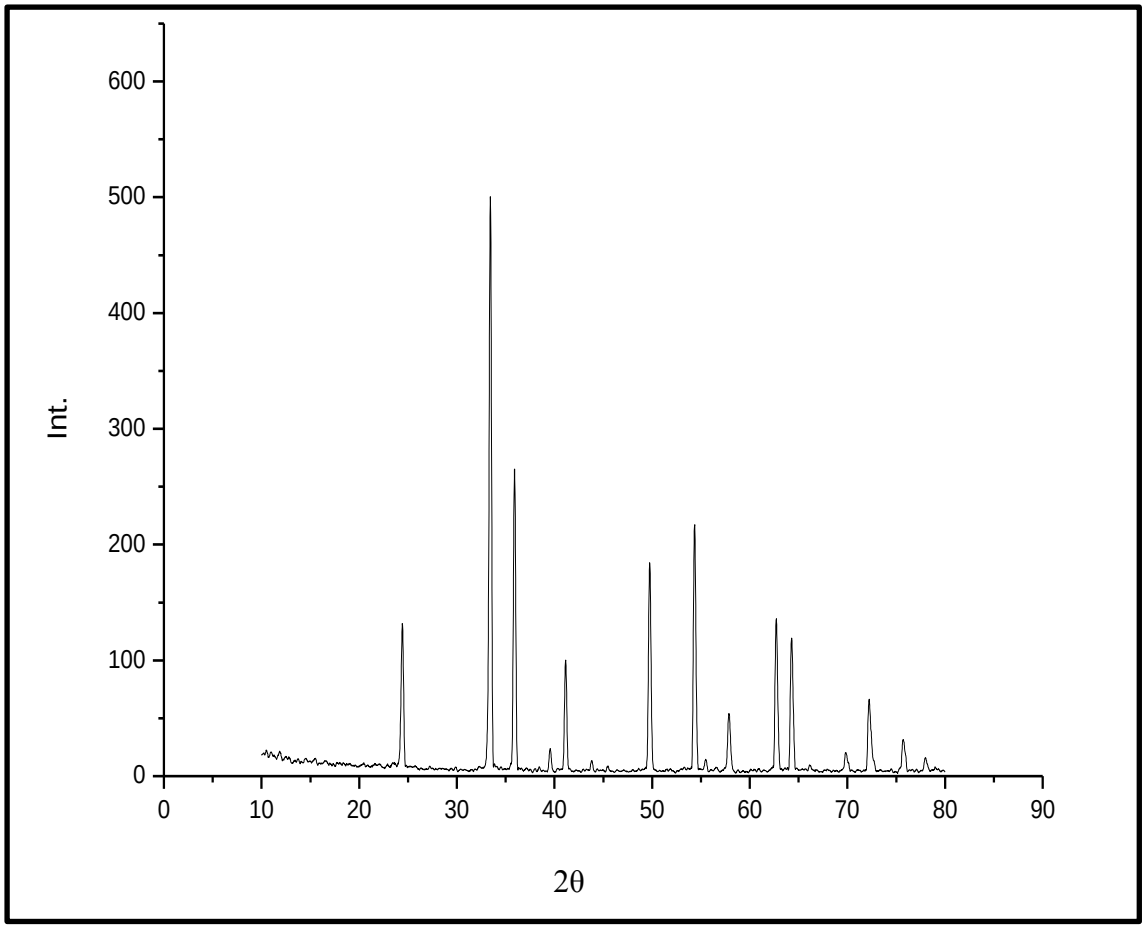

Figure (3.2): XRD pattern of iron oxide nanoparticles, Fe_2O_3

Table (3.3): Strongest three peaks in XRD of copper oxide nanoparticles, CuO

No.	2θ (deg)	d (Å)	FWHM (deg)	Intensity
1	38.6249	2.32916	1.13200	1043
2	35.4796	2.52810	1.17570	821
3	48.7088	1.86794	1.38000	395

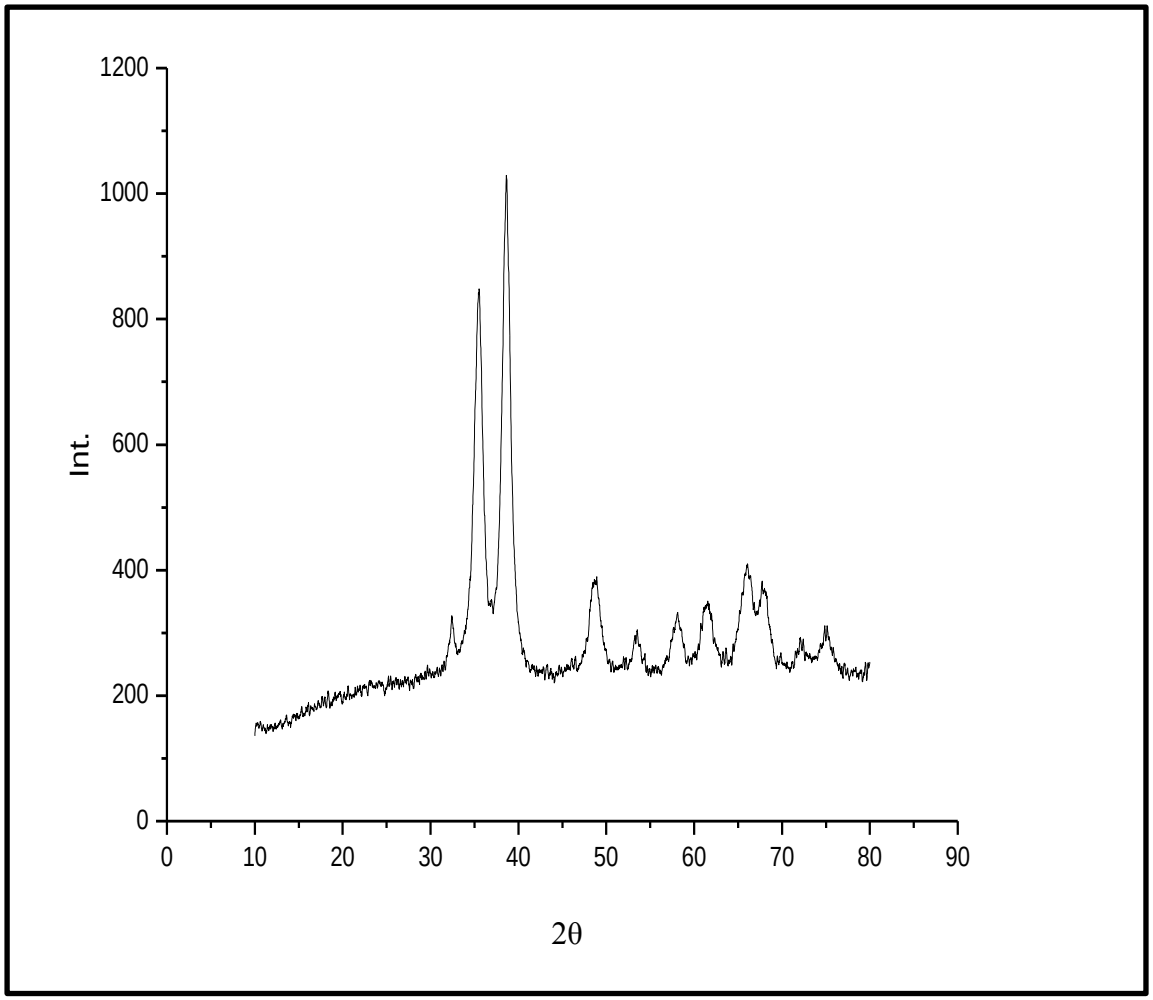

Figure (3.3): XRD pattern of copper oxide nanoparticles, CuO

3.1.1.2: Particle size calculation of metal oxides nanoparticles:

The particle size was calculated from Deby – Scherrer formula in equation **(2.2)** for metal oxide nanoparticles (Fe_3O_4 , Fe_2O_3 , and CuO), The particle size found is 12.04 nm for (Fe_3O_4) nanoparticles. and 39.11 nm for (Fe_2O_3) nanoparticles, and 7.43 nm for (CuO) nanoparticles, The presence of sharp peaks in XRD patterns and particle size of less than 100 nm suggest the nano crystalline nature of all oxides.

3.1.2: Scanning electron microscope

The surface morphology of the prepared metal oxide nanoparticles (Fe_3O_4, Fe_2O_3, and CuO) were revealed through the SEM image and shown in **Figures (3.4, 3.5 and 3.6 respectively)**, all of them show a homogeneous distribution of spherical shape like nanoparticles with irregular distribution. From SEM images it is confirmed that the particles having size in between 60-80 nanometers by simple counting and calculations of number of particles and their sizes and this confirm the nanostructure nature of the oxides.

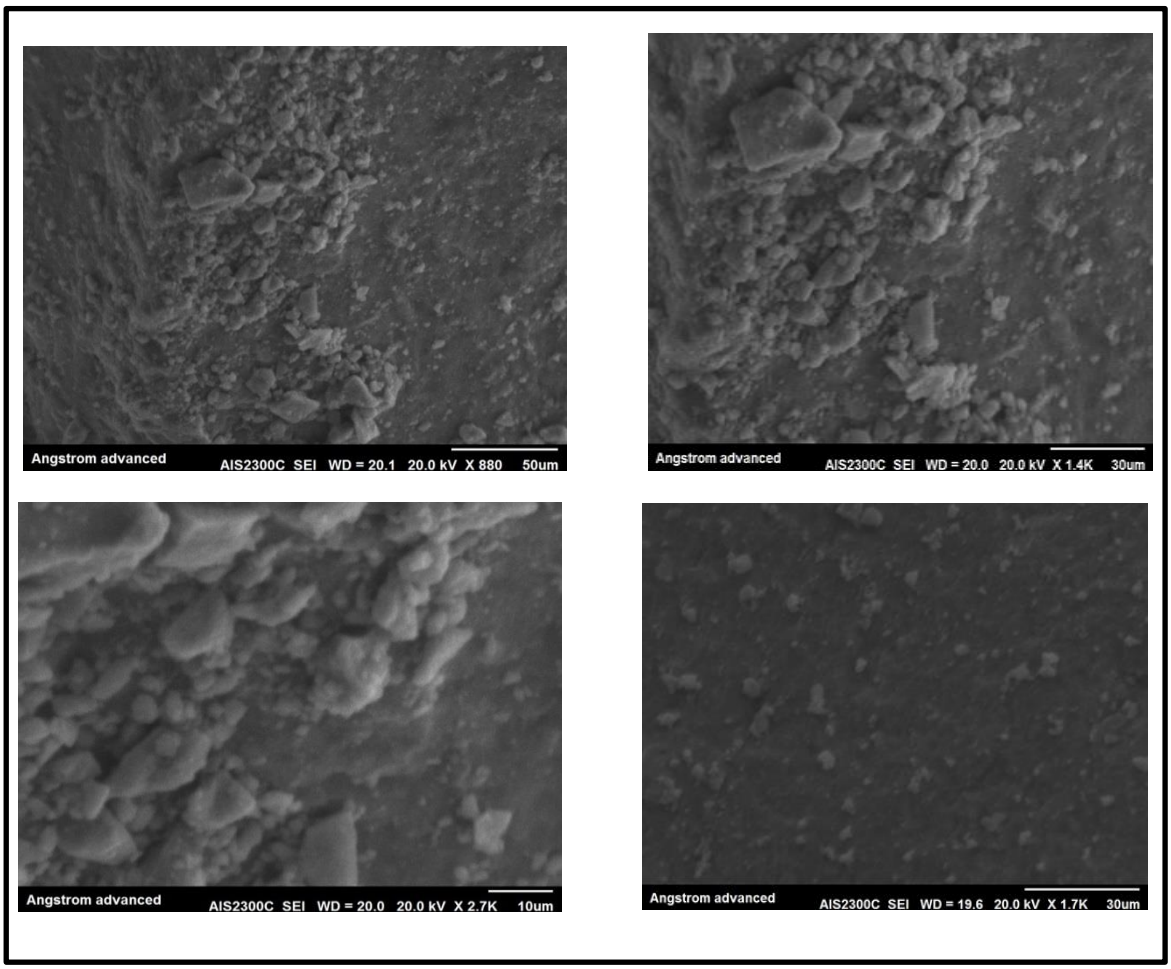

Figure (3.4): SEM images of iron oxide nanoparticles, Fe_3O_4.

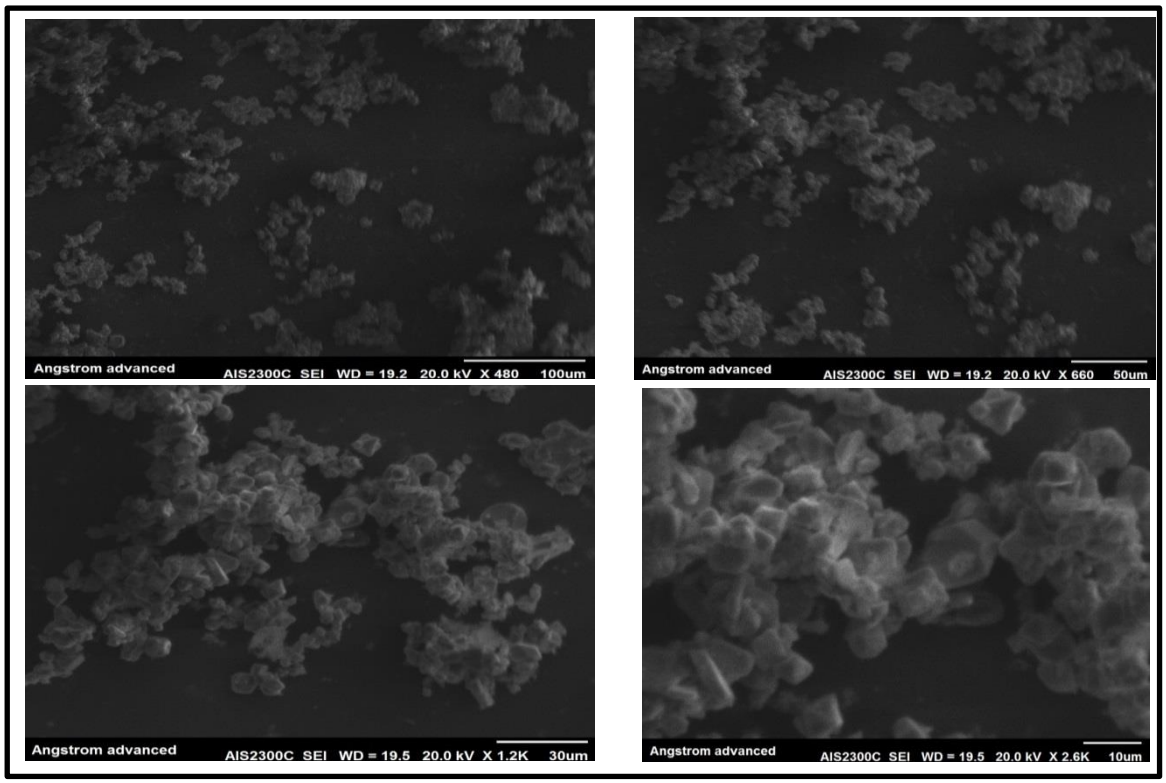

Figure (3.5): SEM images of iron oxide nanoparticles, Fe_2O_3.

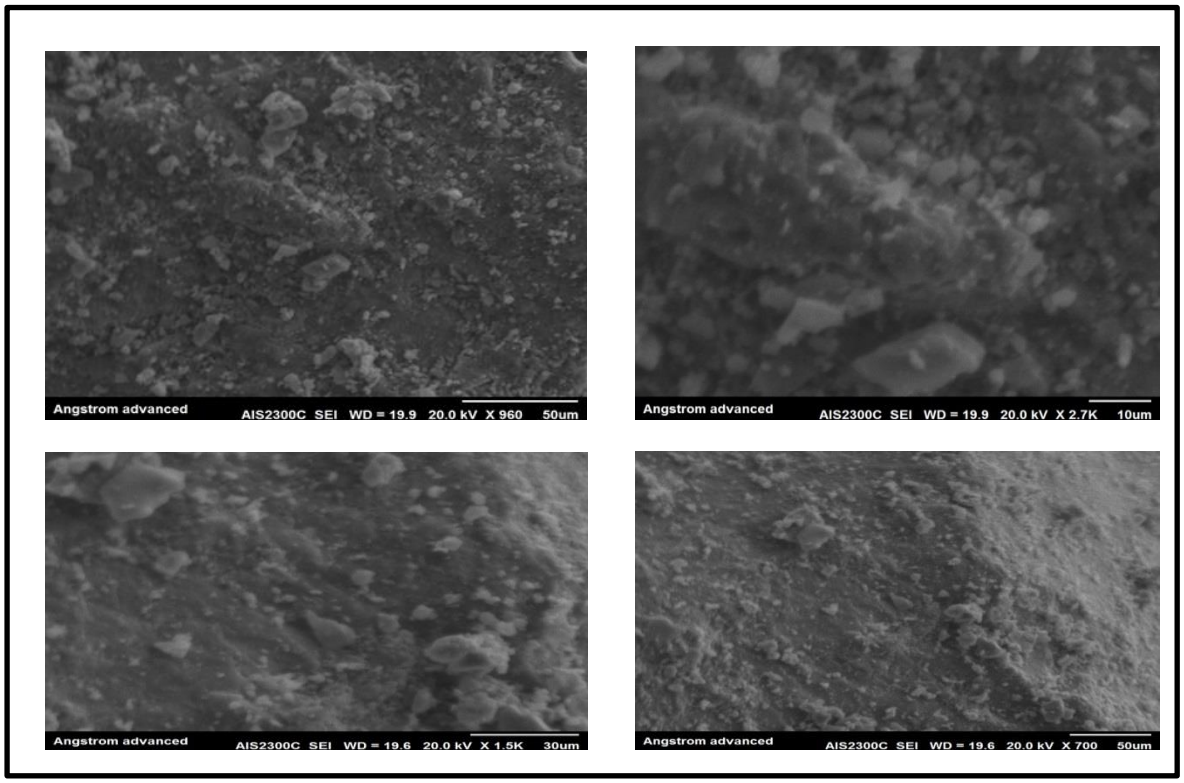

Figure (3.6): SEM images of copper oxide nanoparticles, CuO.

3.1.3 : Atomic force microscope

The AFM analysis provides a measure of average of grain size [106]. **Figures (3.7 , 3.8 , and 3.9)** show a typical AFM images of the three metal oxide nanoparticles.

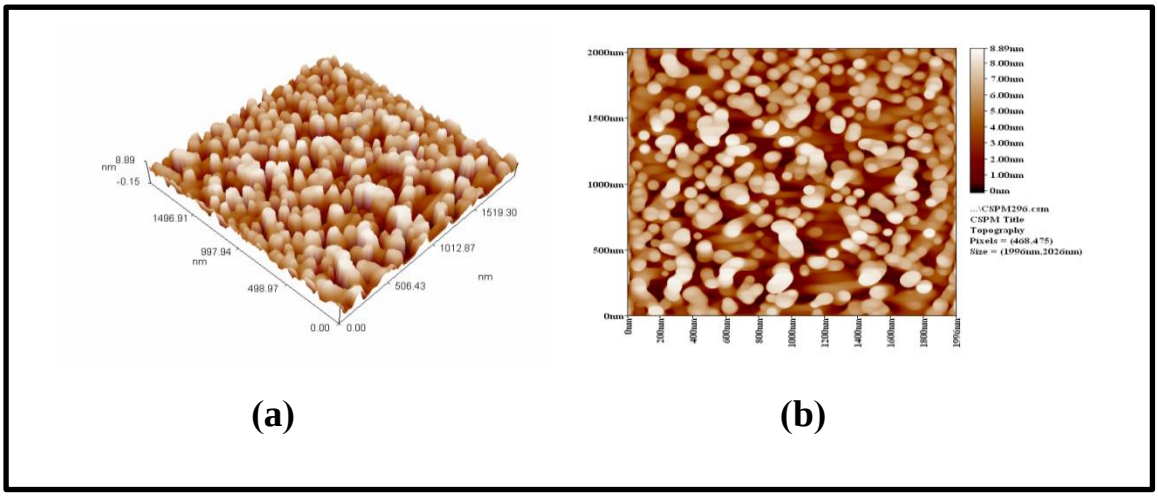

Figure (3.7): AFM images for iron oxide nanoparticles, Fe_3O_4

Figure (3.7) explains images of AFM for (Fe_3O_4) nanoparticles with area (size=1996nmX2026nm) and ability analytical (pixels =468,475 IN). **Figure (3.7-a)** is AFM picture in three dimensions (3D), it explains structural shape for grains, and **Figure (3.7-b)** is AFM picture in two dimensions (2D) it is found that average roughness is 1.96 nm and Root mean square(RMS) is 2.3 and average diameter is 98.57 nm.

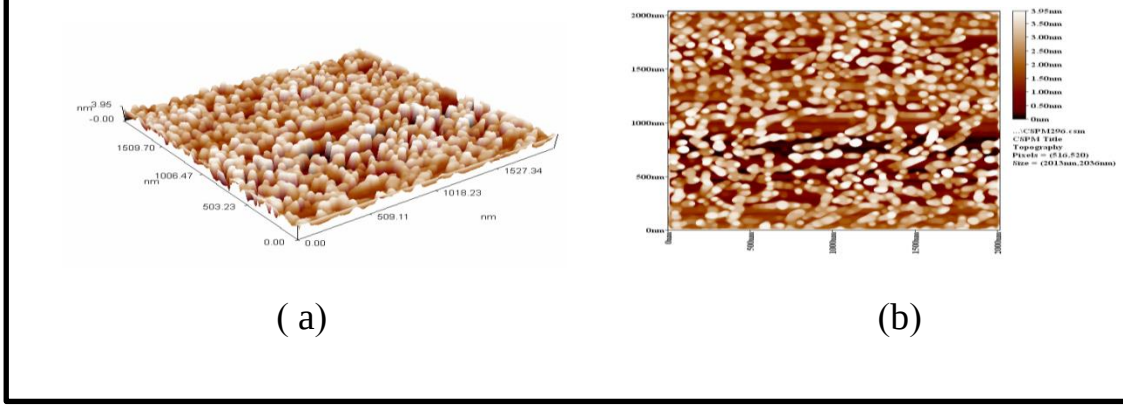

Figure (3.8): AFM images for iron oxide nanoparticles, Fe_2O_3

Figure (3.8) explains images of AFM for (Fe_2O_3) nanoparticles with area (size= 2013 nmX2036nm) and analytical ability (pixels=468,475 IN). Where **Figure (3.8 - a)** is AFM picture in three dimensions (3D) , it explains structural shape for grains , and **Figure (3.8-b)** is AFM picture in two dimensions (2D) it is found that average roughness is 0.931 nm and RMS is 1.09 nm , and average diameter is 64.70 nm.

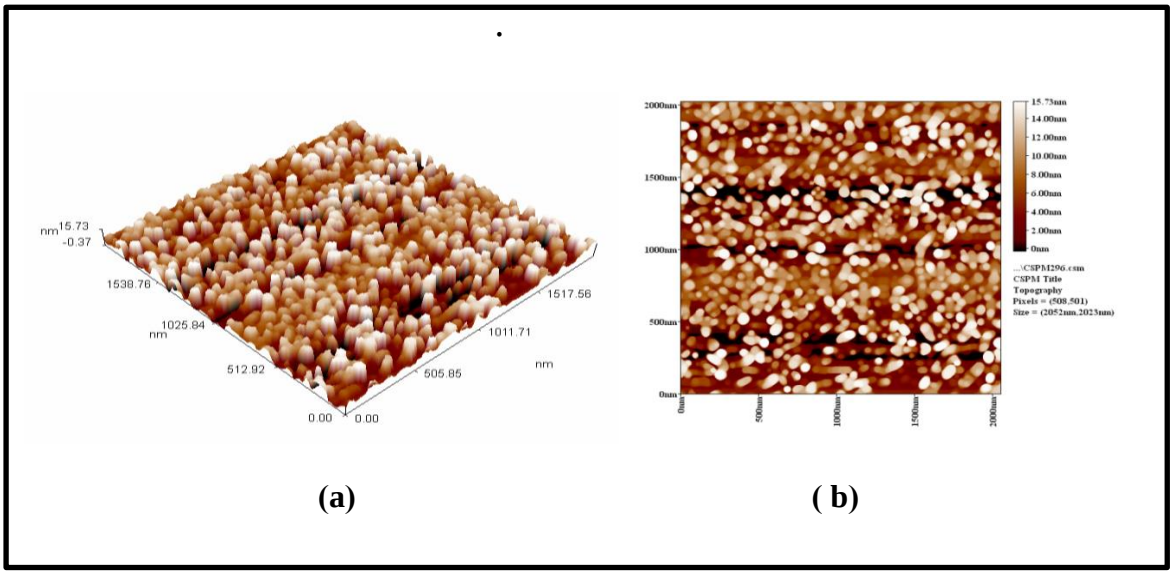

Figure (3.9): AFM images for copper oxide nanoparticles, CuO

Figure (3.9) explains images of AFM for (CuO) nanoparticles, with area (size=2052nm X 2023nm) and ability analytical (pixels=508,501). Where **Figure (3.9-a)** is AFM picture in three dimensions (3D), it explains structural shape for grains, and **Figure (3.9-b)** is AFM picture in two dimensions (2D) it is found that average roughness is 4.04 nm and RMS is 4.67 nm, and average diameter is 68.42 nm.

Tables (3.4, 3.5 , and 3.6) and **Figures (3.10 , 3.11 , and 3. 12)** show the granularity cumulating distribution and average diameter data of (Fe_3O_4) nanoparticles, (Fe_2O_3) nanoparticles , and (CuO) nanoparticles respectively

Table (3.4) : Granularity cumulating distribution and average diameter of iron oxide nanoparticles, Fe_3O_4.

Avg. Diameter:98.57 nm								
Diameter (nm)<	Volume (%)	Cumulation (%)	Diameter (nm)<	Volume (%)	Cumulation (%)	Diameter (nm)<	Volume (%)	Cumulation (%)
80.00	9.03	9.03	110.00	10.42	80.56	140.00	0.69	97.92
85.00	14.58	23.61	115.00	4.17	84.72	145.00	0.69	98.61
90.00	10.42	34.03	120.00	4.86	89.58	150.00	0.69	99.31
95.00	13.19	47.22	125.00	3.47	93.06	180.00	0.69	100.00
100.00	10.42	57.64	130.00	2.78	95.83			
105.00	12.50	70.14	135.00	1.39	97.22			

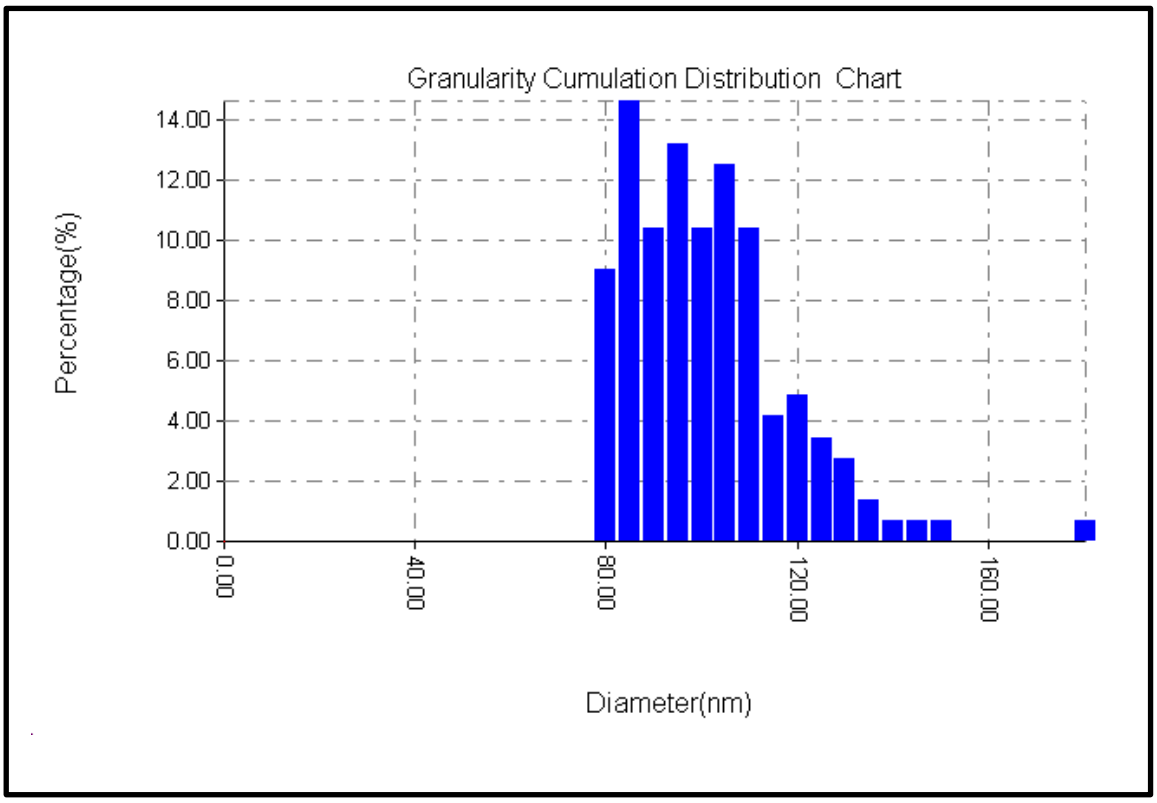

Figure (3.10): Granularity cumulating distribution of iron oxide nanoparticles, Fe_3O_4

Table (3.5) : Granularity cumulating distribution and average diameter of iron oxide nanoparticles, Fe_2O_3

Avg. Diameter:64.70 nm								
Diameter (nm)<	Volume (%)	Cumulation (%)	Diameter (nm)<	Volume (%)	Cumulation (%)	Diameter (nm)<	Volume (%)	Cumulation (%)
35.00	0.98	0.98	70.00	11.55	64.58	105.00	1.57	98.43
40.00	3.13	4.11	75.00	9.20	73.78	110.00	0.59	99.02
45.00	6.07	10.18	80.00	6.85	80.63	115.00	0.59	99.61
50.00	10.96	21.14	85.00	7.63	88.26	120.00	0.20	99.80
55.00	11.55	32.68	90.00	4.89	93.15	125.00	0.20	100.00
60.00	11.15	43.84	95.00	2.35	95.50			
65.00	9.20	53.03	100.00	1.37	96.87			

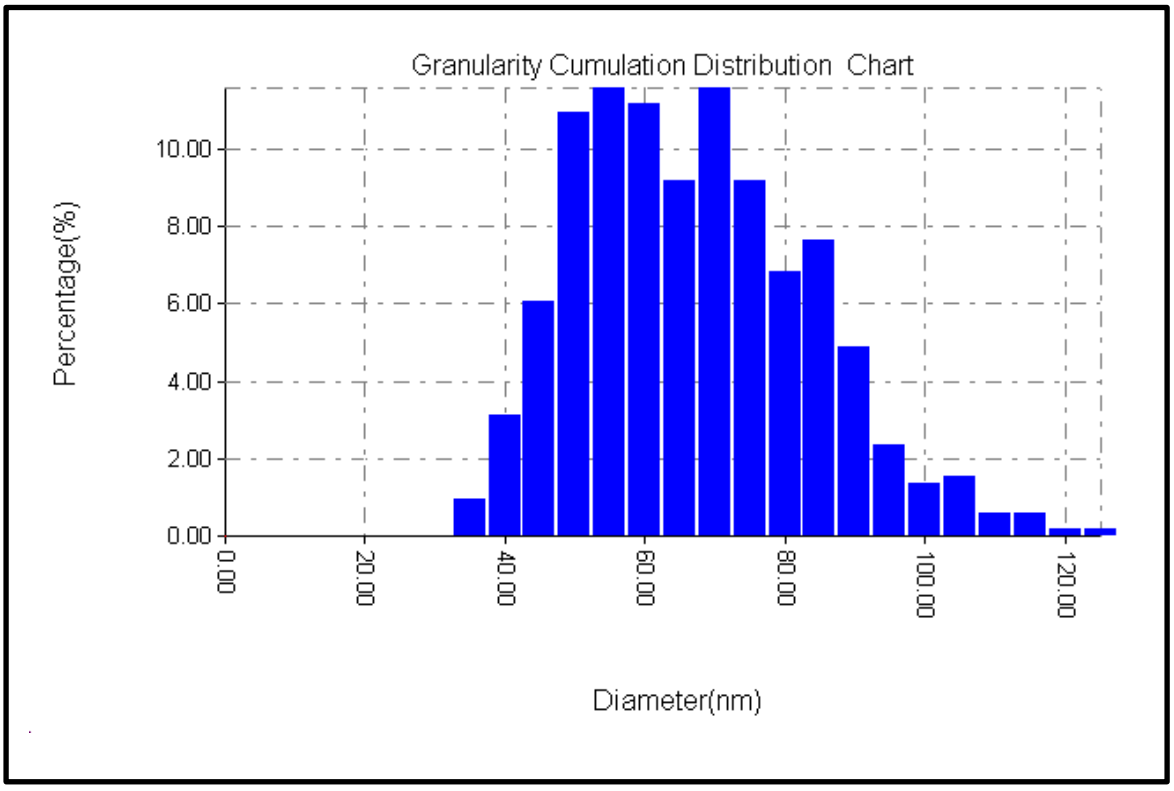

Figure (3.11): Granularity cumulating distribution of iron oxide nanoparticles, Fe_2O_3

Table (3.6): Granularity cumulating distribution and average diameter of copper oxide nanoparticles, CuO.

Avg. Diameter:68.42 nm								
Diameter (nm)<	Volume (%)	Cumulation (%)	Diameter (nm)<	Volume (%)	Cumulation (%)	Diameter (nm)<	Volume (%)	Cumulation (%)
10.00	0.22	0.22	55.00	8.52	26.20	100.00	2.84	93.89
15.00	0.22	0.44	60.00	8.08	34.28	105.00	1.75	95.63
20.00	0.44	0.87	65.00	9.17	43.45	110.00	1.97	97.60
25.00	0.66	1.53	70.00	11.79	55.24	115.00	0.87	98.47
30.00	0.66	2.18	75.00	9.61	64.85	120.00	0.87	99.34
35.00	0.66	2.84	80.00	8.95	73.80	125.00	0.44	99.78
40.00	2.62	5.46	85.00	6.99	80.79	130.00	0.22	100.00
45.00	4.59	10.04	90.00	5.90	86.68			
50.00	7.64	17.69	95.00	4.37	91.05			

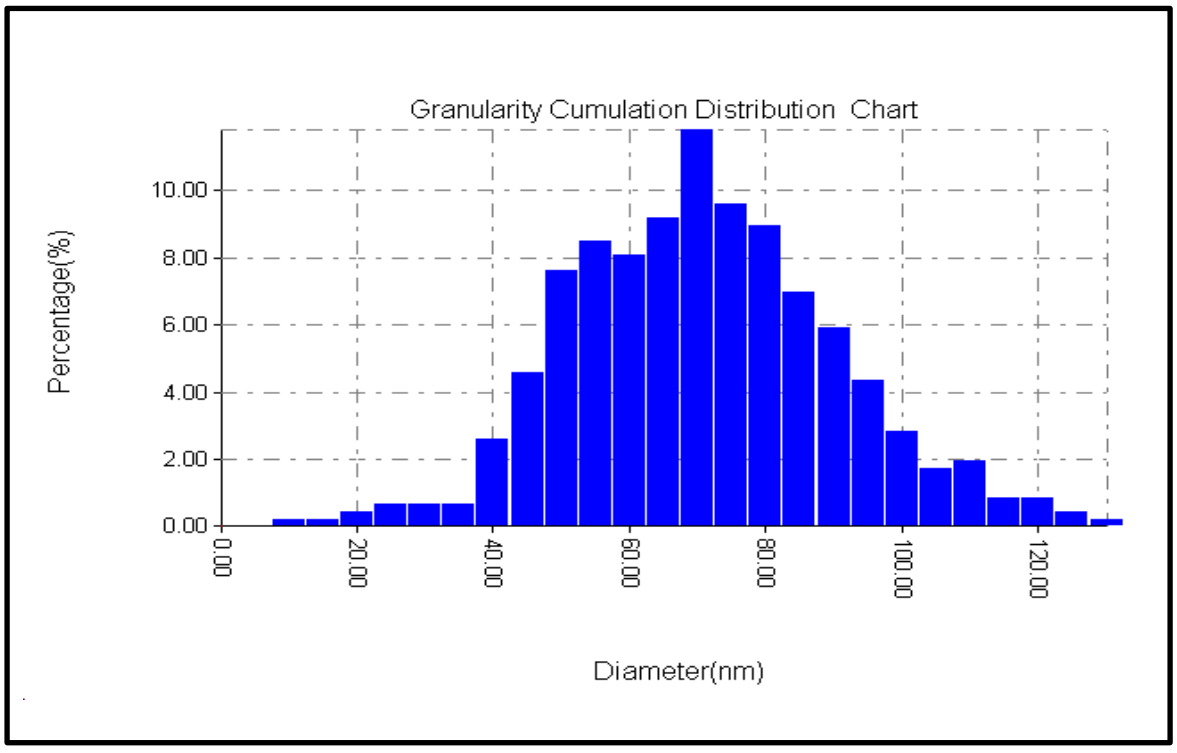

Figure (3.12): Granularity cumulating distribution of copper oxide nanoparticles, CuO

3.2 : Batch Adsorption Separation Method of Nickel and Lead Ions

3.2.1 : Contact time of adsorption :

The contact time between metal oxide nanoparticles (Adsorbent) with nickel and lead ions (adsorbate) is sufficient for the adsorption process to reach equilibrium at room temperature of 25±1^{o}C using a fixed concentration (C_o = 100 mg/L) and adsorbent dosage (0.1g) .and pH of 3.5 are studied at different times (0 , 30 , 60 , 90 and 120) minutes.

3.2.1.1: Contact time of adsorption of nickel ions on metal oxide nanoparticles

Tables (3.7 - 3.15), show the changes of nickel ion removal and percentage removal at contact time of (0 , 30 , 60 , 90 , and 120) minutes using (Fe_3O_4), (Fe_2O_3), and (CuO) nanoparticles respectively, and the results are presented in **Figures (3.13 , 3.14 , 3.15)** also. It is observed that the increasing in contact time lead to increasing in percentage of nickel removal and this due to the larger available surface area of the nanoparticles. .

Nickel adsorption percentage in the initial stage depends on increase abundance in active binding site numbers on the surface of adsorbent. Finite mass transfer of the adsorbate molecules from the bulk to the adsorbent surface cause to be gradual increase in adsorption subsequently realization of the equilibrium adsorption [16, 52, 53, 84]. Among the three oxide nanoparticles observed the results showed that the (CuO) nanoparticles gave the best nickel removal percentage by the time, followed by (Fe_2O_3) nanoparticles, and then (Fe_3O_4) nanoparticles.

Table (3.7): Effect of contact time on the removal of nickel ions using iron oxide nanoparticles, Fe_3O_4 at initial concentration of (100 mg/L).

Time, min	0	30	60	90	120
Residual concentration, (C_t), mg/ L	100	21.811	18.595	16.762	15.175
Removed concentration, (R), mg/ L	0	78.189	81.405	83.238	84.825
Residual (C_t) %	100	21.811	18.595	16.762	15.175
Removed (R) %	0	78.189	81.405	83.238	84.825

Table (3.8): Effect of contact time on the removal of nickel ions using iron oxide nanoparticles, Fe_3O_4 at initial concentration of (200 mg/L).

Time, min	0	30	60	90	120
Residual concentration (C_t), mg/ L	200	53.568	47.566	41.696	39.178
Removed concentration (R), mg/ L	0	146.432	152.434	158.304	160.822
Residual (C_t) %	100	26.784	23.783	20.848	19.589
Removed (R) %	0	73.216	76.217	79.152	80.411

Table (3.9): Effect of contact time on the removal of nickel ions using iron oxide nanoparticles, Fe_3O_4 at initial concentration of (300 mg/L).

Time, min	0	30	60	90	120
Residual concentration (C_t), mg/ L	300	115.653	103.846	91.836	73.455
Removed concentration (R), mg/ L	0	184.347	196.154	208.164	226.545
Residual (C_t)%	100	38.551	34.615	30.612	24.485
Removed (R) %	0	61.449	65.385	69.388	75.515

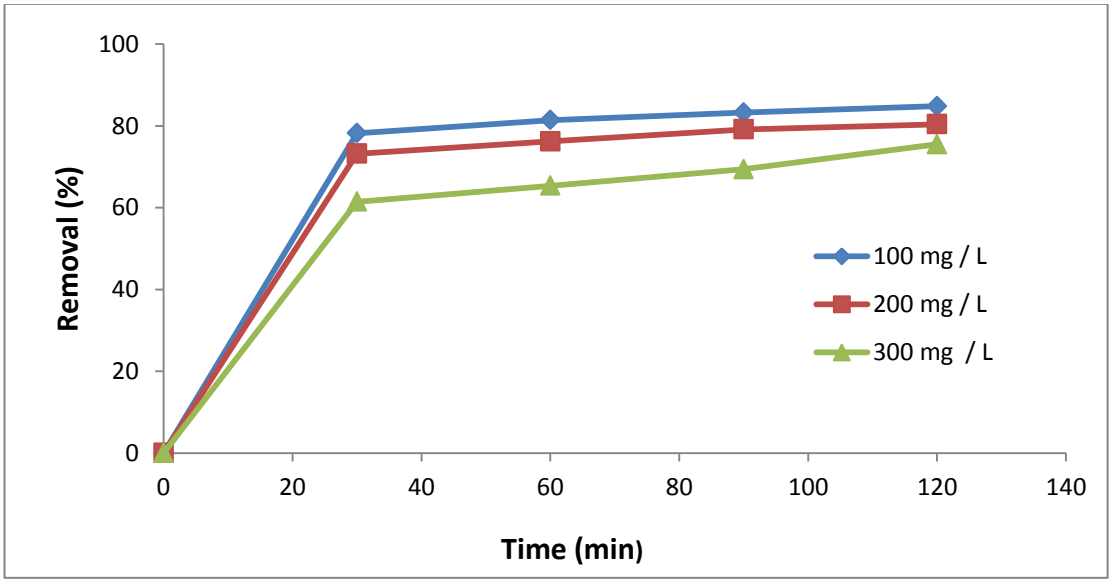

Figure (3.13): Effect of contact time on percentage removal of nickel ions using iron oxide nanoparticles, Fe_3O_4 at different initial concentration.

Table (3.10): Effect of contact time on the removal of nickel ions using iron oxide nanoparticles, Fe_2O_3 at initial concentration of (100 mg/L).

Time, min	0	30	60	90	120
Residual concentration (C_t), mg/ L	100	19.911	16.815	15.567	13.800
Removed concentration (R), mg/ L	0	80.089	83.185	84.433	86.200
Residual (C_t)%	100	19.911	16.815	15.567	13.800
Removed (R) %	0	80.089	83.185	84.433	86.200

Table (3.11): Effect of contact time on the removal of nickel ions using iron oxide nanoparticles, Fe_2O_3 at initial concentration of (200 mg/L).

Time, min	0	30	60	90	120
Residual concentration (C_t), mg/ L	200	51.855	46.934	42.700	38.745
Removed concentration (R), mg/ L	0	148.145	153.066	157.300	161.255
Residual (C_t) %	100	25.927	23.467	21.350	19.373
Removed (R) %	0	74.073	76533	78.650	80.627

Table(3.12): Effect of contact time on the removal of nickel ions using iron oxide nanoparticles, Fe_2O_3 at initial concentration of (300 mg/L).

Time, min	0	30	60	90	120
Residual concentration (C_t), mg/ L	300	101.833	88.895	76.944	68.588
Removed concentration (R), mg/ L	0	198.167	211.105	223.056	231.412
Residual (C_t)%	100	33.944	29.632	25.648	22.862
Removed (R) %	0	66.056	70.368	74.352	77.137

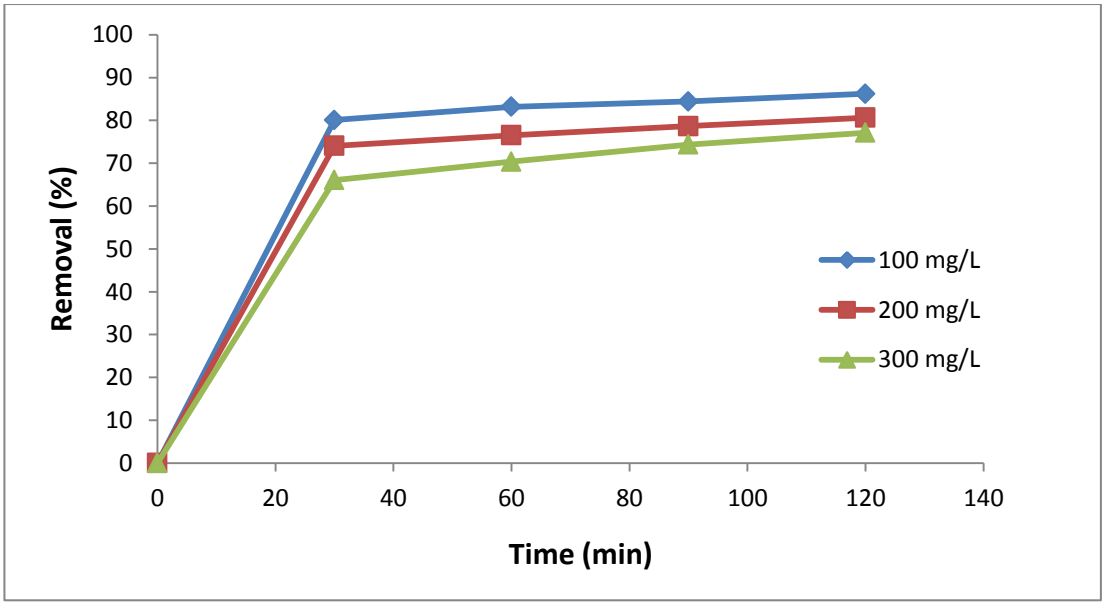

Figure (3.14): Effect of contact time on percentage removal of nickel ions using iron oxide nanoparticles, Fe_2O_3 at different initial concentration .

Table (3.13): Effect of contact time on the removal of nickel ions using copper oxide nanoparticles, CuO at initial concentration of (100 mg/L).

Time, min	0	30	60	90	120
Residual concentration (C_t), mg/ L	100	17.848	16.154	13.056	10.948
Removed concentration (R), mg/ L	0	82.152	83.846	86.944	89.052
Residual (C_t)%	100	17.848	16.154	13.056	10.948
Removed (R) %	0	82.152	83.846	86.944	89.052

Table (3.14): Effect of contact time on the removal of nickel ions using copper oxide nanoparticles, CuO at initial concentration of (200 mg/L).

Time, min	0	30	60	90	120
Residual concentration (C_t), mg/ L	200	55.256	48.614	40.552	37.910
Removed concentration (R), mg/ L	0	144.744	151.386	159.448	162.090
Residual (C_t) %	100	27.628	24.307	20.276	18.955
Removed (R) %	0	72.372	75.693	79.724	81.045

Table(3.15): Effect of contact time on the removal of nickel ions using copper oxide nanoparticles, CuO at initial concentration of (300 mg/L).

Time, min	0	30	60	90	120
Residual concentration (C_t), mg/ L	300	95.247	90.327	83.604	72.978
Removed concentration (R), mg/ L	0	204.753	209.673	216.396	227.022
Residual (C_t)%	100	31.749	30.109	27.868	24.326
Removed (R) %	0	68.251	69.891	72.132	75.674

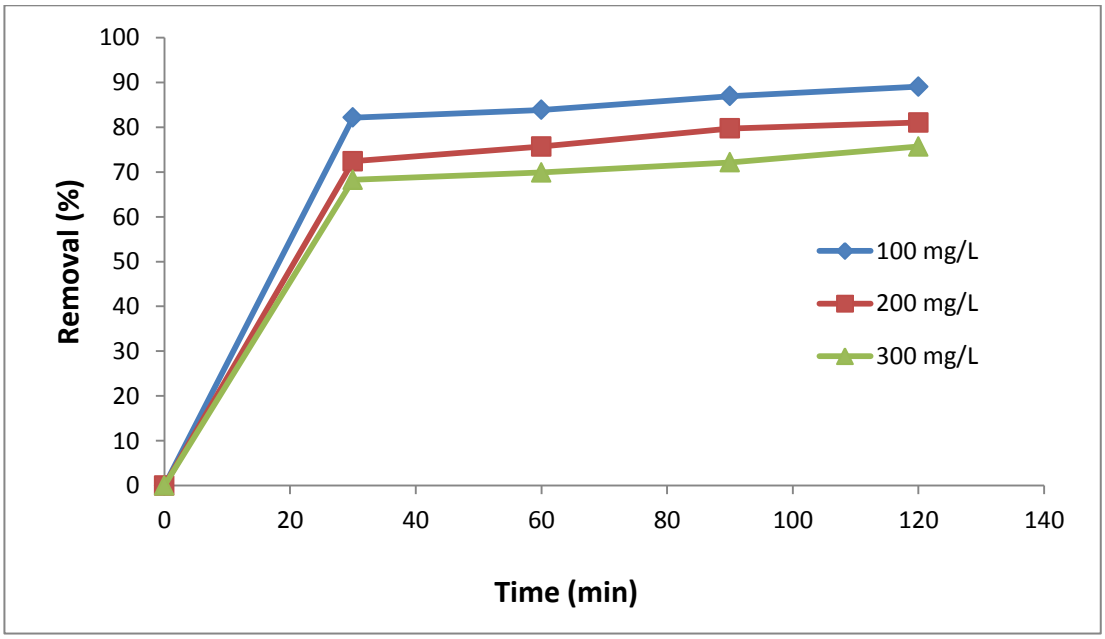

Figure (3.15): Effect of contact time on percentage removal of nickel ions using copper oxide Nanoparticles, CuO at different initial concentration.

3.2.1.2: Contact time of adsorption of lead ions on metal oxide nanoparticles:

Tables (3.16 - 3.24) show the changes of lead ion removal and percentage removal at contact time of (0 , 30 , 60 , 90 , and 120) minutes using (Fe_3O_4) nanoparticles, (Fe_2O_3) nanoparticles, and (CuO) nanoparticles respectively, and the results are presented in **Figures (3.16 , 3.17 , 3.18)** also.

It seems that the percentage removal of lead increased with increase in contact time .This increase is clear from the beginning and up to 90 minutes and then it is significantly reduced and reached to stability and steady state

This explains the fact that all adsorbent sites were free and the solute concentration was high at the beginning and then, the lead adsorption by oxide nanoparticles was decreased comparison with adsorption rate in the beginning due to the number of adsorption sites were decrease and the concentration of lead after adsorption , and this may be due to the saturation of the adsorbent surface with lead ions [17,40,93].

As far as the comparison between the three oxides, the results showed that the (Fe_3O_4) nanoparticles gave the best lead percentage removal with the time, followed by (Fe_2O_3) nanoparticles and finally (CuO) nanoparticles.

Table (3.16): Effect of contact time on the removal of lead ions using iron oxide nanoparticles, Fe_3O_4 at initial concentration of (100 mg/L).

Time, min	0	30	60	90	120
Residual concentration (C_t), mg/ L	100	14.621	11.594	5.123	4.786
Removed concentration (R), mg/ L	0	85.379	88.406	94.877	95.214
Residual (C_t)%	100	14.621	11.594	5.123	4.786
Removed (R) %	0	85.379	88.406	94.877	95.214

Table (3.17): Effect of contact time on the removal of lead ions using iron oxide nanoparticles, Fe_3O_4 at initial concentration of (200 mg/L).

Time,min	0	30	60	90	120
Residual concentration (Ct), mg/ L	200	34.286	27.304	16.124	14.554
Removed concentration (R), mg/ L	0	165.714	172.696	183.876	185.446
Residual (Ct) %	100	17.143	13.652	8.062	7.277
Removed (R) %	0	82.857	86.348	91.938	92.723

Table (3.18): Effect of contact time on the removal of lead ions using iron oxide nanoparticles, Fe_3O_4 at initial concentration of (300 mg/L)

Time,min	0	30	60	90	120
Residual concentration (C_t), mg/ L	300	54.348	43.629	27.261	25.395
Removed concentration (R) , mg/ L	0	245.652	256.371	272.739	274.605
Residual (C_t)%	100	18.116	14.543	9.087	8.465
Removed (R) %	0	81.884	85.457	90.913	91.535

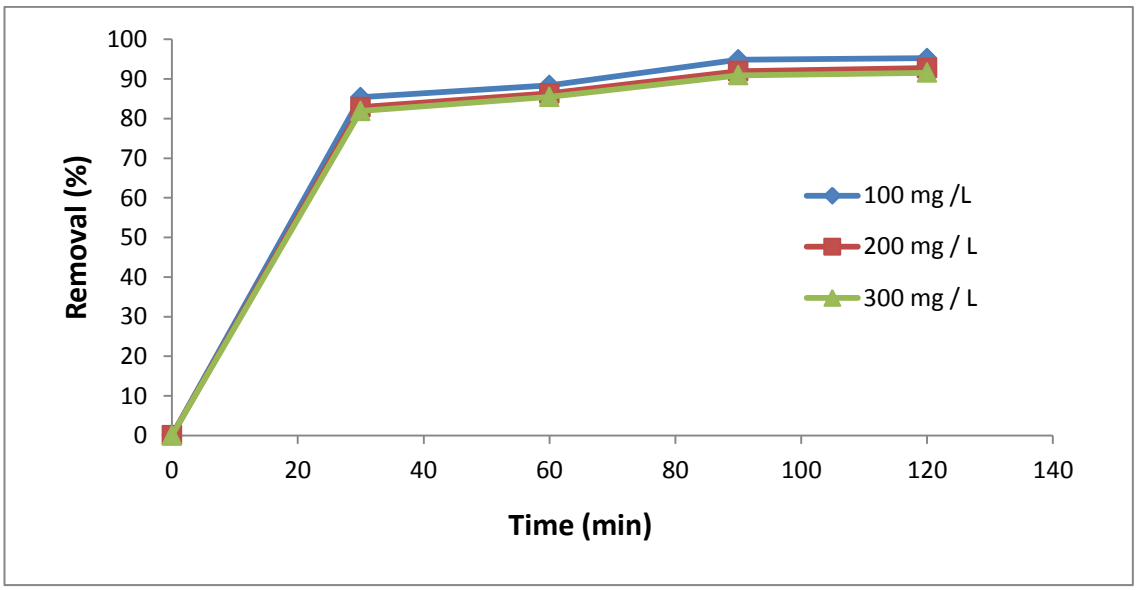

Figure (3.16): Effect of contact time on percentage removal of lead ions using iron oxide nanoparticles, Fe_3O_4 at different initial concentration.

Table (3.19): Effect of contact time on the removal of lead ions using iron oxide nanoparticles, Fe_2O_3 at initial concentration of (100 mg/L).

Time, min	0	30	60	90	120
Residual concentration (C_t), mg/ L	100	15.471	11.910	6.177	5.467
Removed concentration (R), mg/ L	0	84.259	88.090	93.823	94.533
Residual (C_t)%	100	15.471	11.910	6.177	5.467
Removed (R) %	0	84.259	88.090	93.823	94.533

Table (3.20): Effect of contact time on the removal of lead ions Using iron oxide nanoparticles, Fe_2O_3 at initial concentration of (200 mg/L).

Time, min	0	30	60	90	120
Residual concentration (C_t), mg/ L	200	33.200	26.382	18.672	17.328
Removed concentration (R), mg/ L	0	166.800	173.618	181.328	182.672
Residual (C_t) %	100	16.600	13.191	9.366	8.664
Removed (R) %	0	83.400	86.809	90.664	91.336

Table (3.21): Effect of contact time on the removal of lead ions using iron oxide nanoparticles, Fe_2O_3 at initial concentration of (300 mg/L).

Time, min	0	30	60	90	120
Residual concentration (C_t), mg/ L	300	54.048	43.143	32.748	27.393
Removed concentration (R), mg/ L	0	245.952	256.857	267.252	272.607
Residual (C_t)%	100	18.016	14.381	10.916	9.131
Removed (R) %	0	81.984	85.619	89.084	90.869

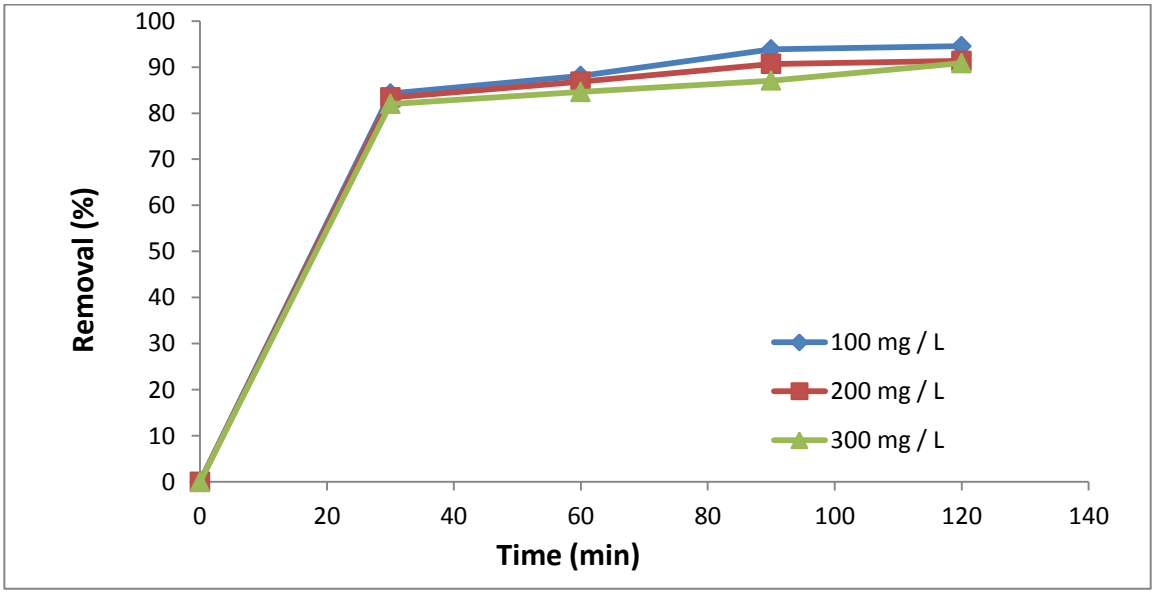

Figure (3.17): Effect of contact time on percentage removal of lead ions using iron oxide nanoparticles, Fe_2O_3 at different initial concentration.

Table (3.22): Effect of contact time on the removal of lead ions using copper oxide nanoparticles, CuO at initial concentration of (100 mg/L).

Time, min	0	30	60	90	120
Residual concentration (C_t), mg/ L	100	20.596	17.601	13.123	12.877
Removed concentration (R), mg/ L	0	79.404	82.399	86.877	87.123
Residual (C_t)%	100	20.596	17.601	13.123	12.877
Removed (R) %	0	79.404	82.399	86.877	87.123

Table (3.23): Effect of contact time on the removal of lead ions using copper oxide nanoparticles, CuO at initial concentration of (200 mg/L).

Time, min	0	30	60	90	120
Residual concentration (C_t), mg/ L	200	43.626	38.822	32.372	30.928
Removed concentration (R), mg/ L	0	156.374	161.178	167.628	169.072
Residual (C) %	100	21.813	19.411	16.186	15.464
Removed (R) %	0	78.187	80.589	83.814	84.536

Table(3.24): Effect of contact time on the removal of lead ions using copper oxide nanoparticles, CuO at initial concentration of (300 mg /L).

Time, min	0	30	60	90	120
Residual concentration (C_t), mg/ L	300	64.137	56.544	51.195	48.438
Removed concentration (R), mg/ L	0	235.863	243.456	248.805	251.562
Residual (C_t)%	100	21.379	18.884	17.064	16.146
Removed (R) %	0	78.621	81.152	82.936	83.854

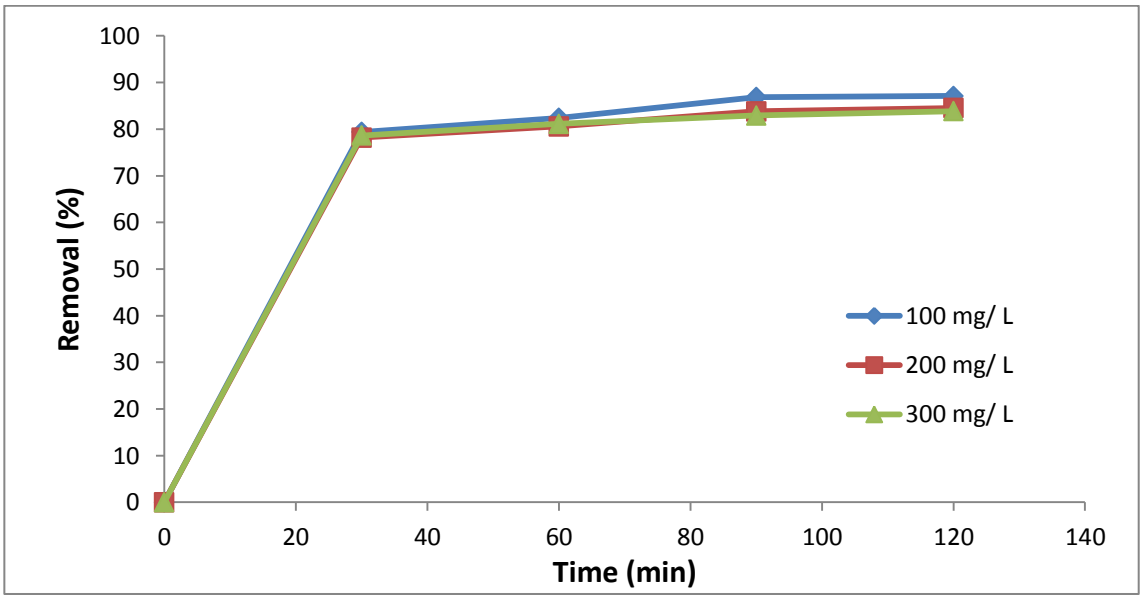

Figure (3.18): Effect of contact time on percentage removal of lead ions using copper oxide Nanoparticles, (CuO) at different initial concentration.

3.2.2: Effect of the initial concentration

The adsorption experiment was carried out at room temperature of 25±1 ^{o}C with different initial concentration C_o (100 , 200 , 300 mg / L) and keeping the adsorbent dosage (0.1g) and pH of 3.5 at contact time of (0 , 30 , 60 , 90 , and 120) minutes. .

3.2.2.1: Effect of the initial concentration of nickel ions on its adsorption

Tables (3.25 - 3.28) show the variation of percentage of nickel ion removal and residual and initial concentration of nickel ions (100 , 200 , 300 mg / L) using (Fe_3O_4) nanoparticles, **Tables (3.29 - 3.32)** using (Fe_2O_3) nanoparticles , and **Tables (3.33 - 3.36)** using (CuO) nanoparticles, and also represented diagrammatically in **Figure (3.19 , 3.20 , and 3.21)** respectively. .

The results indicated that the percentage of nickel ions removal decreases with the increase of initial metal ion concentration, increasing the initial concentration of Ni(II) in a batch study, a saturation point appears which resulted in decreased percentage of Ni(II) removal and this is due to the fact that after the formation of mono ionic layer at low concentration over the adsorbent surface, further formation of the layer is highly hindered at higher concentration due to interaction between nickel ions on the surface and in these solution. Among the three oxide nanoparticles observed, the results showed that the (CuO) nanoparticles gave the best nickel percentage removal with the time, followed by (Fe_2O_3) nanoparticles and then (Fe_3O_4) nanoparticles seem to be show the lowest percentage removal [16,53,84,98] .

.

Table (3.25): Effect of initial concentration of nickel ion on its removal using iron oxide nanoparticles, Fe_3O_4 at contact time of 30 minutes.

Initial Concentration (C_o), mg/L	100	200	300
Residual concentration (C_t), mg/L	21.811	53.568	115.653
Removed concentration (R), mg/L	78.189	146.432	184.347
Residual (C_t)%	21.811	26.784	38.551
Removed (R) %	78.189	73.216	61.449

Table (3.26): Effect of initial concentration of nickel ion on its removal using iron oxide nanoparticles, Fe_3O_4 at contact time of 60 minutes.

Initial Concentration (C_o), mg/L	100	200	300
Residual concentration (C_t), mg/L	18.595	47.566	103.846
Removed concentration (R) , mg/L	81.405	152.434	196.154
Residual (C_t)%	18.595	23.783	34.615
Removed (R) %	81.405	76.217	65.385

Table (3.27): Effect of initial concentration of nickel ion on its removal using iron oxide nanoparticles, Fe_3O_4 at contact time of 90 minutes.

Initial Concentration (C_o), mg/L	100	200	300
Residual concentration (C_t), mg/L	16.762	41.696	91.836
Removed concentration (R), mg/L	83.238	158.304	208.164
Residual (C_t)%	16.762	20.848	30.612
Removed (R) %	83.238	79.152	69.388

Table (3.28): Effect of initial concentration of nickel ion on its removal using iron oxide nanoparticles, Fe_3O_4 at contact time of 120 minutes.

Initial Concentration (C_o), mg/L	100	200	300
Residual concentration (C_t), mg/L	15.175	39.178	73.455
Removed concentration (R), mg/L	84.825	160.822	226.545
Residual (C_t)%	15.175	19.589	24.485
Removed (R) %	84.825	80.411	75.515

Table (3.29): Effect of initial concentration of nickel ion on its removal using iron oxide nanoparticles, Fe_2O_3 at contact time of 30 minutes.

Initial Concentration (C_o), mg/L	100	200	300
Residual concentration (C_t), mg/L	19.911	51.855	101.833
Removed concentration (R), mg/L	80.089	148.145	198.167
Residual (C_t)%	19.911	25.927	33.944
Removed (R) %	80.089	74.073	66.056

Table (3.30): Effect of initial concentration of nickel ion on its removal using iron oxide nanoparticles, Fe_2O_3 at contact time of 60 minutes.

Initial Concentration (Co), mg/L	100	200	300
Residual concentration (Ct), mg/L	16.815	46.934	88.895
Removed concentration (R), mg/L	83.185	153.066	211.105
Residual (Ct)%	16.815	23.467	29.632
Removed (R) %	83.185	76533	70.368

Table (3.31): Effect of initial concentration of nickel ion on its removal using iron oxide nanoparticles, Fe_2O_3 at contact time of 90 minutes.

Initial Concentration (C_o), mg/L	100	200	300
Residual concentration (C_t), mg/L	15.567	42.700	76.944
Removed concentration (R), mg/L	84.433	157.300	223.056
Residual (C_t)%	15.567	21.350	25.648
Removed (R) %	84.433	78.650	74.352

Table (3. 32): Effect of initial concentration of nickel ion on its removal using iron oxide nanoparticles, Fe_2O_3 at contact time of 120 minutes.

Initial Concentration (C_o), mg/L	100	200	300
Residual concentration (C_t), mg/L	13.800	38.745	68.588
Removed concentration (R), mg/L	86.200	161.255	231.412
Residual (C_t)%	13.800	19.373	22.862
Removed (R) %	86.200	80.627	77.137

Table (3.33): Effect of initial concentration of nickel ion on its removal using copper oxide nanoparticles, CuO at contact time of 30 minutes.

Initial Concentration (C_o), mg/L	100	200	300
Residual concentration (C_t), mg/L	17.848	55.256	95.247
Removed concentration (R), mg/L	82.152	144.744	204.753
Residual (C_t)%	17.848	27.628	31.749
Removed (R) %	82.152	72.372	68.251

Table (3.34): Effect of initial concentration of nickel ion on its removal using copper oxide nanoparticles, CuO at contact time of 60 minutes.

Initial Concentration (C_o), mg/L	100	200	300
Residual concentration (C_t), mg/L	16.154	48.614	90.327
Removed concentration (R), mg/L	83.846	151.386	209.673
Residual (C_t)%	16.154	24.307	30.109
Removed (R) %	83.846	75.693	69.891

Table (3.35): Effect of initial concentration of nickel ion on its removal using copper oxide nanoparticles, CuO at contact time of 90 minutes.

Initial Concentration (C_o), mg/L	100	200	300
Residual concentration (C_t), mg/L	13.056	40.552	83.604
Removed concentration (R), mg/L	86.944	159.448	216.396
Residual (C_t)%	13.056	20.276	27.868
Removed (R) %	86.944	79.724	72.132

Table (3.36): Effect of initial concentration of nickel ion on its removal using copper oxide nanoparticles, CuO at contact time of 120 minutes.

Initial Concentration (C_o), mg/L	100	200	300
Residual concentration (C_t), mg/L	10.948	37.910	72.978
Removed concentration (R), mg/L	89.052	162.090	227.022
Residual (C_t)%	10.948	18.955	24.326
Removed (R) %	89.052	81.045	75.674

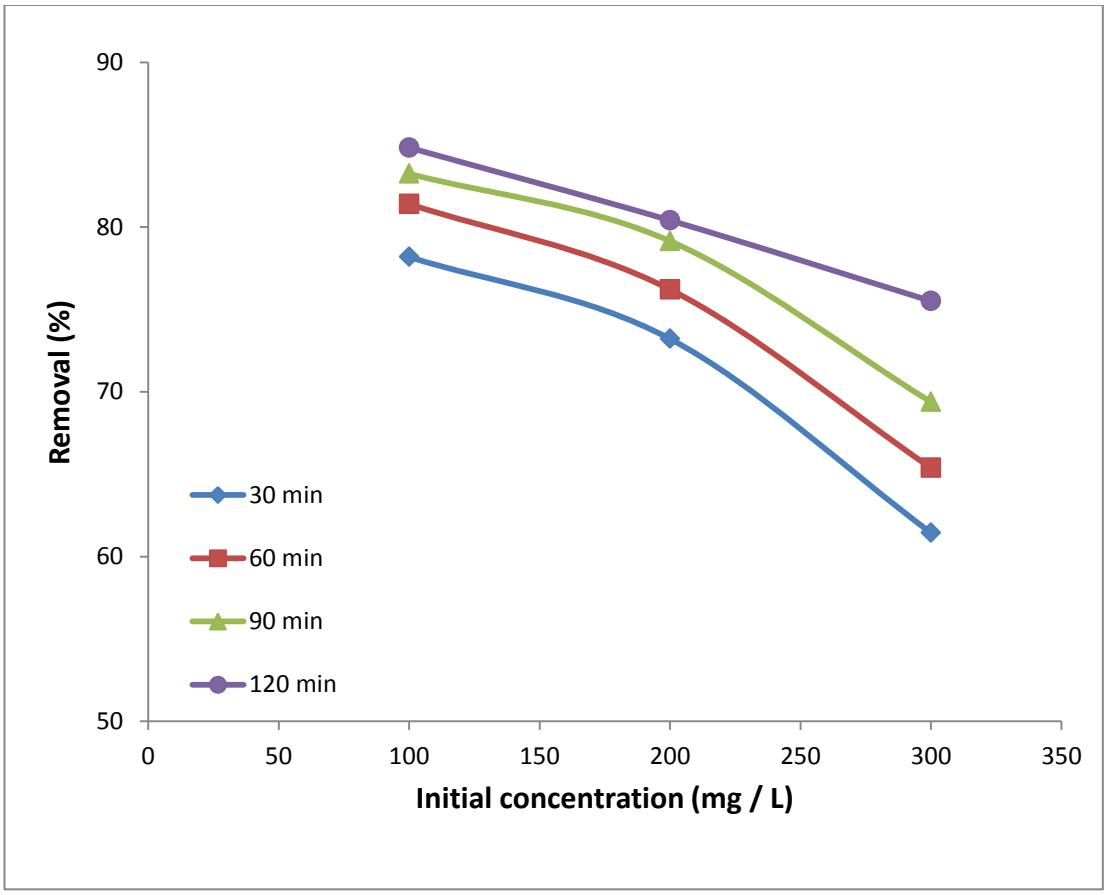

Figure (3.19): Relationship between initial concentration of nickel ion (100, 200, and 300 mg/ L) and percentage removal of it by adsorption on iron oxide nanoparticles, Fe_3O_4 at different contact times.

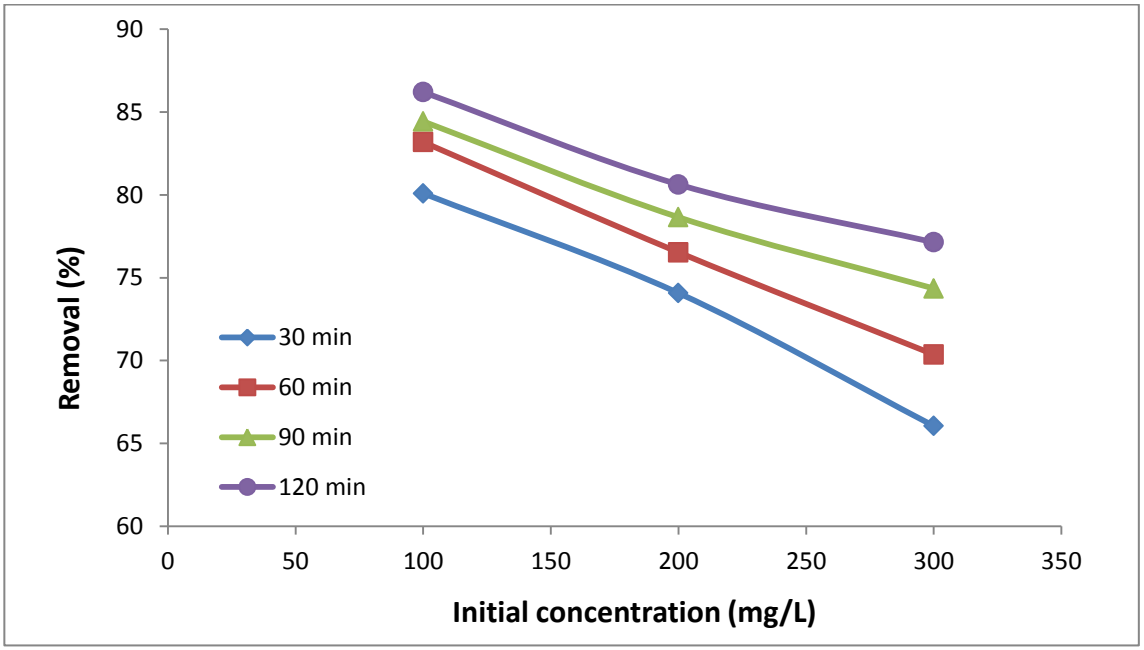

Figure (3.20) : Relationship between initial concentration of nickel ion (100, 200, and 300 mg/L) on the percentage removal of it by adsorption on iron oxide nanoparticles, Fe_2O_3 at different contact times .

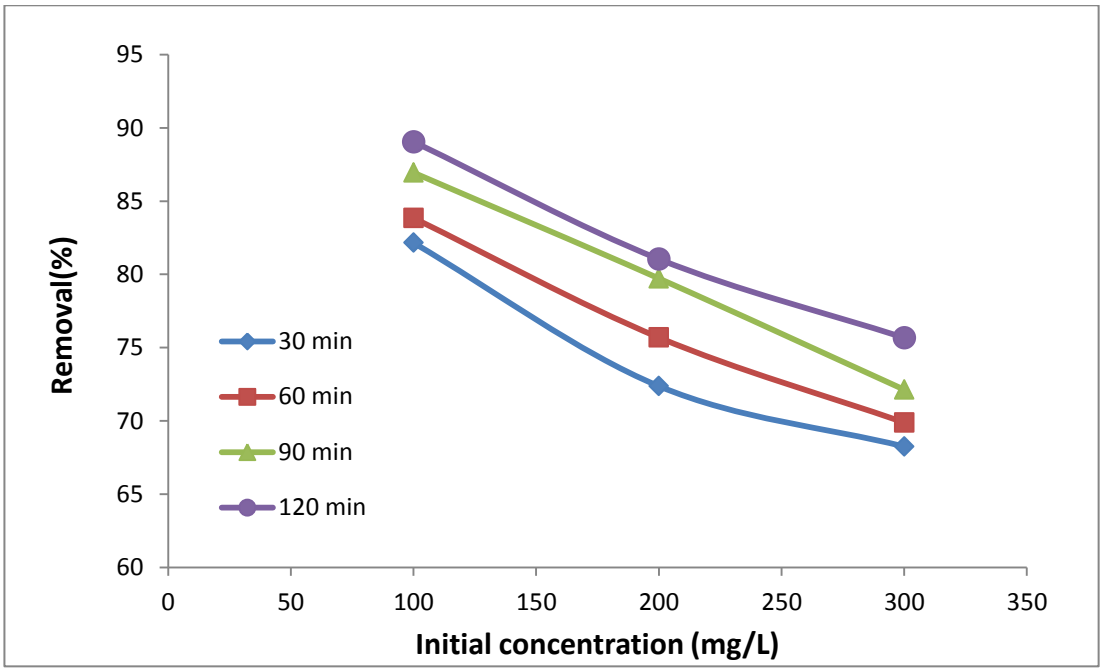

Figure (3.21): Relationship between initial concentration of nickel ion (100, 200, and 300 mg/L) on the percentage removal of it by adsorption on copper oxide nanoparticles, CuO at different contact times .

3.2.2.2: Effect of the initial concentration of lead ions on its adsorption

Tables (3.37 - 3.40) show the variation of percentage lead ion residual and removal with different initial concentration of lead ions (100 , 200 , 300 mg/L) using (Fe_3O_4) nanoparticles, **Tables (3.41 - 3.44)** using (Fe_2O_3) nanoparticles , and **Tables (3.45 - 3.48)** using (CuO) nanoparticles, and also diagrammatically represented in **Figures (3.22 , 3.23 , and 3.24)** respectively.

The effect of initial concentration on the lead ion percentage removal by metal oxides nanoparticles plays an important role in the adsorption process. It is observed that the percentage removal decreases with the increasing of initial lead ion concentration which is due to increase in the driving force of the concentration gradient. When the concentrations decreased, the percentages removals were higher due to a larger surface area of the adsorbent being available for the adsorption of metal ions. When the concentration is high, the percentages removals are low because the available sites of the adsorption became less and when initial concentration increased until it reached the saturation point with time until no more lead ions was further removed from solution. Thus maximum adsorption of lead was recorded with 100 mg/L for the three nanoparticle oxides but the (Fe_3O_4) nanoparticle gave the best lead ion percentage removal followed by (Fe_2O_3) nanoparticles, followed by (CuO) nanoparticles [17,40,93] .

Table (3.37): Effect of initial concentration of lead ion on its removal using iron oxide nanoparticles, Fe_3O_4 at contact time of 30 minutes.

Initial concentration (C_o), mg/L	100	200	300
Residual concentration (C_t), mg/L	14.621	34.286	54.348
Removed concentration (R) , mg/L	85.379	165.714	245.652
Residual (C_t)%	14.621	17.143	18.116
Removed (R) %	85.379	82.857	81.884

Table (3.38): Effect of initial concentration of lead ion on its removal using iron oxide nanoparticles, Fe_3O_4 at contact time of 60 minutes.

Initial Concentration (C_o) , mg/L	100	200	300
Residual concentration (C_t), mg/L	11.594	27.304	43.629
Removed concentration (R), mg/L	88.406	172.696	256.371
Residual (C_t)%	11.594	13.652	14.543
Removed (R) %	88.406	86.348	85.457

Table (3.39): Effect of initial concentration of lead ion on its removal using iron oxide nanoparticles, Fe_3O_4 at contact time of 90 minutes.

Initial concentration (C_o), mg/L	100	200	300
Residual concentration, (C_t), mg/L	5.123	16.124	27.261
Removed concentration, (R), mg/L	94.877	183.876	272.739
Residual (C_t)%	5.123	8.062	9.087
Removed (R) %	94.877	91.938	90.913

Table (3.40): Effect of initial concentration of lead ion on its removal using iron oxide nanoparticles, Fe_3O_4 at contact time of 120 minutes.

Initial concentration (C_o), mg/L	100	200	300
Residual concentration (C_t), mg/L	4.786	14.554	25.395
Removed concentration (R), mg/L	95.214	185.446	274.605
Residual (C_t)%	4.786	7.277	8.465
Removed (R) %	95.214	92.723	91.535

Table (3.41): Effect of initial concentration of lead ion on its removal using iron oxide nanoparticles, Fe_2O_3 at contact time of 30 minutes.

Initial concentration (C_o), mg/L	100	200	300
Residual concentration (C_t), mg/L	15.471	33.200	54.048
Removed concentration (R), mg/L	84.259	166.800	245.952
Residual (C_t)%	15.471	16.600	18.016
Removed (R) %	84.259	83.400	81.984

Table (3.42): Effect of initial concentration of lead ion on its removal using iron oxide nanoparticles, Fe_2O_3 at contact time of 60 minutes.

Initial concentration (C_o), mg/L	100	200	300
Residual concentration (C_t), mg/L	11.910	26.382	43.143
Removed concentration (R), mg/L	88.090	173.618	256.857
Residual (Ct)%	11.910	13.191	14.381
Removed (R) %	88.090	86.809	85.619

Table (3.43): Effect of initial concentration of lead ion on its removal using iron oxide nanoparticles, Fe_2O_3 at contact time of 90 minutes.

Initial concentration (C_o), mg/L	100	200	300
Residual concentration, (C_t), mg/L	6.177	18.672	32.748
Removed concentration, (R), mg/L	93.823	181.328	267.252
Residual (C_t)%	6.177	9.366	10.916
Removed (R) %	93.823	90.664	89.084

Table (3.44): Effect of initial concentration of lead ion on its removal using iron oxide nanoparticles, Fe_2O_3 at contact time of 120 minutes.

Initial concentration (C_o) , mg/L	100	200	300
Residual concentration (C_t), mg/L	5.467	17.328	27.393
Removed concentration, (R) , mg/L	94.533	182.672	272.607
Residual (C_t)%	5.467	8.664	9.131
Removed (R) %	94.533	91.336	90.869

Table (3.45): Effect of initial concentration of lead ion on its removal using copper oxide nanoparticles, CuO at contact time of 30 minutes.

Initial concentration (C_o), mg/L	100	200	300
Residual concentration (C_t), mg/L	20.596	43.626	64.137
Removed concentration (R), mg/L	79.404	156.374	235.863
Residual (C_t)%	20.596	21.813	21.379
Removed (R) %	79.404	78.187	78.621

Table (3.46): Effect of initial concentration of lead ion on its removal using copper oxide nanoparticles, CuO at contact time of 60 minutes.

Initial concentration (C_o), mg/L	100	200	300
Residual concentration (C_t), mg/L	17.601	38.822	56.544
Removed concentration (R), mg/L	82.399	161.178	243.456
Residual (C_t)%	17.601	19.411	18.884
Removed (R) %	82.399	80.589	81.152

Table (3.47): Effect of initial concentration of lead ion on its removal using copper oxide nanoparticles, CuO at contact time of 90 minutes.

Initial concentration (C_o), mg/L	100	200	300
Residual concentration (C_t), mg/L	13.123	32.372	51.195
Removed concentration (R), mg/L	86.877	167.628	248.805
Residual (C_t)%	13.123	16.186	17.064
Removed (R) %	86.877	83.814	82.936

Table (3.48): Effect of initial concentration of lead ion on its removal using copper oxide nanoparticles, CuO at contact time of 120 minutes.

Initial Concentration (C_o), mg/L	100	200	300
Residual concentration (C_t), mg/L	12.877	30.928	48.438
Removed concentration (R), mg/L	87.123	169.072	251.562
Residual (C_t)%	12.877	15.464	16.146
Removed (R) %	87.123	84.536	83.854

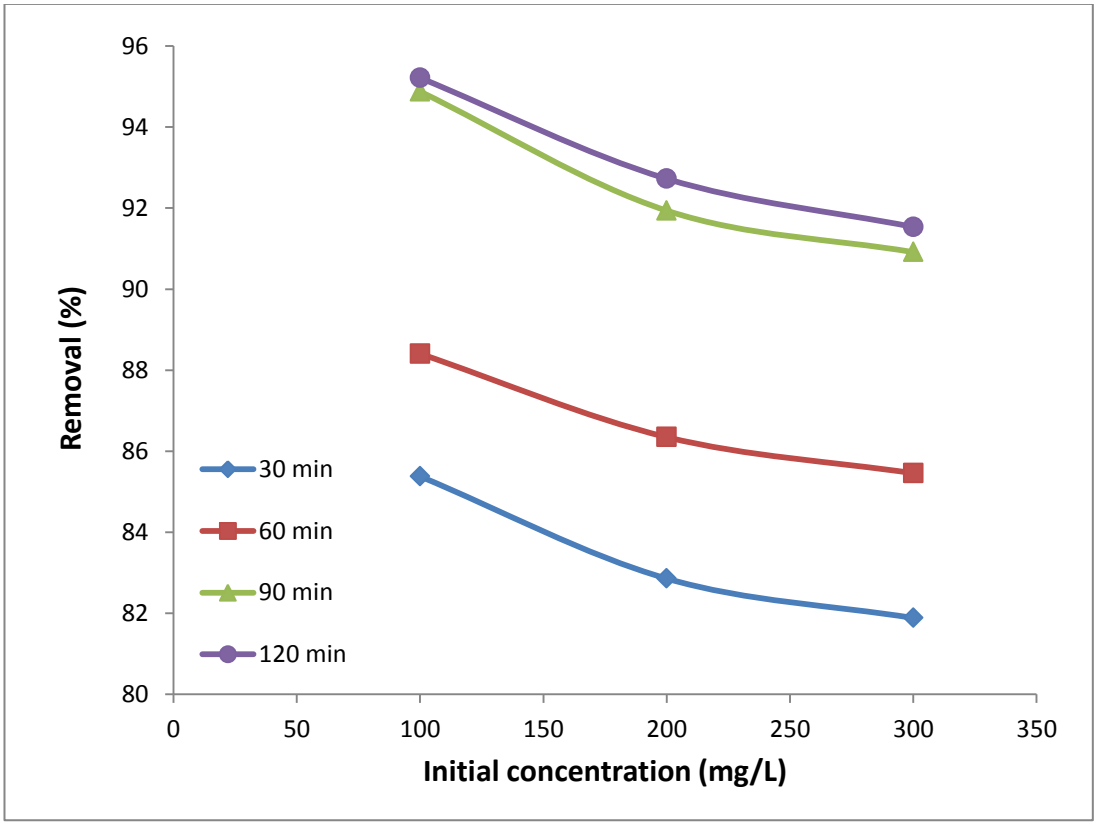

Figure (3.22): Relationship between initial concentration of lead ion (100, 200, and 300 mg/L) and percentage removal of it by adsorption on iron oxide nanoparticles, Fe_3O_4 at different contact times.

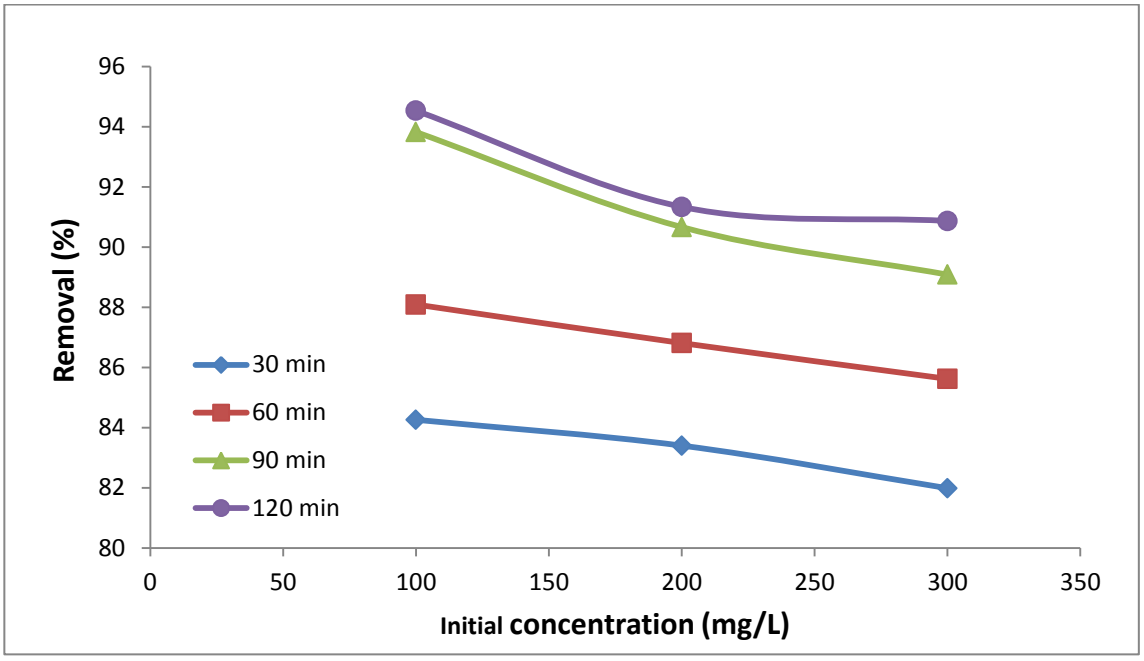

Figure (3.23): Relationship between initial concentration of lead ion (100, 200,and 300 mg/L) and percentage removal of it by adsorption on iron oxide nanoparticles, Fe_2O_3 at different contact times .

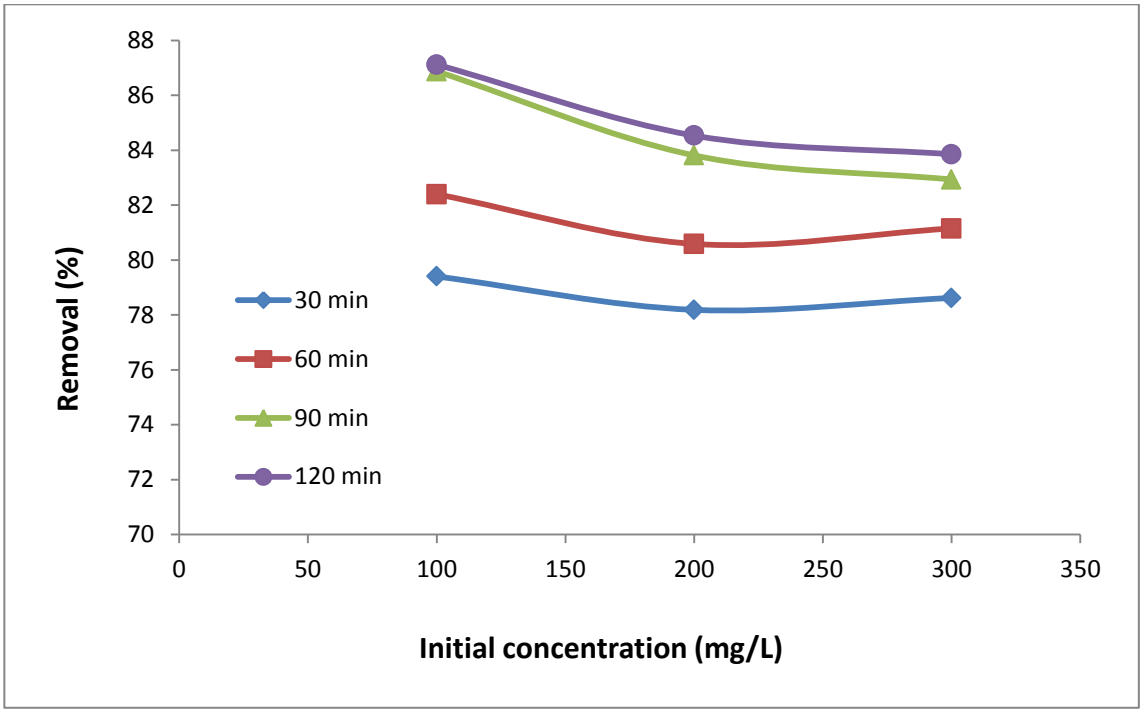

Figure (3.24): Relationship between initial concentration of lead ion (100, 200, and 300 mg/L) and percentage removal by adsorption on copper oxide nanoparticles, CuO at different contact times .

3.2.3: The adsorption isotherm

Adsorption of nickel and lead ions from an aqueous solutions by using (Fe_3O_4) nanoparticles, (Fe_2O_3) nanoparticles , and (CuO) nanoparticles, are studied at room temperature 25±1˚C and keeping the pH of solution at 3.5 using a different concentration (C_o =100 , 200 , and 300 mg/L), adsorbent dosage (0.1g) and different times (30 , 60 , 90 and 120) minutes.

The results are represented by initial concentration of nickel and lead ions $\mathbf{C_o}$, the equilibrium concentration $\mathbf{C_e}$ measured at equilibrium time and quantity adsorbed $\mathbf{Q_e}$, $\mathbf{Q_e}$ values were calculated from experimental data by using equation **(2.4)** , and are listed in **Tables (3.49) and (3.50)**for nickel and lead ions respectively .

The quantities adsorbed $\mathbf{Q_e}$ are plotted versus equilibrium concentration $\mathbf{C_e}$ to obtain general adsorption isotherms of nickel ions removal which are shown in **Figures (3.25 , 3.26 , and 3.27)** using (Fe_3O_4) nanoparticles, (Fe_2O_3) nanoparticles , and (CuO) nanoparticles respectively, and also adsorption isotherms of lead ions removal which are shown in **Figures (3.28 , 3.29, and 3.30)** using (Fe_3O_4) nanoparticles, (Fe_2O_3) nanoparticles , and (CuO) nanoparticles respectively.

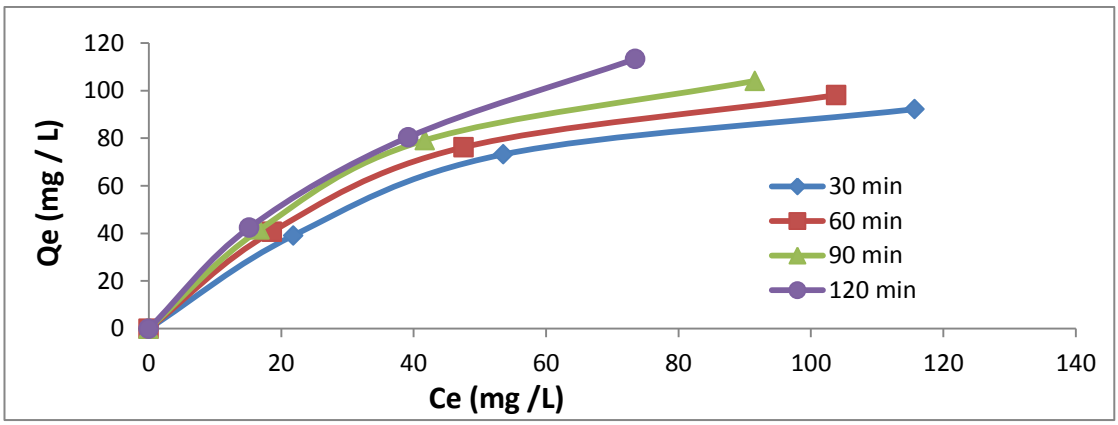

Figure (3.25): Adsorption isotherm of nickel ions removal on iron oxide nanoparticle, Fe_3O_4 surface at different contact times.

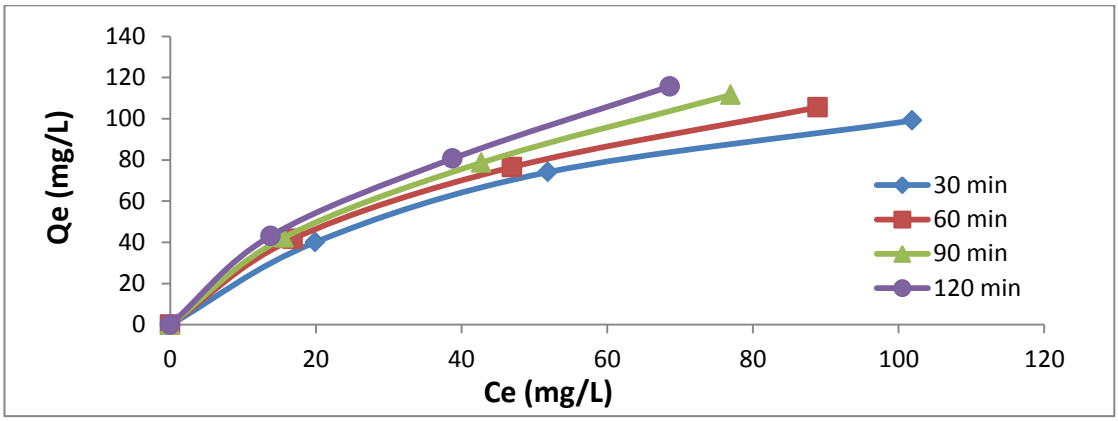

Figure (3.26): Adsorption isotherm of nickel ions removal on iron oxide nanoparticle, Fe_2O_3 surface at different contact times.

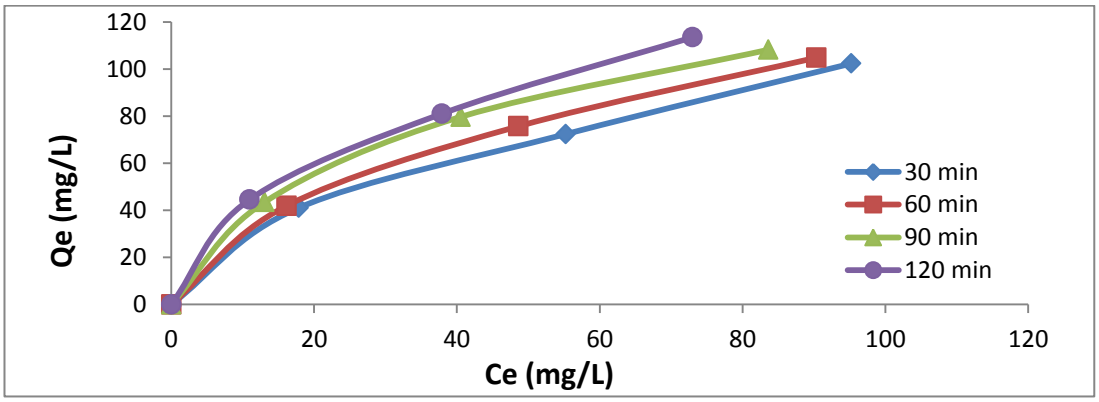

Figure (3.27): Adsorption isotherm of nickel ions removal on copper oxide nanoparticle, CuO surface at different contact times

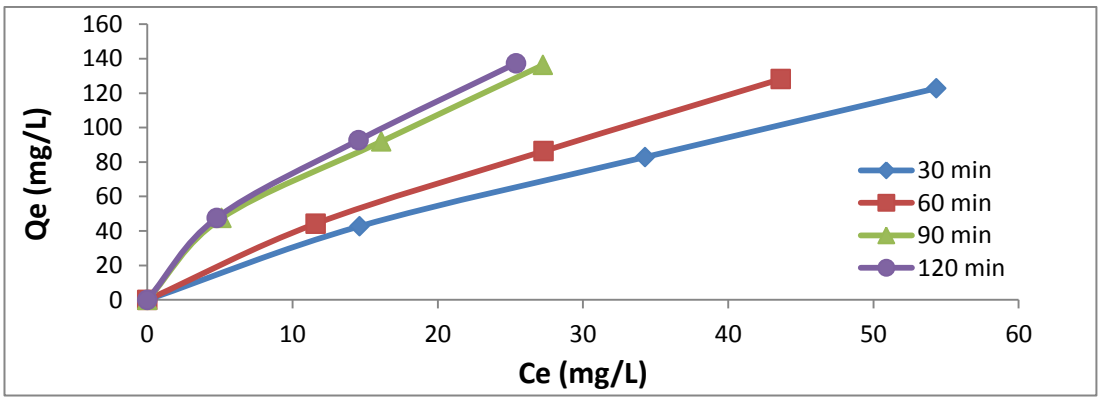

Figure (3.28): Adsorption isotherm of lead ions removal on iron oxide nanoparticle, Fe_3O_4 surface at different contact times.

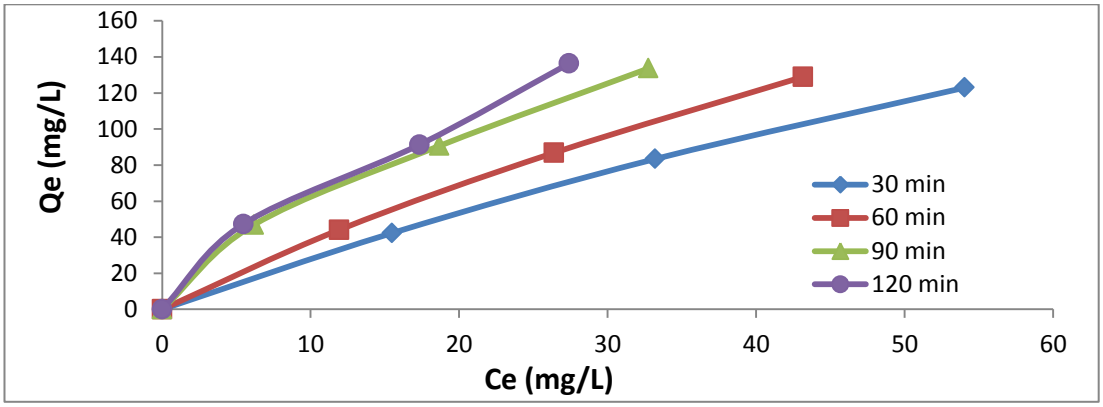

Figure (3.29): Adsorption isotherm of lead ions removal on iron oxide nanoparticle, Fe_2O_3 surface at different contact times.

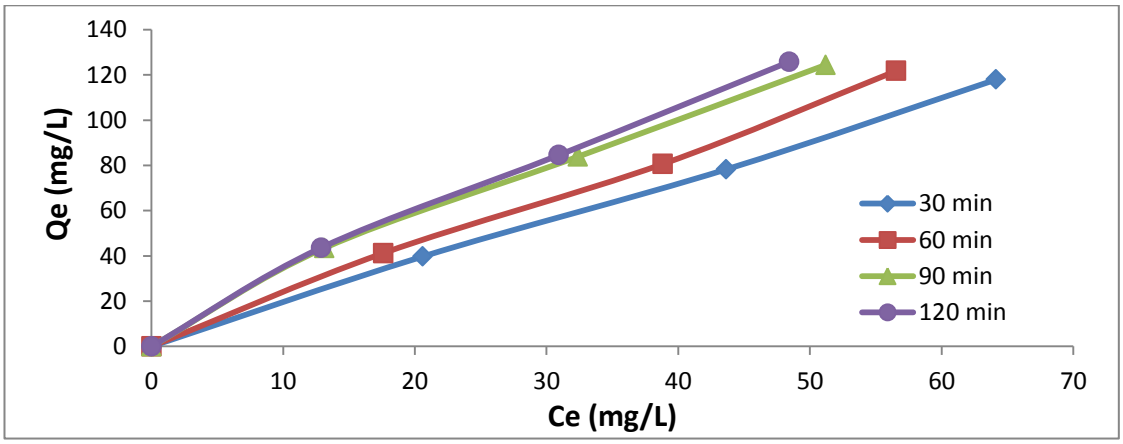

Figure (3.30): Adsorption isotherm of lead ions removal on copper oxide nanoparticle, CuO surface at different contact times.

The results showed increase in adsorption capacities of the (Fe_3O_4) nanoparticles, (Fe_2O_3) nanoparticles, and (CuO) nanoparticles with the equilibrium concentration of solutions, and reached high values. The general shape of the adsorption isotherms of nickel and lead ions removal on the (Fe_3O_4) nanoparticles, (Fe_2O_3) nanoparticles, and (CuO) nanoparticles is consistent with L-Type of Giles classification shown in **Figure (1.1).** The isotherm of the mentioned system obeyed to the assumption of high adsorption of nickel and lead ions on adsorbent surfaces at the beginning . This strongly adsorbed on the adsorbent because there is no competition from solvent for adsorbent sites [72].

Langmuir equation **(1. 1)** and Freundlich equation **(1. 3)** are applied for adsorption equilibrium for the (Fe_3O_4) nanoparticles, (Fe_2O_3) nanoparticles, and (CuO) nanoparticles at different times in order to see the best model that describe the adsorption phenomena. .

Adsorption isotherm data for nickel ions removal are plotted and presented in **Tables (3.51) and (3.52) , and Figures (3.31) – (3.36).**

. The values of the Langmuir isotherm constants, ***a*** , which is the monolayer adsorption capacity , ***b***, which is constantly related to the energy of adsorption were calculated from the slope and intercept of plots of (C_e /Q_e) versus C_e of equation (1.1), and the Freundlich isotherm constants , K_f , which is the adsorption capacity of the adsorbent , and ***n*** , which is the adsorption intensity being calculated from the slope and intercept of plots of (log Q_e) versus (log C_e) of equation (1.3) , and the results are shown in **Table (3.53).** .

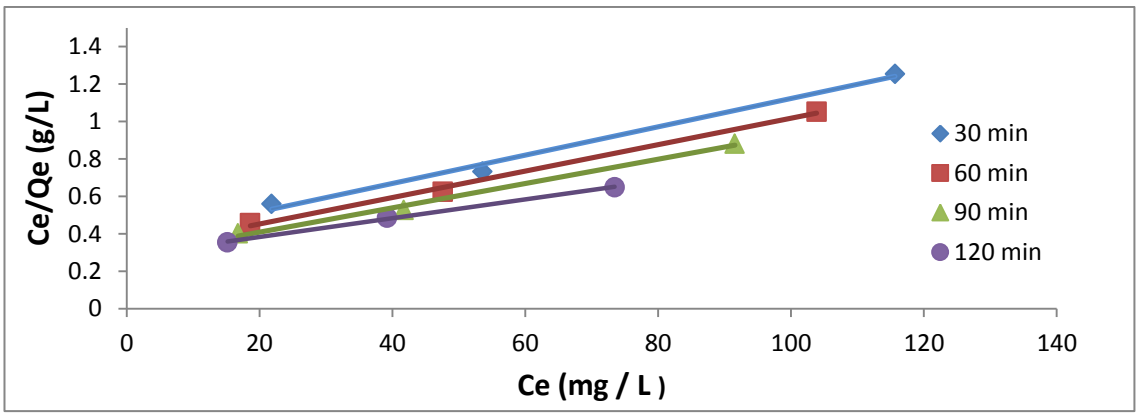

Figure (3.31): Linear Langmuir isotherm of nickel ions adsorption on iron oxide nanoparticle, Fe_3O_4 surface at different contact times.

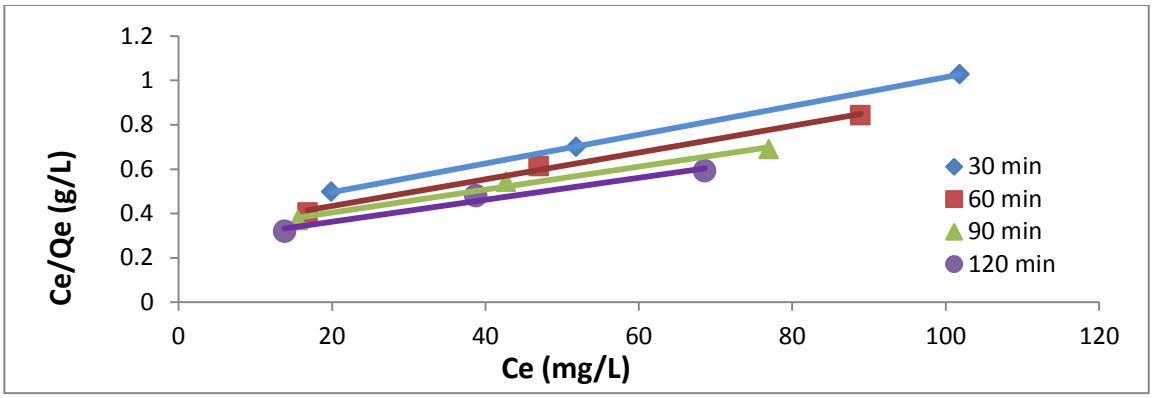

Figure (3.32): Linear Langmuir isotherm of nickel ions adsorption on iron oxide nanoparticle, Fe_2O_3 surface at different contact times

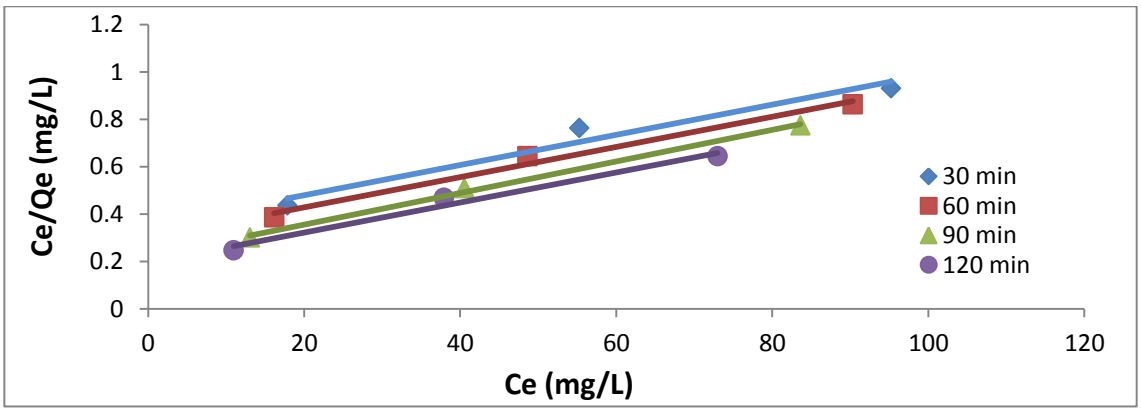

Figure (3.33) : Linear Langmuir isotherm of nickel ions adsorption copper oxide nanoparticle, CuO surface at different contact times

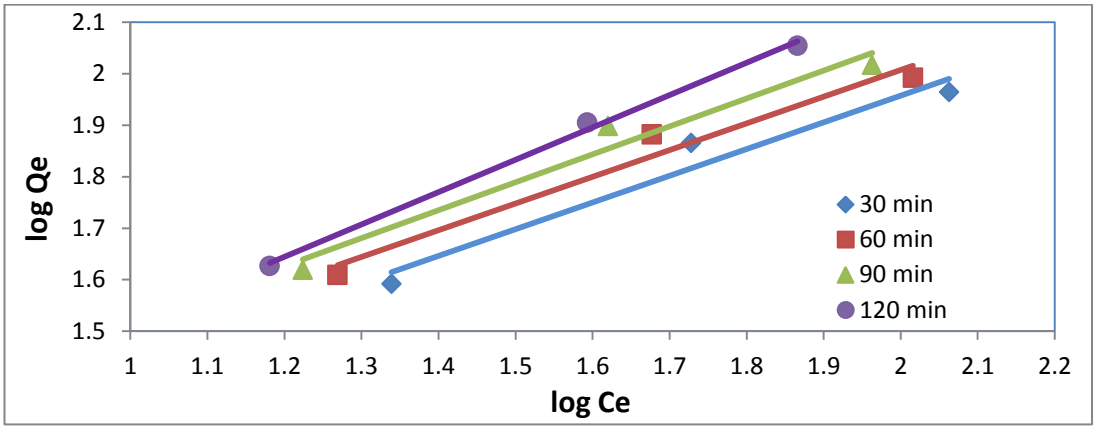

Figure (3.34): Linear freundlich isotherm of nickel ions adsorption on iron oxide nanoparticle, Fe_3O_4 surface at different contact times.

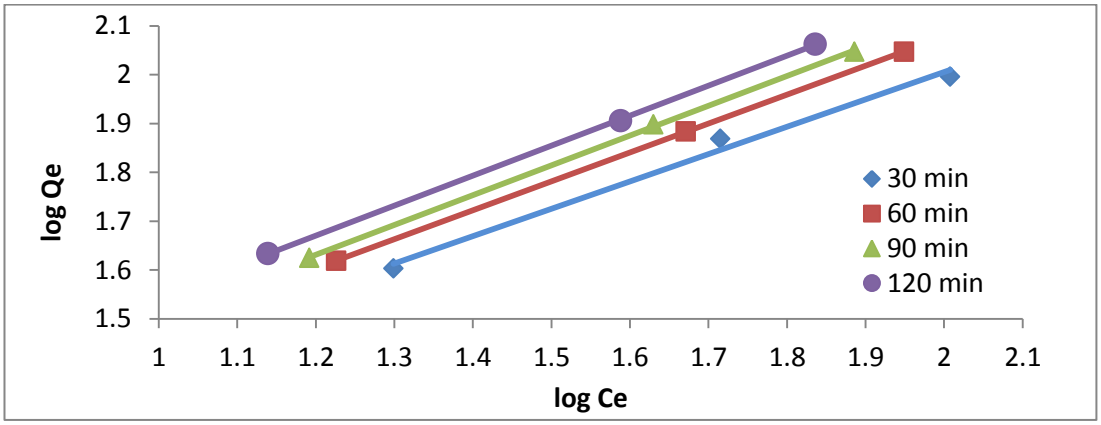

Figure (3.35): Linear freundlich isotherm of nickel ions adsorption on iron oxide nanoparticle, Fe_2O_3 surface at different contact times

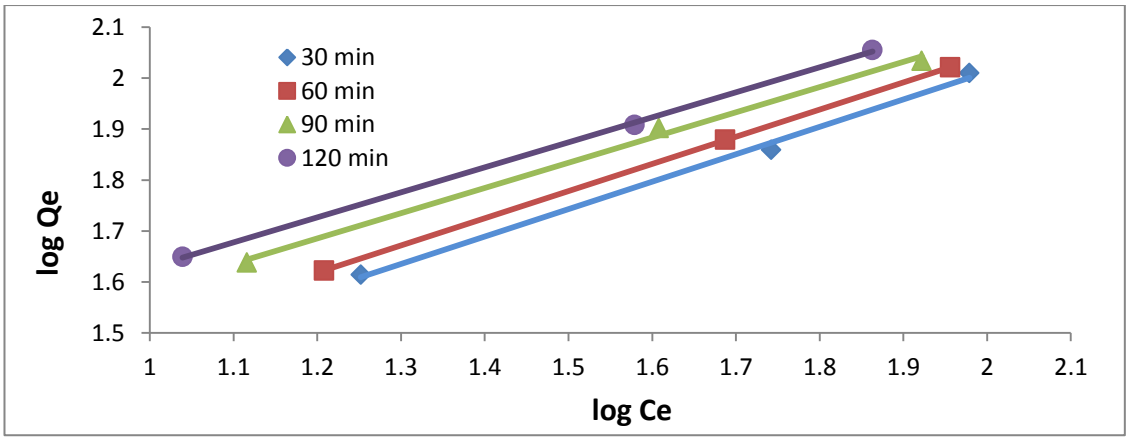

Figure (3.36): Linear freundlich isotherm of nickel ions adsortion on copper oxide nanoparticle, CuO surface at different contact times.

From **Table (3.53)**, the correlation coefficient for the linear Langmuir regression fits is higher than that for the Freundlich plot for the (Fe_3O_4) nanoparticles, so the Langmuir model can describe the adsorption isotherm for the uptake of nickel ions from aqueous solution on (Fe_3O_4) nanoparticles surfaces, indicating the applicability of monolayer coverage of the nickel ions on the surfaces of adsorbents and basing on assumption that the surfaces are homogeneous [16,52] , but with (Fe_2O_3) nanoparticles, and (CuO) nanoparticles , the results show what is otherwise based on the correlation coefficient data for adsorption of nickel ions from aqueous solution on each of (Fe_2O_3) nanoparticles, and (CuO) nanoparticles, which fit better to Freundlich isotherm model than the Langmuir one. So the adsorption of nickel ions is best described by the Freundlich isotherm model [16].The results indicated that the mono layer adsorption capacity ***a*** , energy of adsorption ***b***, adsorption capacities K_f , and adsorption intensity ***n*** of nickel ions removal on (Fe_3O_4) nanoparticles, (Fe_2O_3) nanoparticles, and (CuO) nanoparticles are increase with an increase of contact time.

Adsorption isotherm data for lead ions removal are plotted and presented in **Tables (3.54) and (3.55), and Figures (3.37 – 3.42).**
The values of the Langmuir and Freundlich isotherm constants are shown in **Table (3.56).**

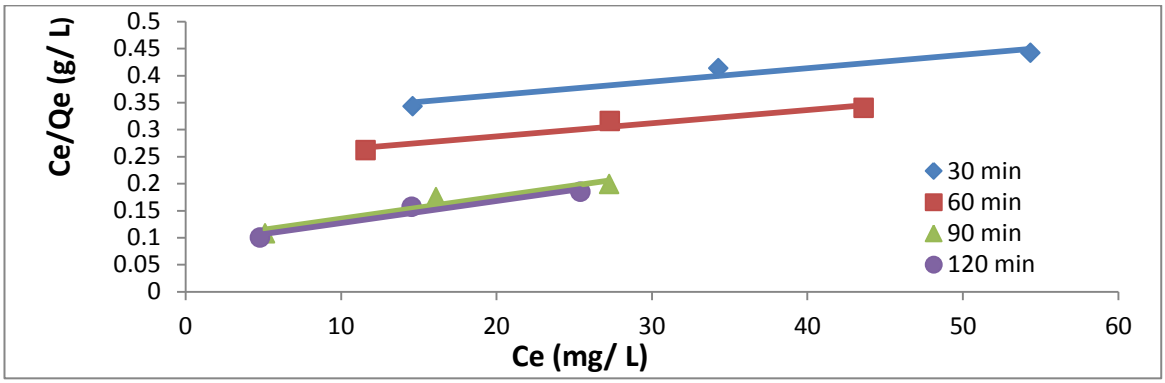

Figure (3.37): Linear Langmuir isotherm of lead ions adsorption on iron oxide nanoparticle, (Fe_3O_4) surface at different contact times.

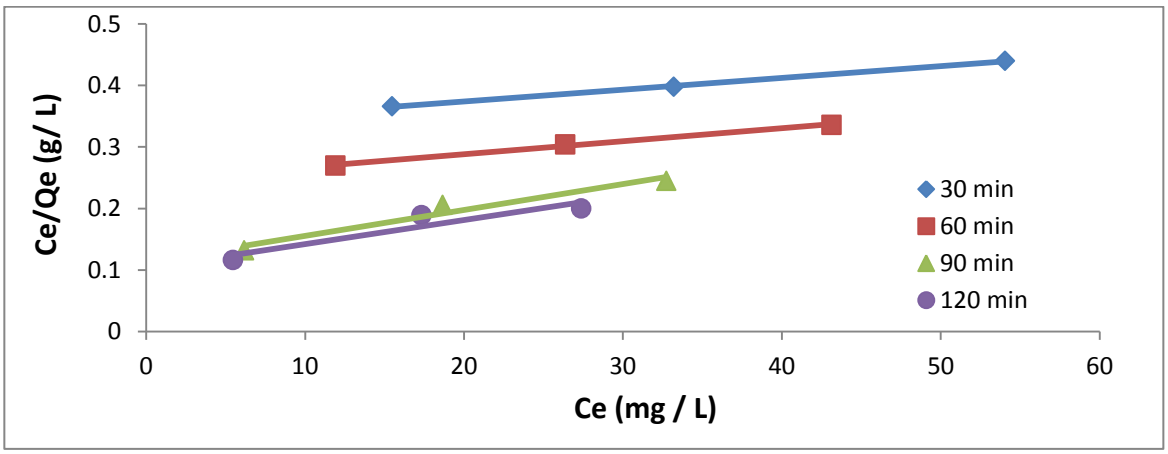

Figure (3.38): Linear Langmuir isotherm of lead ions adsorption on iron oxide nanoparticle, Fe_2O_3 surface at different contact times

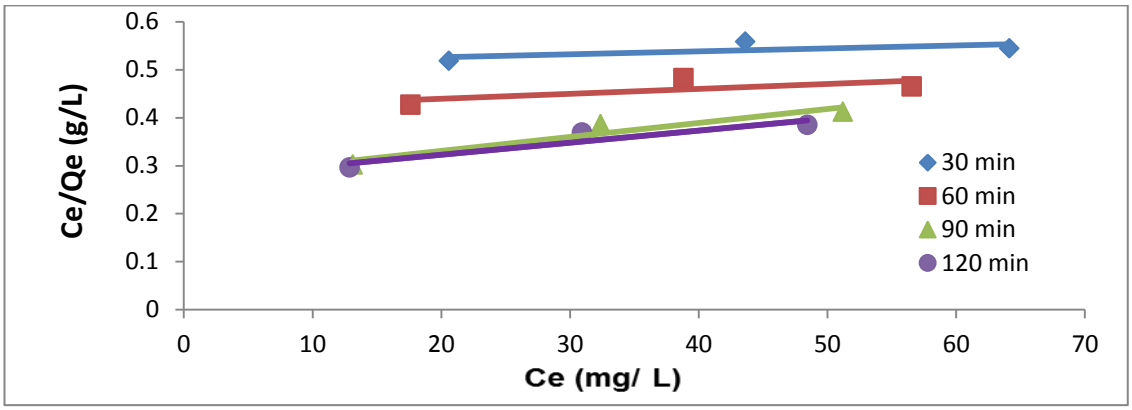

Figure (3.39): Linear Langmuir isotherm of lead ions adsorption on copper oxide nanoparticle, CuO surface at different contact times

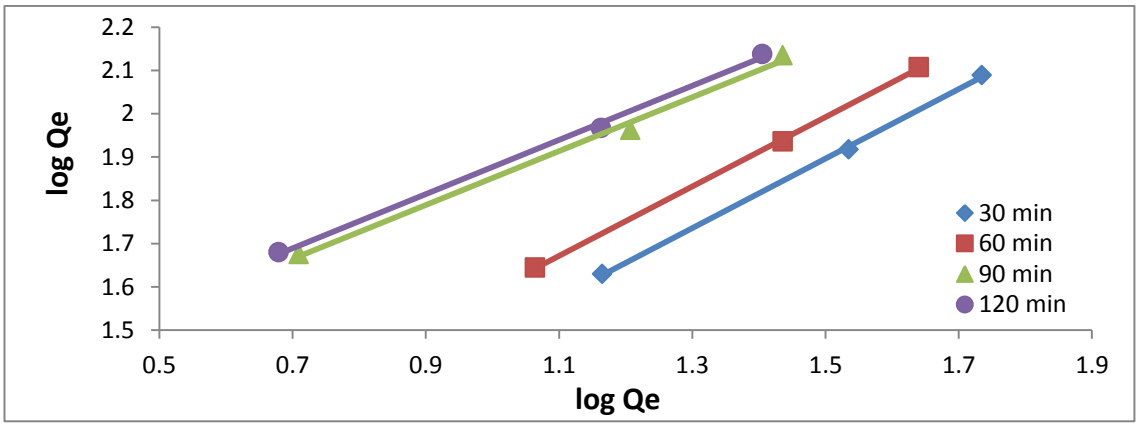

Figure (3.40): Linear Freundlich isotherm of lead ions adsorption on iron oxide nanoparticle, Fe_3O_4 surface at different contact times.

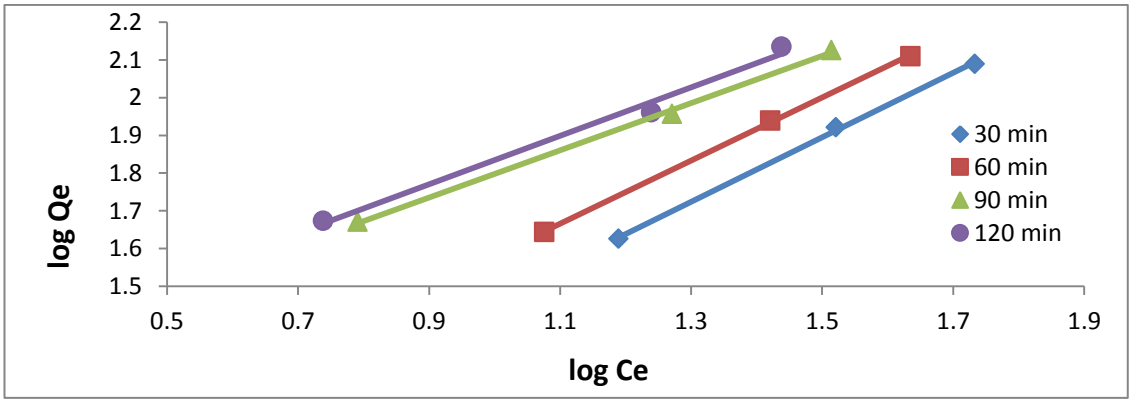

Figure (3.41): Linear Freundlich isotherm of lead ions adsorption on iron oxide nanoparticle, Fe_2O_3 surface at different contact times

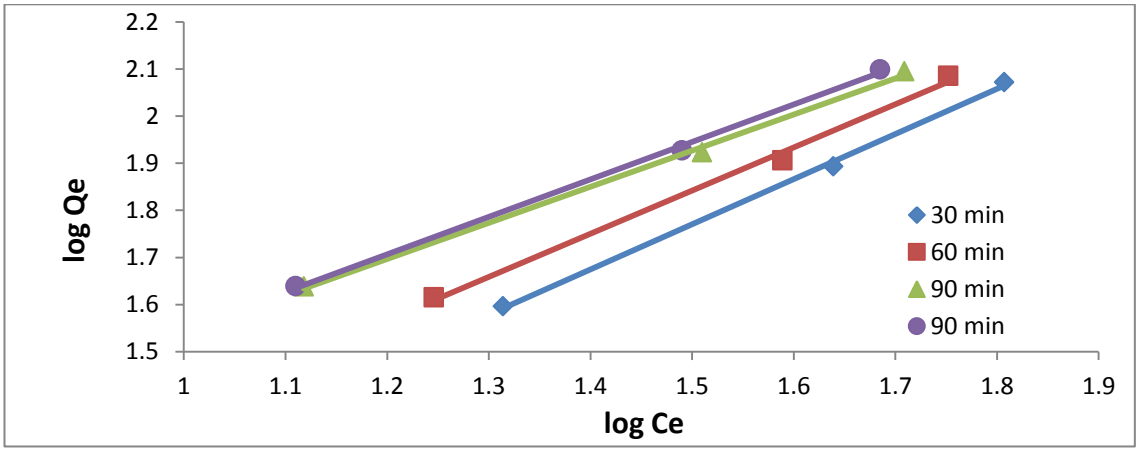

Figure (3.42): Linear Freundlich isotherm of lead ions adsorption on copper oxide nanoparticle, CuO surface at different contact times.

As presented in **Table (3.56)** ,the correlation coefficient for the linear Freundlich regression fits is higher than that for the Langmuir plot for of the three oxide nanoparticles ,(Fe_3O_4) , (Fe_2O_3), and (CuO), so the Freundlich model could describe the adsorption isotherm for the uptake of lead ions from aqueous solution using the three oxide nanoparticles, (Fe_3O_4),(Fe_2O_3),and(CuO)surfaces [45,99].

The results indicated that the mono layer adsorption capacity ***a*** , energy of adsorption ***b***, adsorption capacities K_f , and adsorption intensity ***n*** of lead ions uptake on (Fe_3O_4) nanoparticles, (Fe_2O_3) nanoparticles, and (CuO) nanoparticles are increase with an increase of contact time .

3.2.4: Kinetic study of adsorption of nickel and lead ions by metal oxide nanoparticles

Kinetic studies are carried out using (0.1g) of (Fe_3O_4) or (Fe_2O_3) or (CuO) nanoparticles add to Ni (II) ion solution with initial concentration (100 mg /L) at 25±2℃ and pH of 3.5 with constant stirring speed 150 rpm and intervals times (30, 60, 90, 120) minute.

The order of adsorbate – adsorbent interaction is described using various kinetic models. **Tables (3.57, 3.58)**, show the kinetic data for adsorption of nickel ion on (Fe_3O_4) or (Fe_2O_3) or (CuO) nanoparticles surface using pseudo-first and second order model where the pseudo-first and second order models are describe by the equations (2.5 and 2.6) respectively .

The slope and intercept of plots of (ln C_2/C_1) versus *t* in **Figure (3.43)** are used to determine the pseudo-first order rate constant k_1 and the correlation coefficient R^2.

The plots of ($1/C_2$) against t give a linear relationship , and k_2 and the correlation coefficient R^2 where calculated from the slope and intercept of line of **Figure (3.44).**

Table (3.57): Pseudo-first order kinetic data for adsorption of nickel ion on Fe_3O_4, Fe_2O_3 , and CuO nanoparticles surfaces.

Time	C_1	Fe_3O_4		Fe_2O_3		CuO	
		C_2	$\ln (C_2/C_1)$	C_2	$\ln (C_2/C_1)$	C_2	$\ln (C_2/C_1)$
30	100	21.811	-1.5228	19.911	1.6139	17.848	1.7233
60	100	18.595	-1.6823	16.815	1.7829	16.154	1.8230
90	100	16.762	-1.7861	15.567	1.8600	13.056	2.0359
120	100	15.175	-1.8855	13.800	1.9805	10.948	2.2120

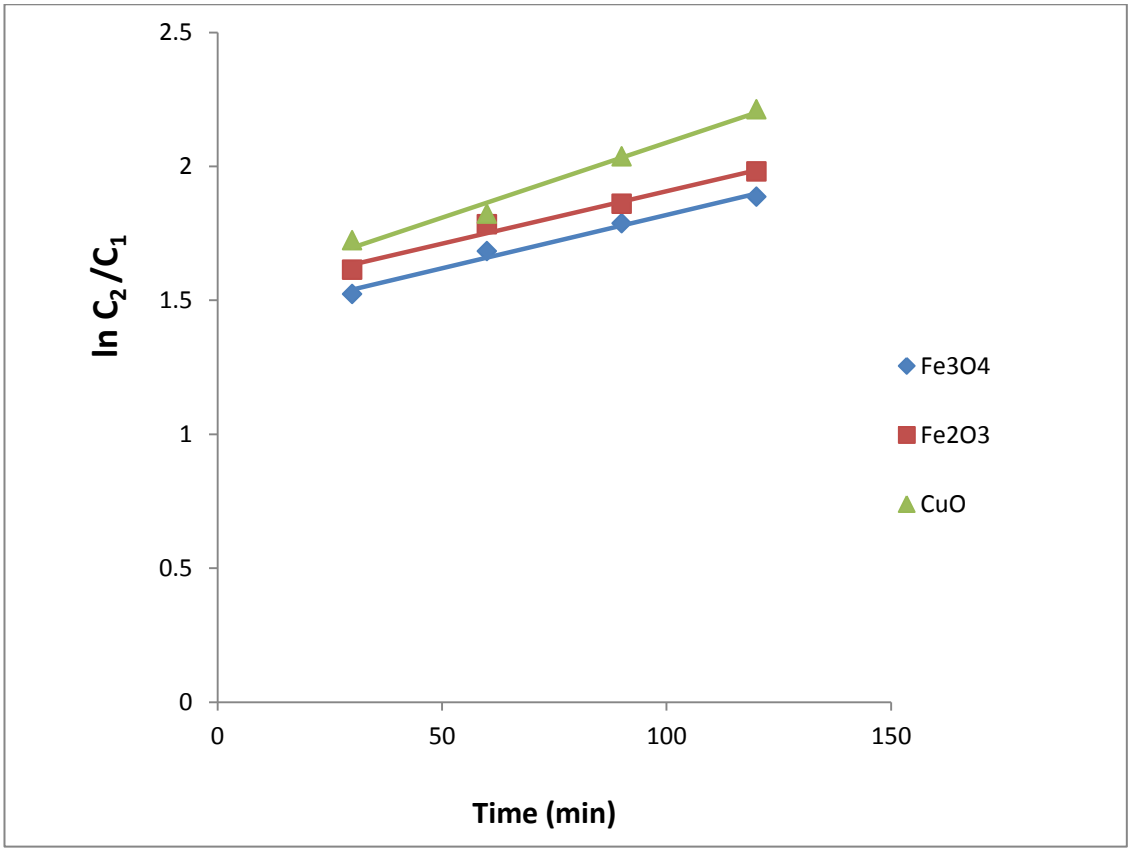

Figure (3.43): Pseudo-first order kinetic plot for the adsorption of nickel ion on Fe_3O_4 , Fe_2O_3, and CuO nanoparticles surfaces.

Table (3.58): Pseudo-second order kinetic data for adsorption of nickel ion on Fe_3O_4, Fe_2O_3, and CuO nanoparticles surfaces.

Time	C_1	Fe_3O_4		Fe_2O_3		CuO	
		C_2	$1/C_2$	C_2	$1/C_2$	C_2	$1/C_2$
30	100	21.811	0.0458	19.911	0.0502	17.848	0.056
60	100	18.595	0.0538	16.815	0.0595	16.154	0.0619
90	100	16.762	0.0597	15.567	0.0642	13.056	0.0766
120	100	15.175	0.0659	13.800	0.0725	10.948	0.0913

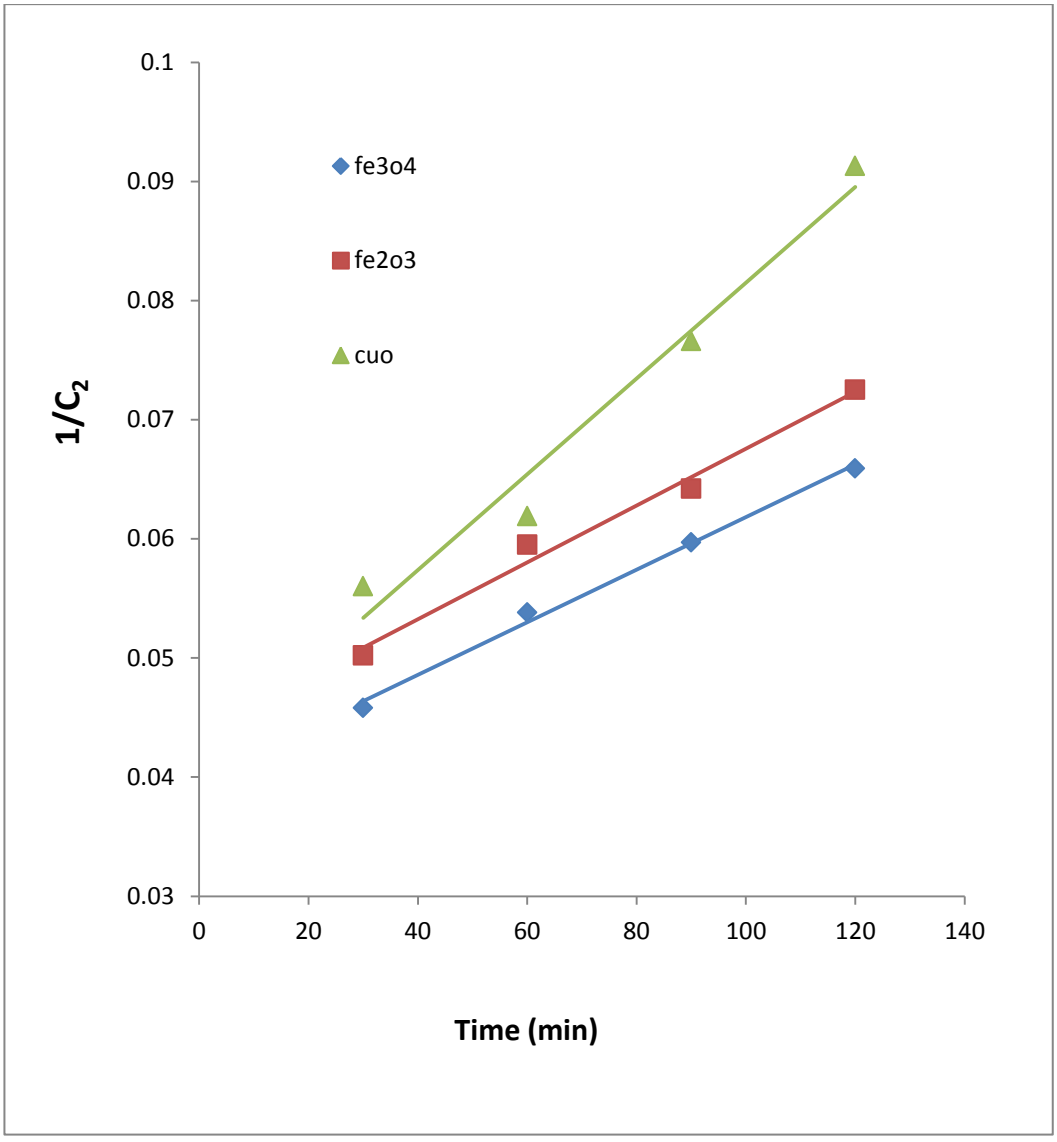

Figure (3.44): Pseudo-second order kinetic plot for the adsorption of nickel ion on Fe_3O_4, Fe_2O_3, and CuO nanoparticles surfaces

Table (3.59): The Pseudo-first, and second orders and their correlation coefficient of nickel adsorption

Oxide nanoparticles	k_1	R^2	k_2	R^2
Fe_3O_4	0.0040	0.9856	0.0002	0.995
Fe_2O_3	0.0039	0.9788	0.0002	0.9861
CuO	0.0056	0.982	0.0004	0.996

The result in **Table (3.59)** show the correlation coefficient of pseudo-second order as higher in comparison with the pseudo-first order and the kinetic data fits well with a pseudo-second order for nickel ions adsorption on the (Fe_3O_4), (Fe_2O_3) and (CuO) nanoparticles surface[16,23,52].

The calculated above is repeated for the orders of adsorption reaction of lead by using Pb (II) ion solution with initial concentration (100 mg /L) also . **Tables (3.60, 3.61)** and **Figures (3.45, 3.46)** show the kinetic data for adsorption of lead ion on (Fe_3O_4), (Fe_2O_3), and (CuO) nanoparticles surface which for pseudo-first and second order model respectively.

Table (3.60): Pseudo-first order kinetic data for adsorption of lead ion on Fe_3O_4 , Fe_2O_3, and CuO nanoparticles surfaces

Time	C_1	Fe_3O_4		Fe_2O_3		CuO	
		C_2	$\ln (C_2/C_1)$	C_2	$\ln (C_2/C_1)$	C_2	$\ln (C_2/C_1)$
30	100	14.621	1.9227	15.471	1.8662	20.596	1.5801
60	100	11.594	2.1547	11.910	2.1278	17.601	1.7372
90	100	5.123	2.9714	6.177	2.784	13.123	2.0308
120	100	4.786	3.0395	5.467	2.9064	12.123	2.0497

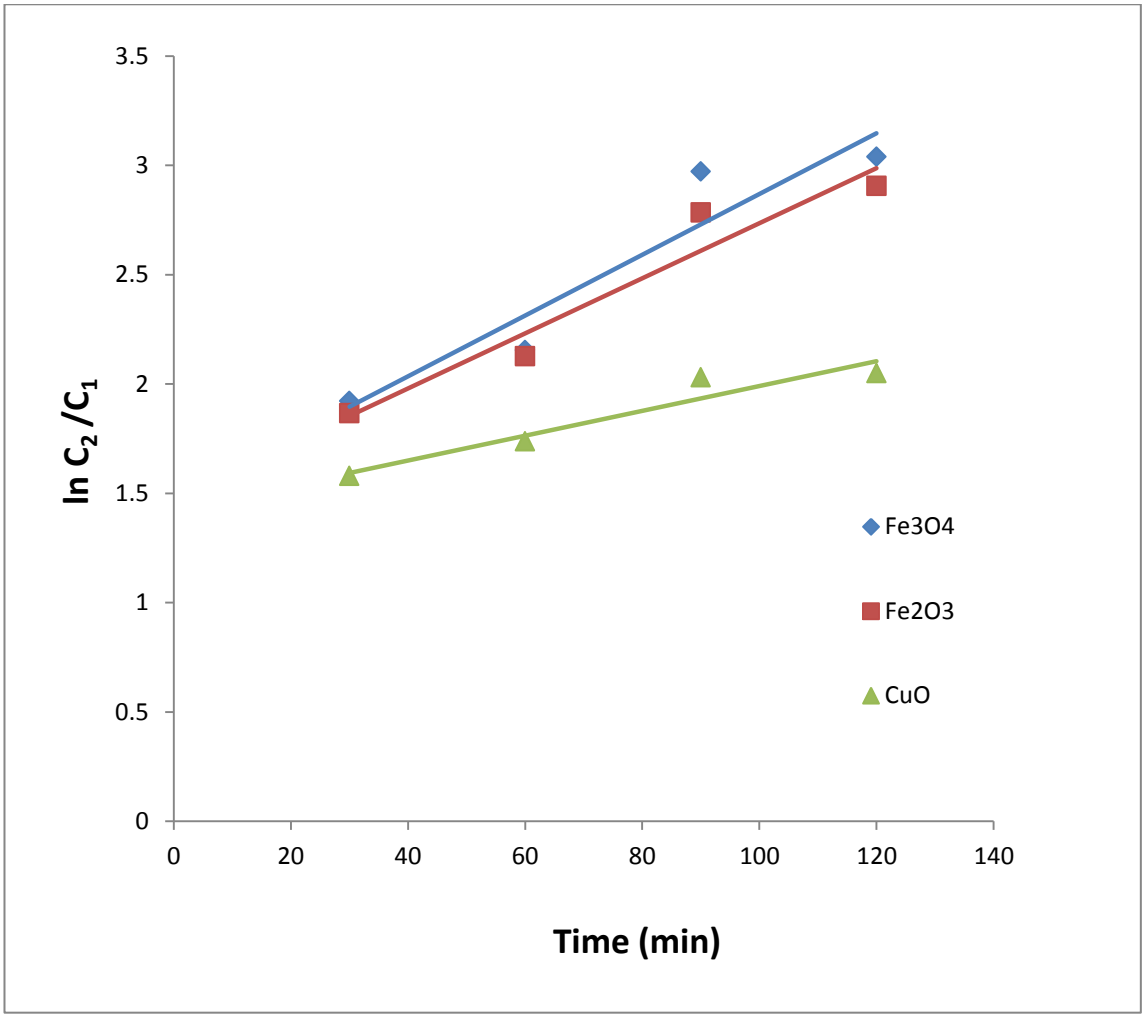

Figure (3.45): Pseudo-first order kinetic plot for the adsorption of lead ion on Fe_3O_4, Fe_2O_3, and CuO nanoparticles surface

Table (3.61): Pseudo-second order kinetic data for adsorption of lead ion on Fe_3O_4, Fe_2O_3, and CuO nanoparticles surface

Time	C_1	Fe_3O_4		Fe_2O_3		CuO	
		C_2	$1/C_2$	C_2	$1/C_2$	C_2	$1/C_2$
30	100	14.621	0.0683	15.471	0.0646	20.596	0.0485
60	100	11.594	0.0862	11.910	0.0839	17.601	0.0568
90	100	5.123	0.1951	6.177	0.1618	13.123	0.0762
120	100	4.786	0.2089	5.467	0.1829	12.123	0.0776

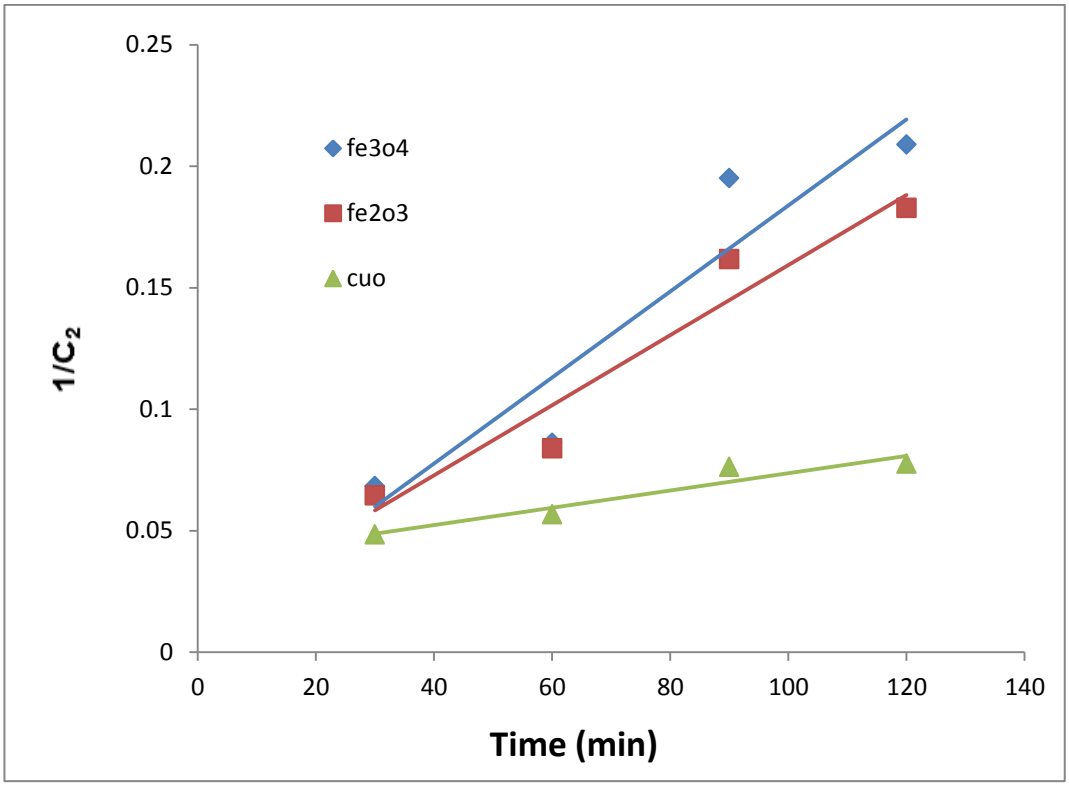

Figure (3.46): Pseudo-second order kinetic plot for the adsorption of lead ion on Fe_3O_4 , Fe_2O_3 , and CuO nanoparticles surfaces

Table (3.62) : The Pseudo-first, and second orders and their correlation coefficient of lead adsorption

Oxide nanoparticles	k_1	R^2	k_2	R^2
Fe_3O_4	0.0139	0.9008	0.0018	0.910
Fe_2O_3	0.0126	0.937	0.0014	0.939
CuO	0.0057	0.9163	0.0004	0.918

The result in **Table (3.62)** shows the correlation coefficient of pseudo-second order as higher in comparison with the pseudo-first order and the kinetic data fits well with a pseudo-second order for lead ions adsorption on the (Fe_3O_4) , (Fe_2O_3) and (CuO) nanoparticles surface [17,34,93].

3.3 : Conclusions

- It is concluded through the present study that the three oxide nanoparticles (Fe_3O_4), (Fe_2O_3), and (CuO), can be prepared by a simple precipitation method. XRD spectrum revealed that particle size obtained is around 12.04 nm for (Fe_3O_4), nanoparticles and 39.11 nm for (Fe_2O_3), nanoparticles, and 7.43 nm for (CuO), nanoparticles which agreed fairly well with SEM and AFM data. Surface morphology as a main nanoparticles phenomenon is studied in terms of SEM and AFM spectroscopic techniques which prove XRD data.
- The metal oxide nanoparticles which are used in the research (Fe_3O_4, Fe_2O_3, and CuO nanoparticles) have a high ability for removing heavy metal ions from aqueous solution especially nickel and lead ions.
- By increasing in the contact time, the nickel and lead ions percentage removal increases. Among the three oxide nanoparticles observed results showed that the (CuO), nanoparticles gave the best nickel ion removal percentage with time, followed by (Fe_2O_3), nanoparticles and last (Fe_3O_4), nanoparticles. As for lead ions removal percentage, results showed that the (Fe_3O_4), nanoparticles gave the best lead removal percentage with time, followed by (Fe_2O_3), nanoparticles and then (CuO) nanoparticles.
- By increasing in the initial concentration of adsorbate, the nickel and lead ions percentage removal decreases . So the maximum adsorption of nickel and lead ions is recorded using 100 mg/L for the three oxides nanoparticle and the (CuO) nanoparticles gave the best nickel removal percentage with time, followed by (Fe_2O_3) nanoparticles and

then (Fe_3O_4) nanoparticles. Also the results showed the (Fe_3O_4) nanoparticles gave the best lead removal percentage followed by (Fe_2O_3) nanoparticles and finally (CuO) nanoparticles.

- The correlation coefficient for the linear Langmuir regression fits is higher than that for the Freundlich one for (Fe_3O_4) nanoparticles, so the Langmuir model could describe the adsorption isotherm for the uptake of nickel ions from aqueous solution on (Fe_3O_4), nanoparticles surfaces. (Fe_2O_3), and(CuO) nanoparticles show what is otherwise because they fit better to the model of Freundlich isotherm than the model of Langmuir isotherm, so Freundlich model could describe the adsorption isotherm of removal for nickel ions from its aqueous solution on both oxides nanoparticles surfaces.
- The correlation coefficient for the linear Freundlich regression fits is higher than that for the Langmuir plot for of the three oxide nanoparticles (Fe_3O_4) , (Fe_2O_3), and (CuO), so the Freundlich model could describe the adsorption isotherm for the removal of lead ions from aqueous solution on the three oxide nanoparticles surfaces.
- Nickel ions and lead ions adsorption on (Fe_3O_4), (Fe_2O_3), and (CuO) nanoparticles surfaces obey pseudo-second order equation with a good correlation.

3.4 : Future Studies

- Preparation the three oxide nanoparticles (Fe_3O_4), (Fe_2O_3), and (CuO) by other methods like sol-gel, electrochemical method …etc.
- Change the quantity of the adsorbent dosage and calculate the removal percentage of nickel and lead ions.
- Calculate the removal percentage of nickel and lead ions at different pH.
- Change temperature and calculate the removal percentage of nickel and lead ions and the thermodynamic study of adsorption.
- Using initial concentration of nickel or lead ions less than 100 mg/L.
- Calculate the removal percentage of nickel and lead ions at contact time less than 30 (min) and more than 120 min
- Using the three oxide nanoparticles (Fe_3O_4), (Fe_2O_3), and (CuO) to remove the other heavy metals such Cr , Cd , Al …etc. .
- Using the three oxide nanoparticles (Fe_3O_4), (Fe_2O_3), and (CuO) for other applications like catalyst, and study their activity.

Table (3.49) : Data of nickel ion removal by iron oxide nanoparticle, Fe_3O_4, and iron oxide nanoparticle, Fe_2O_3, and copper oxide nanoparticle, CuO surfaces at different contact times .

Metal oxide nanoparticle	Co mg/L	30 Min		60 Min		90 Min		120 Min	
		Ce mg/L	Qe mg/g	Ce mg/L	Qe mg/g	Ce mg/L	Qe mg/g	Ce mg/L	Qe mg/g
Iron oxide nanoparticle (Fe_3O_4)	100	21.811	39.094	18.595	40.702	16.762	41.619	15.175	42.413
	200	53.568	73.216	47.566	76.217	41.696	79.152	39.178	80.411
	300	115.653	92.187	103.846	98.077	91.536	104.082	73.455	113.273
Iron oxide nanoparticle (Fe_2O_3)	100	19.911	40.045	16.815	41.593	15.567	42.217	13.800	43.100
	200	51.855	74.073	46.934	76.533	42.700	78.65	38.745	80.627
	300	101.833	99.084	88.895	105.553	76.944	111.528	68.588	115.706
Copper oxide nanoparticle (CuO)	100	17.848	41.076	16.154	41.923	13.056	43.472	10.948	44.526
	200	55.256	72.372	48.614	75.693	40.552	79.724	37.91	81.045
	300	95.247	102.376	90.327	104.837	83.604	108.198	72.978	113.511

Table (3.50) : Data of lead ion removal by iron oxide nanoparticle, Fe_3O_4 , and iron oxide nanoparticle Fe_2O_3 , and copper oxide nanoparticle, CuO surfaces at different contact times.

Metal oxide nanoparticle	Co mg/L	30 Min		60 Min		90 Min		120 Min	
		Ce mg/L	Qe mg/g	Ce mg/L	Qe mg/g	Ce mg/L	Qe mg/g	Ce mg/L	Qe mg/g
Iron oxide nanoparticle (Fe_3O_4)	100	14.621	42.689	11.594	44.203	5.123	47.439	4.786	47.607
	200	34.286	82.857	27.304	86.348	16.124	91.938	14.554	92.723
	300	54.348	122.826	43.629	128.186	27.261	136.370	25.395	137.303
Iron oxide nanoparticle (Fe_2O_3)	100	15.471	42.265	11.910	44.545	6.177	46.912	5.467	47.267
	200	33.200	83.400	26.382	86.809	18.672	90.664	17.328	91.436
	300	54.048	122.976	43.143	128.429	32.748	133.626	27.393	136.304
Copper oxide nanoparticle (CuO)	100	20.596	39.702	17.601	41.199	13.123	43.439	12.877	43.562
	200	43.626	78.187	38.822	80.589	32.372	83.814	30.928	84.536
	300	64.137	117.930	56.544	121.728	51.195	124.403	48.438	125.781

Table (3.51) : Adsorption parameters values of nickel ions on iron oxide nanoparticle, Fe_3O_4, and iron oxide nanoparticle, Fe_2O_3, copper oxide nanoparticle, CuO surfaces at different times for the application of Langmuir isotherm equation.

Metal oxide nanoparticle	C_o mg/L	30 Min			60 Min			90 Min			120 Min		
		C_e mg/L	Q_e mg/g	C_e/Q_e	C_e mg/L	Q_e mg/g	C_e/Q_e	C_e mg/L	Q_e mg/g	C_e/Q_e	C_e mg/L	Q_e mg/g	C_e/Q_e
Iron oxide nanoparticle (Fe_3O_4)	100	21.811	39.094	0.559	18.595	40.702	0.457	16.762	41.619	0.403	15.175	42.413	0.354
	200	53.568	73.216	0.732	47.566	76.217	0.624	41.696	79.152	0.527	39.178	80.411	0.487
	300	115.653	92.187	1.255	103.846	98.077	1.052	91.536	104.082	0.882	73.455	113.273	0.648
Iron oxide nanoparticle (Fe_2O_3)	100	19.911	40.045	0.497	16.815	41.593	0.404	15.567	42.217	0.369	13.800	43.100	0.320
	200	51.855	74.073	0.700	46.934	76.533	0.613	42.700	78.650	0.542	38.745	80.627	0.480
	300	101.833	99.084	1.028	88.895	105.553	0.842	76.944	111.528	0.689	68.588	115.706	0.593
Copper oxide nanoparticle (CuO)	100	17.848	41.076	0.435	16.154	41.923	0.385	13.056	43.472	0.300	10.948	44.526	0.240
	200	55.256	72.372	0.763	48.614	75.693	0.643	40.552	79.724	0.509	37.91	81.045	0.468
	300	95.247	102.376	0.930	90.327	104.837	0.862	83.604	108.198	0.773	72.978	113.511	0.643

Table (3.52):Adsorption parameters values of nickel ions on iron oxide nanoparticle, Fe_3O_4, and iron oxide nanoparticle, Fe_2O_3, and copper oxide nanoparticle, CuO surfaces at different times for the application of Freundlich isotherm equation.

Metal oxide nanoparticles	C_o mg/L	30 Min				60 Min				90 Min				120 Min			
		C_e mg/L	Q_e mg/g	Log C_e	Log Q_e	C_e mg/L	Q_e mg/g	Log C_e	Log Q_e	C_e mg/L	Q_e mg/g	Log C_e	Log Q_e	C_e mg/L	Q_e mg/g	Log C_e	Log Q_e
(Fe_3O_4)	100	21.811	39.094	1.339	1.592	18.595	40.702	1.269	1.609	16.762	41.619	1.224	1.619	15.175	42.413	1.181	1.627
	200	53.568	73.216	1.728	1.865	47.566	76.217	1.677	1.882	41.696	79.152	1.62	1.898	39.178	80.411	1.593	1.905
	300	115.653	92.187	2.063	1.964	103.846	98.077	2.016	1.992	91.536	104.082	1.963	2.017	73.455	113.273	1.866	2.054
(Fe_2O_3)	100	19.911	40.045	1.299	1.603	16.815	41.593	1.226	1.619	15.567	42.217	1.192	1.625	13.8	43.100	1.139	1.634
	200	51.855	74.073	1.715	1.869	46.934	76.533	1.671	1.884	42.700	78.650	1.630	1.898	38.745	80.627	1.588	1.906
	300	101.833	99.084	2.008	1.996	88.895	105.553	1.949	2.047	76.944	111.528	1.886	2.047	68.588	115.706	1.836	2.063
(CuO)	100	17.848	41.076	1.252	1.614	16.154	41.923	1.208	1.622	13.056	43.472	1.116	1.638	10.948	44.526	1.039	1.649
	200	55.256	72.372	1.742	1.859	48.614	75.693	1.687	1.879	40.552	79.724	1.608	1.902	37.91	81.045	1.579	1.908
	300	95.247	102.376	1.979	2.01	90.327	104.837	1.956	2.021	83.604	108.198	1.922	2.034	72.978	113.511	1.863	2.055

Table (3.53): Langmuir and Freundlich constants and the correlation coefficients for the adsorption of nickel ions by iron oxide nanoparticle, Fe_3O_4 , iron oxide nanoparticle, Fe_2O_3, and copper oxide nanoparticle , CuO , surfaces at different contact times

Metal oxide nanoparticle	Time (min)	Langmuir model					Freundlich model				
		1/a	a	1/ab	b	R^2	1/n	n	$\log K_f$	K_f	R^2
Iron oxide nanoparticle Fe_3O_4	30	0.0076	131.5789	0.3676	0.0207	0.9904	0.5188	1.9275	0.9198	8.3138	0.9521
	60	0.0071	140.8450	0.3107	0.0229	0.9958	0.5180	1.9305	0.9710	9.3541	0.9652
	90	0.0065	153.8462	0.2786	0.0233	0.9934	0.5428	1.8423	0.9749	9.4384	0.9656
	120	0.0050	200	0.2824	0.0177	0.9978	0.6275	1.5936	0.8915	7.7893	0.9969
Iron oxide nanoparticle Fe_2O_3	30	0.0065	153.8462	0.3662	0.0177	0.9999	0.5600	1.7857	0.8852	7.6771	0.9897
	60	0.0060	166.6667	0.3125	0.0192	0.9954	0.5923	1.6883	0.8932	7.8198	1
	90	0.0052	192.3077	0.3001	0.0173	0.9871	0.6097	1.6402	0.8998	7.9396	0.9997
	120	0.0049	204.0816	0.2647	0.0185	0.9775	0.6143	1.6279	0.9333	8.5763	0.9999
Copper oxide nanoparticle CuO	30	0.0064	156.2500	0.3519	0.0182	0.9586	0.5380	1.8587	0.9359	8.6278	0.9962
	60	0.0064	156.2500	0.3004	0.0213	0.9859	0.5338	1.8734	0.9775	9.4951	1
	90	0.0067	149.2537	0.2230	0.0300	0.9965	0.4953	2.0189	1.0909	12.3282	0.9960
	120	0.0063	158.7302	0.1952	0.0323	0.9795	0.4910	2.0367	1.1373	13.7183	0.9996

Table (3.54) : Adsorption parameters values of lead ions removal on iron oxide nanoparticle , Fe_3O_4 , and iron oxide nanoparticle, Fe_2O_3 , copper oxide nanoparticle, CuO, surfaces at different times for the application of Langmuir isotherm equation.

Metal oxide nanoparticle	C_o mg/L	30 Min			60 Min			90 Min			120 Min		
		C_e mg/L	Q_e mg/g	C_e/Q_e	C_e mg/L	Q_e mg/g	C_e/Q_e	C_e mg/L	Q_e mg/g	C_e/Q_e	C_e mg/L	Q_e mg/g	C_e/Q_e
Iron oxide nanoparticle (Fe_3O_4)	100	14.621	42.689	0.343	11.594	44.203	0.262	5.123	47.439	0.108	4.786	47.607	0.100
	200	34.286	82.857	0.414	27.304	86.348	0.316	16.124	91.938	0.175	14.554	92.723	0.157
	300	54.348	122.826	0.442	43.629	128.186	0.340	27.261	136.370	0.199	25.395	137.303	0.185
Iron oxide nanoparticle (Fe_2O_3)	100	15.471	42.265	0.366	11.910	44.045	0.270	6.177	46.912	0.132	5.467	47.267	0.116
	200	33.200	83.400	0.398	26.382	86.809	0.304	18.672	90.664	0.206	17.328	91.336	0.189
	300	54.048	122.976	0.440	43.143	128.429	0.336	32.748	133.626	0.245	27.393	136.304	0.200
Copper oxide nanoparticle (CuO)	100	20.596	39.702	0.518	17.601	41.199	0.427	13.123	43.439	0.302	12.877	43.562	0.296
	200	43.626	78.187	0.558	38.822	80.589	0.482	32.372	83.814	0.386	30.928	84.536	0.369
	300	64.137	117.930	0.544	56.544	121.728	0.465	51.195	124.403	0.412	48.438	125.781	0.385

Table (3.55) : Adsorption parameters values of lead ions removal on iron oxide nanoparticle, Fe_3O_4 , and iron oxide nanoparticle, Fe_2O_3, and copper oxide nanoparticle, CuO, surfaces at different times for the application of Freundlich isotherm equation.

Metal oxide nanoparticles	C_o mg/L	30 Min				60 Min				90 Min				120 Min			
		C_e mg/L	Q_e mg/g	Log C_e	Log Q_e	C_e mg/L	Q_e mg/g	Log C_e	Log Q_e	C_e mg/L	Q_e mg/g	Log C_e	Log Q_e	C_e mg/L	Q_e mg/g	Log C_e	Log Q_e
(Fe_3O_4)	100	14.621	42.689	1.165	1.630	11.594	44.203	1.064	1.645	5.123	47.439	0.709	1.676	4.786	47.607	0.679	1.680
	200	34.286	82.857	1.535	1.918	27.304	86.348	1.436	1.936	16.124	91.938	1.207	1.963	14.554	92.723	1.163	1.967
	300	54.348	122.826	1.735	2.089	43.629	128.186	1.640	2.108	27.261	136.370	1.436	2.135	25.395	137.303	1.405	2.138
(Fe_2O_3)	100	15.471	42.265	1.189	1.626	11.910	44.045	1.076	1.644	6.177	46.912	0.791	1.671	5.467	47.267	0.738	1.674
	200	33.200	83.400	1.521	1.921	26.382	86.809	1.421	1.939	18.672	90.664	1.271	1.957	17.328	91.336	1.239	1.961
	300	54.048	122.976	1.733	2.089	43.143	128.929	1.635	2.110	32.748	133.626	1.514	2.126	27.393	136.304	1.438	2.135
(CuO)	100	20.596	39.702	1.314	1.596	17.601	41.199	1.246	1.615	13.123	43.439	1.118	1.638	12.877	43.562	1.110	1.639
	200	43.626	78.187	1.639	1.893	38.822	80.589	1.589	1.906	32.372	83.814	1.510	1.923	30.928	84.536	1.490	1.927
	300	64.137	117.930	1.807	2.072	56.544	121.728	1.752	2.085	51.195	124.403	1.709	2.095	48.438	125.781	1.685	2.099

Table (3.56) : Langmuir and Freundlich constants and the correlation coefficients for the adsorption of lead ions by iron oxide nanoparticle, Fe_3O_4 , iron oxide nanoparticle, Fe_2O_3 , and copper oxide nanoparticle, CuO, surfaces at different contact times .

Metal oxide nanoparticle	Time (min)	Langmuir model					Freundlich model				
		1/a	a	1/ab	b	R^2	1/n	n	Log K_f	K_f	R^2
Iron oxide nanoparticle Fe_3O_4	30	0.0025	400	0.314	3.1848	0.9381	0.8019	1.2471	0.6935	4.9374	0.9994
	60	0.0024	416.6667	0.2392	4.1807	0.9482	0.8012	1.2482	0.7907	6.1759	0.9996
	90	0.0041	243.9025	0.0943	10.6045	0.9289	0.6225	1.6065	1.2292	16.9512	0.9955
	120	0.0041	243.9025	0.0863	11.5875	0.9504	0.6254	1.5989	1.2514	17.8402	0.998
Iron oxide nanoparticle Fe_2O_3	30	0.0019	526.3158	0.3356	2.9798	0.999	0.8544	1.1705	0.6133	4.1049	0.9991
	60	0.0021	476.1905	0.2461	4.0634	0.9964	0.8357	1.1967	0.7467	5.5808	0.9997
	90	0.0042	238.0953	0.1133	8.8262	0.956	0.6246	1.6011	1.1734	14.9073	0.9984
	120	0.0039	256.4103	0.1031	9.6994	0.8788	0.642	1.5577	1.1926	15.5812	0.9893
Copper oxide nanoparticle CuO	30	0.0006	1666.6667	0.5135	1.9475	0.4432	0.9585	1.0433	0.3328	2.1518	0.9984
	60	0.001	1000	0.4193	2.3849	0.507	0.9164	1.0913	0.4674	2.9336	0.9957
	90	0.0029	344.8276	0.2734	3.6577	0.9188	0.7668	1.3042	0.7768	5.9814	0.998
	120	0.0025	400	0.2728	3.6657	0.8854	0.7942	1.2592	0.7539	5.6741	0.9985

REFERENCES

[1] Singh**,** P. **(2010).** ***Environment and ecology*****.** 1st ed**.** India: New Age International (P) Ltd.

[2] Percival, R.V., Miller, A.S., and Schroeder, C.H. (2014). ***Environmental regulation , law, science, and policy*****.** 6th ed. Content Technology Inc.

[3] Schultz, R.A.,(2014) ***.Technology versus ecology: Human superiority and the ongoing conflict with nature.*** 1st ed. USA. Idea Group Inc.

[4] Akankali, J.A., and Abowei, J.F.N. (2010). **The intuitional perspective of environment pollutants impact severity on artisanal fisheries resources in Niger delta, Nigeria .** Current Research Journal of Economic Theory**.** 2 (2): 76-81.

[5] Bartram,J. and Balance, R. (1996**).** ***Water quality monitoring: A practical guide to the design and implementation of fresh water quality studies and monitoring programmes***. London. E & FN Spon an imprint of Chapman and Hall.

[6] Alrumman, S.A., El-kott, A.F., Keshk, S.M.A.S. (2016).**Water pollution : Source and treatment**. American Journal of Environmental Engineering . 6 (3): 88-98.

[7] Kurniawana, T.A., Chan, G.Y.S., Lo, W.H., Babel, S. (2006). **Physico –chemical treatment techniques for wastewater laden with heavy metals.** Chemical Engineering Journal. 118 (1-2): 83-98.

[8] Panneerselvam, P., Bala, V.S.S., Thiruvengadaravi, K.V., Nandagopal, J., Palanichamy, M., and Sivanesan, S. (2009). **The removal of copper ions from aqueous solution using phosphoric acid modified β- zeolites**. Indian Journal of Science and Technology. 2 (2): 63-66.

[9] Sayilgan, S.C. (2013). **Determination of characteristics of adsorbent for adsorption heat pumps.** Turkey. M.Sc. thesis, The Graduate School of Engineering and Sciences of İzmir Institute of Technology.

[10] Bhargavi, R.J., Maheshwari, U., and Gupta, S. (2015). **Synthesis and use of alumina nanoparticles as an adsorbent for the removal of Zn(II) and CBG dye from wastewater**. International Journal of Industrial Chemistry. 6 (1): 31- 41.

[11] Taman, R., Ossman, M.E., Mansour, M.S. and Farag, H.A. (2015). **Metal Oxide Nano-particles as an Adsorbent for Removal of Heavy Metals.** Journal of Advanced Chemical Engineering**.** 5 (3) : 1- 8

[12] Parmar, M., and Thakur, L. (2013). **Heavy metal Cu, Ni and Zn: Toxicity, health hazards and their removal techniques by low cost adsorbents: A short overview.** International Journal of Plant, Animal and Environmental Sciences. 3 (3) : 143-157.

[13] Nomanbhay, S.M., and Palanisamy, K. (2005). **Removal of heavy metal from industrial wastewater using chitosan coated oil palm shell charcoal**. Electronic Journal of Biotechnology. 8 (1): 43-53.

[14] Ahmed, R.A., and Fekry, A.M. (2013). **Preparation and characterization of a nanoparticles modified chitosan sensor and its application for the determination of heavy metals from different aqueous media**. International Journal of Electrochemical Science. 8: 6692-6708.

[15] Pandharipande, S.L., and Deshmukh, A.R. (2013). **Artificial neural network approach for modeling of Ni (II) adsorption from aqueous solution using aegel marmelos fruit shell adsorbent.** International Journal of Engineering Sciences and Emerging Technologies. 4 (2): 27-36.

[16] Sharma, S.K., Mahiya, S., and Lofrano, G. (2015). **Removal of divalent nickel from aqueous solutions using *Carissa carandas* and *Syzygium aromaticum* : isothermal studies and kinetic modeling**. Applied Water Science, DOI 10.1007/s13201-015-0359-y.

[17] Akkaya, G., and Guzel, F.(2013). **Optimization of copper and lead removal by a novel biosorbent : Cucumber (*Cucumis Sativus*) peels kinetic, equilibrium, and desorption studies.** Journal of Dispersion Science and Technology. 34:1295-1307.

.

[18] Egirani, D.**,** and Wessey, N. (2015). **Effect of clay and goethite mineral systems on lead removal from aqueous solution – Paper II**. International Journal of Multidisciplinary Academic Research. 3 (4): 83-92.

[19] Mehdipour, S., Vatanpour, V., and Kariminia, H.R. (2015). **Influence of ion interaction on lead removal by a polyamide nanofiltration membrane**. Desalination. 362: 84–92.

[20] Bystrzejewski, M., and Pyrzynska, K. (2011). **Kinetics of copper ions sorption onto activated carbon, carbon nanotubes and carbon-encapsulated magnetic nanoparticles.** Colloids and Surfaces A: Physicochemical and Engineering Aspects. 377: 402-408.

[21] Zolfaghari, G., Sari, A.E., Anbia, M., Younesi, H., and Ghasemian, M.B. (2013). **Zinc oxide-coated nanoporous carbon adsorbent for lead removal from water:Optimization, equilibrium modeling, and kinetics studies**. International Journal of Environmental Science and Technology.10: 325-340.

[22] Kremplova, M., Fialova, D., Hynek, D., Adam, V., and Kizek R. (2013).**Utilization of the iron nanoparticles for heavy metal removal from the environment**. proceedings of Mendelne2013 Conference. Faculty of Agronomy. Mendel University. Czech Republic. Brno. 20th and 21st November. 924-928.

[23] Haladu, S.A., Muhammad, A.M., Saleh, T.A., and Ali, S.A.(2016). **Synthesis of novel cross-linked cyclopolymer bearing polyzwitterion-dianionic moieties and its sorption efficiency for Ni(II) removal from waters**. Chemical Engineering Research and Design.106: 337-346.

[24] Das, K.K., Das S.N., and Dhundasi, S.A. (2008). **Nickel, its adverse health effects & oxidative stress**. Indian Journal of Medical Research.128: 412-425.

[25] Petrucci, F., Bocca, B. Forte, G., Caimi, S., and Cristaudo, A. (2009). **Role of diet in nickel dermatitis**. The Open Chemical and Biomedical Methods Journal. 2: 55-57.

[26] Singh, R.S., Singh, V.K., Tiwari, P.N., Singh, U.N., and Sharma, Y.C. (2009).**An Economic Removal of Ni(II) from Aqueous Solutions Using an Indigenous Adsorbent**. The Open Environmental Engineering Journal. 2: 30-36.

[27] Ricciardi, L., Gangemi, S., Isola, S., Fogliani, O., Saitta, S., and Ambrosio, F.P. (2001). **Nickel allergy, a model of food cellular hypersensitivity?**. Allergy. 56 (67): 109-112.

[28] U.S. Department of health and human services**.** Public health service**.** ***Toxicological Profile for Nickel***. (2005). USA: Agency for Toxic Substances and Disease Registry .

.

[29] Saravanan, A., Kumar, P.S., and Preetha, B. (2015).**Optimization of process parameters for the removal of chromium (VI) and nickel (II) from aqueous solutions by mixed biosorbents (custard apple seeds and Aspergillus niger) using response surface methodology**. Desalination and Water Treatment DOI:10.1080/19443994.2015.1064034 .

[30] Uzun, I., Guler, B., Ozyurek, T., Ucarli, O., Bodrumlu, E., and Menek, N. (2014).**Assessment of the nickel ion releases from the broken stainless steel and nickel titanium endodontic instruments**. International Journal of Electochemical Science. 9: 5812-5819.

[31] Varma, S., Sarode, D., Wakale, S., Bhanvas, B.A., and Deosarkar, M.B. (2013). **Removal of nickel from waste water using graphene nanocomposite**. International Journal of Chemical and Physical Sciences. 2 (Special Issue): 132-139.

[32] Sparrow, G. (2005). ***Nickel***. 1st ed. New York: Marshall Cavendish.

[33] Housecroft, C.E., and Edwin C. Constable, E.C. (2010). ***Chemistry: An introduction to organic, inorganic and physical chemistry*.** 4th ed. Italy Printic Hall, printed and bound by Rotolito Lombarda .

[34] Yin, R., Zhai, Q., Yu, L., Xiao, Y., Wang, G.,Yu, R., Tian, F., and Chen, W. (2016). **The binding characters study of lead removal by *Lactobacillus plantarum***. European Food Research and Technology. 242 (10): 1621-1629.

[35] Al-Rufaie, E.M., and Fahad, F.D. (2016). **Spectrophotometric studies for the effect of Pb^{+2} ion on some chelators**. Journal of Kufa for Chemical Science. 2 (1) : 76-86.

[36] Bahadir, T., Bakan, G., Altas, L., and Buyukgungor, H. (2007).**The investigation of lead removal by biosorption: An application at storage battery industry wastewaters.** Enzyme and Microbial Technology. 41: 98-102.

[37] Shanmugavalli, R., Shabudeen, P.S.S., Venckatesh, R., Kadirvelu, K., Madhavakrishnan, S., and Pattabhi, S. (2006). **Uptak of Pb (II) ion from aqueous solution using silk cotton hull carbon: An agricultural waste biomass.** E-Journal of Chemistry. 3 (4) : 218-229.

[38] Rahimi, S., Moattari, R.M., Rajabi, L., and Derakhshan, A.A. (2015). **Optimization of lead removal from aqueous solution using goethite/chitosan nanocomposite by response surface methodology**. Colloids and Surfaces A : Physicochemical and Engineering Aspects. 484: 216-225.

[39] Egirani, D. and Wessey, N. (2015). **Effect of mineral systems on lead removal from aqueous solution Part I**. Asian Journal of Basic and Applied Sciences. 2 (2) : 61-73.

[40] Al-Homaidan, A.A., Al-Abbad, A.F., Al-Hazzani, A.A., Al-Ghanayem, A.A., and Alabdullatif, J.A. (2016). **Lead removal by Spirulina platensis biomass.** International of Phytoremedlation. 18 (2) : 184-189.

[41] Gidlow, D.A. (2004). **Lead toxicity**. Occupational Medicine. 54: 76-81.

[42] Flora, G., Gupta, D., and Tiwari, A.(2012). **Toxicity of lead**. Interdiscip Toxicology, 5 (2) : 47-58.

[43] Agency for Toxic Substances and Disease Registry(ATSDR). [2015]. **Priority list of hazardous substances (online).**Available from http://www.atsdr.cdc.gov/SPL/index.html . [2014].

[44] Yuan, L., Zhi, W.,Liu, Y., Karyala, S., Vikesland, P.J., Chen, X., and Zhang, H. (2015). **Lead toxicity to the performance, viability, and community composition of activated sludge microorganisms.** Environmental Science and Technology. 49 (2) : 824-830.

[45] Bhattacharyya, K.G., and Sharma, A. (2004).**Adsorption of Pb(II) from aqueous solution by *Azadirachta indica* (Neem) leaf powder.** Journal of Hazardous Materials B. 113: 97-109.

[46] Yuan, L., Zhi, W., Xie, Q., Chen, X., and Liu**,** Y. (2015). **Lead removal from solution by a porous ceramisite made from bentonite, metallic iron, and activated carbon**. Environmental Science Water Research and Technology. 1: 814-822.

[47] Casas, J.S., Sordo, J. (2006). ***Lead: chemistry, analytical aspects, environmental impact and health effects***. 1st ed. Elsevier B.V.

[48] Fu, F., and Wang, Q. (2011). **Removal of heavy metal ions from waste waters: A review**. Journal of Environmental Management. 92 : 407-418.

[49] Predescu, A., and Nicolae, A. (2012). **Adsorption of Zn, Cu and Cd from wastewaters by means of meghemite nanoparticles.** University Politehnica of Bucharest Scientific Bulletin.74 (1) : 255-264.

[50] Meng, W., and Shibao, C. (2012). **Removal of Cd, Pb and Cu from water using thiol and humic acid functionalized Fe_2O_3 nanoparticles**. Advanced Materials Research. 518 (523) : 1956-1963.

[51] Predescu, A., Matei, E., Berbecaru, A., , and Vidu, R. (2014). **Synthesis of Magnetic Nanoparticles for the removal of heavy metal ions from wastewaters**. Proceedings 38th Annual Congress of American Romanian Academy of Arts and Science .California Institute of Technology . Pasadena. California. USA. July 23-27. (2014): 37- 42.

[52] Judith, T.R., Arivoli, S., and Marimuthu, V. (2014). **Kinetic, equilibrium and mechanistic studies of nickel adsorption on activated *Pistia stratiotes* leaves.** European Journal of Applied Sciences and Technology.1 (1) : 15-22.

[53] Mustaqeem, M., Bagwan, M.S., and Patil, P.R. (2015). **Adsorption of Ni (II) ion from metal solution using natural adsorbents**. International Journal of Emerging Trends in Engineering and Development, 4 (5) : 33-43.

[54] Borba, C.E., Guirardello, R., Silva, E.A., Veit, M.T., and Tavares, C.R.G. (2006). **Removal of nickel (II) ions from aqueous solution by biosorption in a fixed bed column: Experimental and theoretical breakthrough curves.** Biochemical Engineering Journal. 30: 184-191.

[55] Zuolian Cheng, Z., Tan, A.L.K., Tao, Y., Shan, D., Ting, K.E., and Yin, X.J. (2012). **Synthesis and characterization of iron oxide nanoparticles and applications in the removal of heavy metals from industrial wastewater**. International Journal of Photoenergy. 2012 : 1-5.

[56] Min, L., Xiao-hui, G., and De-zhou, W. (2011). **Removing Cd^{2+} by composite adsorbent nano-Fe_3O_4 / bacterial cellulose**. Chemical Research in Chinese Universities. 27 (6) : 1031-1034.

[57] Nazari , A.M., Cox, P.W. and Waters, K.E. (2015).**Copper and nickel ion removal from synthesized process water using BSA-coated bubbles**. Separation and Purification Technology. 156: 459-464.

[58] Dabrowski, A. (2001). **Adsorption from theory to practice**. Advances in Colloid and Interface Science. 93: 135-224.

[59] Bolis, V. (2013). **Fundamentals in adsorption at the solid-gas interface,concepts and thermodynamics.** In A. Auroux, ed. ***Calorimetry and Thermal Methods***. Verlag Berlin Heidelberg: Springer, pp. 3-49.

[60] Worch, E. (2012). ***Adsorption technology in water treatment fundamentals, processes, and modeling***. 1st ed. Berlin, Boston: Walter de Gruyter GmbH and Co. KG.

[61] Qiu, H., Lv, L., Pan, B., Zhang, Q.C., Zhang, W. M., and Zhang, Q.X. (2009). **Critical review in adsorption kinetic models.** Journal of Zhejiang University Science A. 10 (5) : 716-724.

[62] Suzuki, M. (1990). ***Adsorption engineering***. Tokyo / Amsterdam : Kodansha Ltd., and ELSsevier Science Puplishers B.V.

[63] Atkins, P., and Paula, J.D. (2006). ***Physical Chemistry***. 8th ed. New York: W. H. Freeman and Company.

[64] Walter, J., Weber, J.R. (1974). **Adsorption process** . XXIVth International Congress of Pure and Applied Chemistry. 375-392.

[65] Silbey, R.J., Alberty, R.A., and Bawendi, M.G. (2005). ***Physical chemistry***. 4th ed. John Wiley & Sons, Inc.

[66] Jaafar, S.N.B.S. (2006). ***Adsorption study– Dye removal using clay*.** 1st ed.

Malaysia**:** Faculty of Chemical Engineering and Natural Resources. University College of Engineering and Technology .

[67] Lofrano, G. (2012). ***Emerging compounds removal from wastewater: natural and solar based treatments***. 1st ed. Springer Science & Business Media.

[68] Jarullah**,** A.A.(2013). ***Removal of Ni (II) ions from aqueous solutions by adsorption technique using activated carbon as adsorbent*.** Iraq: Ph.D. thesis , college of science for women, university of Baghdad.

[69] Wang, X., Guo, Y., Yang, L., Han, M., Zhao, J., and Cheng, X. (2012).**Nanomaterials as sorbents to remove heavy metal ions in wastewater treatment**. Environmental and Analytical Toxicology. 2 (7) : 1-5. .

[70] Jain D.V.S., and Jauhar S.P. (1998). ***Physical chemistry: principle and problems***. 1st ed. New Delhi: Tata McGrew-Hill.

[71] Foo, K.Y., and Hameed, B.H. (2010).**Insights into the modeling of adsorption isotherm systems**. Chemical Engineering Journal. 156 : 2-10.

[72] Giles,C.H., Smith, D., and Huitson, A. (1974). **A general treatment and classification of the solute adsorption isotherm.** Journal of Colloid and Interface Science. 47 (3) : 755-765.

.

[73] Giles, C.H., MacEwan, T.H., Nakhwa, S.N., and Smith, D. (1960). **A system of classification of solution adsorption isotherms, and its use in diagnosis of adsorption mechanisms and in measurement of specific surface areas of solids.** Journal of the Chemical Society. 786 : 3973-3993.

[74] Mohamed, A.M.O., and Antia, H.E. (1998). ***Geoenvironmental engineering*** . Elsevier science B.V.

[75] Meisslamawy H.A.J. (2006)**.** ***Sorption capacity measurement of sulphuric acid in the active mass of Iraq lead acid strong battery***. Iraq: M.Sc. thesis , Collage of Science for Women-University of Baghdad.

[76] Waly, T.A., Dakroury, A.M., El-Sayed, G.O. and El-Salam, S.A. (2010). **Assessment removal of heavy metals ions from wastewater by Cement Kiln Dust**. Journal of American Science, 6 (12) : 910-917.

[77] Abdeen, Z., and Mohammad, S.G. (2014). **Study of the adsorption efficiency of an eco-friendly carbohydrate polymer for contaminated aqueous solution by organophosphorus pesticide**. Open Journal of Organic Polymer Materials. 4 (1) : 16-28.

[78] Aksu , Z., and Donmez, G. (2006). **Binary biosorption of cadmium (II) and nickel (II) onto dried *Chlorella vulgaris*: Co-ion effect on mono-component isotherm parameters**. Process Biochemistry.41(4) : 860-868.

[79] Laidler K.J., and Meiser J.H., (1982). ***Physical chemistry***. 6th ed.California: Benjamin Cummings Puplishing Company.

[80] Pal, S.L., Jana, U., Manna, P.K., Mohanta, G.P., and Manavalan, R. (2011). **Nanoparticle:An overview of preparation and characterization.** Journal of Applied Pharmaceutical Science. 1 (6) : 228-234 .

[81] Shakibabarough, A., Valinejadshoubi, M., and Valinejadshoubi, M. (2014). **Useable and precautionary aspects of using nanotechnology and nano-materials in the construction industry.** International Journal of Science, Engineering and Technology Research . 3 (4) : 841-847.

[82] Qiu,Y., Yu, J., Zhou, X., Tan, C., and Yin, J.(2009). **Synthesis of porous NiO and ZnO submicro and nanofibers from electrospun polymer fiber templates.** Nanoscale Research Letters. 4 : 173-177.

[83] Andujar, C.D., Ortega, D., Pankhurst, Q.A., and Thanh, N.T.K. (2012). **Elucidating the morphological and structural evolution of iron oxide nanoparticles formed by sodium carbonate in aqueous medium**. Journal of Materials Chemistry**.** 22 : 12498-12506.

[84] Palanisamy, K.L., Devabharathi V., and Sundaram, N.M. (2013). **The utility of magnetic iron oxide nanoparticles stabilized by carrier oils in removal of heavy metals from waste water**. International Journal of Research in Applied, Natural and Social Sciences. 1(4) : 15-22. .

[85] Dozier, D., Palchoudhury, Ph.D. S, and Bao, Y. (2010). **Synthesis of iron oxide nanoparticles with biological coatings.** The Journal of Science and Health at The University of Alabama. 7 : 16-18.

[86] Wang, J., Zheng; S., Shao, Y., Liu, J., Xu, Z., , Zhu, D. (2010). **Amino-functionalized Fe_3O_4 / SiO_2 core–shell magnetic nanomaterial as a novel adsorbent for aqueous heavy metals removal .** Journal of Colloid and Interface Science. 349: 293-299.

[87] Cao, C.Y., Qu, J., Yan, W.S., Zhu, J.F., Wu, Z.Y. and Song, W.G. (2012). **Low cost synthesis of flowerlike α-Fe_2O_3 nanostructures for heavy metal ion removal : Adsorption Property and Mechanism.** Langmuir. 28: 4573-4579. .

[88] Bhargav,S.S., and Prabha, I. (2013). **Removal of arsenic and copper metals from contaminated water using iron (III) oxide nanoparticle**. International Journal of Chemistry and Chemical Engineering. 3 (2) : 107-112.

[89] Nithya, K., Yuvasree, P., Neelakandeswari, N., Rajasekaran, N., Uthayarani, K., Chitra, M., and Kumar, S.S. (2014). **Preparation and characterization of copper oxide nanoparticles.** International Journal of ChemTech Research. 6 (3) : 2220-2222. .

[90] Phiwdang, K., Suphankij, S., Mekprasart, W., and Pecharapa, W. (2013). **Synthesis of CuO nanoparticles by precipitation method using different precursors**. Energy Procedia. 34: 740-745. . .

[91] Ahamed, M., Alhadlaq, H.A., Khan, M.A.M., Karuppiah, P., and Al-Dhabi, N.A. (2014). **Synthesis, characterization, and antimicrobial activity of copper oxide nanoparticles**. Journal of Nanomaterials. 2014: 1-4. .

[92] Srivastava, S., Kumar, M., Agrawal, A., and Dwivedi, S.K. (2013). **Synthesis and characterisation of copper oxide nanoparticles**. IOSR Journal of Applied Physics. 5 (4) : 61-65.

[93] Farghali, A.A., Bahgat, M., EnaietAllah. A., and Khedr, M.H. (2013). **Adsorption of Pb (II) ions from aqueous solutions using copper oxide nanostructures**. Benisuef University Journal of Basic and Applied Sciences . 2: 61-71.

[94] Devi, H.S., and Singh, T.D. (2014). **Synthesis of copper oxide nanoparticles by a novel method and its application in the degradation of methyl orange.** Advance in Electronic and Electric Engineering. 4 (1) : 83-88.

[95] Lanje, A.S., Sharma, S.J., Pode, R.B., and Ningthoujam , R.S. (2010). **Synthesis and optical characterization of copper oxide nanoparticles**. Advances in Applied Science Research.1 (2) : 36-40.

[96] Elshazly, A.H. and Konsowa, A.H. (2003). **Removal of nickel ions from wastewater using a cation-exchange resin in a batch-stirred tank reactor**. Desalination. 158 : 189-193.

[97] Onundi, Y.B., Mamun, A.A., Al Khatib, M.F., and Ahmed, Y.M. (2010). **Adsorption of copper, nickel and lead ions from synthetic semiconductor industrial wastewater by palm shell activated carbon**. International Journal of Environmental Science and Technology.7 (4): 751-758.

[98] Jarullah, A.A., Hassan, K.H., and Alias, M.F. (2012). **Removal of nickel (II) from aqueous solution using activated charcoal derived from the leaves of bitter**

orange tree (*Citrus aurantium*). Journal of Chemistry and Chemical Engineering. 6: 1003-1009.

[99] Ali, R.M. , Hamad, H.A., Hussein, M.M., and Gihan F. Malash, G.F. (2016). **Potential of using green adsorbent of heavy metal removal from aqueoussolutions:Adsorption,kinetics,isotherm,thermodynamic,mechanism and economic analysis**. Ecological Engineering . 91: 317-332.

[100] Liu, J., Chen, J., and Huang, L. (2015). **Heavy metal removal from MSS fly ash by thermal and chlorination treatments**. Scientific Reports. DOI: 10.1038/srep17270.

[101] Theivasanthi, T. and Alagar, M. (2010). **X-Ray diffraction studies of copper nanopowder**. Scholars Research Library. 1 (2): 112-117.

[102] Cullity, B.D. (1978). ***Elements of X-ray Diffraction***. 2nd ed. London : Addison-Wesley Publishing Company.

[103] **Solid State Physics X-ray Scattering III: Debye-Scherrer Method.** (2012). Physics. 340. Spring (3).

[104] Wang, J., Neaton, J.B., Zheng, H., Nagarajan, V., Ogale, S.B., Liu, B., Viehland, D., Vaithyanathan, V., Schlo,. D.G., Waghmare, U.V., Spaldin, N.A., Rabe, K.M., Wuttig, M., and Ramesh, R.(2003). **Epitaxial $BiFeO_3$ multiferroic thin film heterostructures.** Science. 299 (5613) : 1719-1722.

[105] Rozaini, C.A., Jain, K., Oo, C.W., Tan, K.W., Tan, L.S., Azraa, A. and Tong, K.S. (2010). **Optimization of nickel and copper ions removal by modified mangrove barks**. International Journal of Chemical Engineering and Applications. 1(1): 84-89.

[106] Kumar, B.R., and Rao, T.S. (2011). **Effect of substrate temperature on structural properties of nanostructure zinc oxide thin films prepared by reactive DC magnetron sputtering** . Digest Journal of Nano Materials and Bio Structures. 6(3): 1281-1287.

الملخص

في هذه الدراسة، تم تحضير ثلاث اكاسيد نانوية مختلفة باستخدام طريقة الترسيب البسيط وهذه الاكاسيد تتضمن نوعين من اوكسيد الحديد النانوي (Fe_3O_4، Fe_2O_3)، واوكسيد النحاس النانوي (CuO) ،و تم تشخيص خصائص وصفات هذه الاكاسيد النانوية الثلاثة باستخدام عدة تقنيات مثل حيود الأشعة السينية(XRD)، ومجهر المسح الالكتروني (SEM)، ومجهر القوة الذرية (AFM). حيث اظهرت النتائج لقياس (XRD) ان حجم الجسيمات كانت (١٢,٠٤ ، ٣٩,١١ ، ٧,٤٣) نانومتر ل (Fe_3O_4، Fe_2O_3، CuO) النانوية على التوالي ، وهذا ما اكدته نتائج قياسات (SEM و AFM) التي تم اجرائها.

استخدمت هذه الاكاسيد النانوية المحضرة تطبيقيا لإزالة ايونات النيكل و الرصاص من مياه المخلفات الصناعية وذلك باستخدام محلول مائي لهذه الأيونات وتحديد أفضل نسبة مئوية لازالة هذه الايونات في ازمنة مختلف (٣٠، ٦٠، ٩٠، و ١٢٠ دقيقة) وكذلك تراكيز محاليل مائية ابتدائية مختلفة (١٠٠، ٢٠٠، و ٣٠٠ ملغم / لتر) مع تثبيت الظروف الاخرى كالرقم الهيدروجيني عند ٣,٥، وكمية المادة المازة (الاوكسيد النانوي) كانت ٠,١ غرام ، وعند درجة حرارة الغرفة (٢٥ مْ).

أظهرت النتائج ان نسبة إزالة ايونات النيكل و الرصاص تزداد مع زيادة الزمن ، وكما سجلت النتائج ان اعلى امتزاز كان عند تركيز ١٠٠ ملغم / لتر بالنسبة للاكاسيد النانوية الثلاثة المستخدمة وهذا يدل ان نسبة الازالة تنخفض مع زيادة التركيز الابتدائي للمادة الممتزة .

معامل الارتباط اظهر قيمة اكبر لايزوثرم Langmuir عند امتزاز ايونات النيكل على سطح (Fe_3O_4) النانوي مقارنة بمعامل الارتباط لايزوثرم Freundlich وهذا يدل ان معادلة Langmuir تصف سلوك (Fe_3O_4) النانوي عند امتصاص ايونات النيكل ، بينما اكاسيد (Fe_2O_3، CuO) النانوية اظهرت العكس حيث كان معامل الارتباط لايزوثرم Freundlich اكبر لذلك فأن معادلة Freundlich تصف امتصاص هذه الاكاسيد لايون النيكل.

اما عند ازالة او امتزاز ايون الرصاص فأن معامل الارتباط لايزوثرم Freundlich للاكاسيد النانوية الثلاثة المستخدمة كانت قيمته اكبر لذلك فأن معادلته تصف امتزاز ايون الرصاص من قبل الاكاسيد الثلاثة . كما اوضحت النتائج الحركية ان امتزاز ايونات النيكل والرصاص على سطوح الاكاسيد النانوية المحضرة الثلاثة يخضع لقانون المرتبة الثانية .

وزارة التعليم العالي والبحث العلمي
جامعة ديالى
كلية العلوم

تحضير وتشخيص بعض الاكاسيد النانوية واستخدامها لازالة العناصر الثقيلة من مياه المخلفات الصناعية

رسالة مقدمة الى مجلس كلية العلوم- جامعة ديالى وهي جزء من متطلبات نيل درجة الماجستير في علوم الكيمياء

من قبل الطالبة
ايمان رحمن مهدي
بكالوريوس علوم كيمياء
كلية العلوم – جامعة ديالى ٢٠١١

اشراف
أ.د. كريم هنيكش حسن

٢٠١٦ م العراق ١٤٣٨ هـ